TEHNIČKI GLASNIK

TEHNIČKI GLASNIK / TECHNICAL JOURNAL – GODIŠTE / VOLUME 11 – BROJ / NUMBER 3

RUJAN 2017 / SEPTEMBER 2017 – STRANICA / PAGES 67-142

/

SVEUČILIŠTE SJEVER / UNIVERSITY NORTH – CROATIA – EUROPE

ISSN 1846-6168 (PRINT) / ISSN 1848-5588 (ONLINE)

TECHNICAL JOURNAL

ISSN 1846-6168 (Print) ISSN 1848-5588 (Online)

TEHNIČKI GLASNIK - TECHNICAL JOURNAL

Scientific-professional journal of University North

Volume 11 Number 3
Varaždin, July-September 2017 Pages 67–142

Editorial Office:
Sveučilište Sjever – Tehnički glasnik
Sveučilišni centar Varaždin
104. brigade 3, 42000 Varaždin, Hrvatska
Tel. ++385/ 42/ 493 328, Fax.++385/ 42/ 493 333
e-mail: tehnickiglasnik@unin.hr
http://tehnickiglasnik.unin.hr
http://www.unin.hr/djelatnost/izdavastvo/tehnicki-glasnik/
http://hrcak.srce.hr/tehnickiglasnik

Founder and Publisher:
Sveučilište Sjever / University North

Print:
Centar za digitalno nakladništvo, Sveučilište Sjever

All manuscripts published in journal have been reviewed.
Manuscripts are not returned.

The journal is free of charge and four issues per year are published.
Circulation: 100 copies

Journal is indexed and abstracted in:
Web of Science Core Collection (Emerging Sources Citation Index - ESCI), EBSCOhost Academic Search Complete, EBSCOhost – One Belt, One Road Reference Source Product,
ERIH PLUS, CITEFACTOR – Academic Scientific Journals, Hrčak - Portal znanstvenih časopisa RH

Registration of journal:
The journal "Tehnički glasnik" is listed in the HGK Register on the issuance and distribution of printed editions on the 18th October 2007 under number 825.

Preparation ended:
September 2017

Note from the Editor-in-Chief

Dear readers,

It is my great pleasure to present to you a new issue of Tehnički Glasnik-Technical Journal, number 3, year 11. As you can see, 15 articles have been published (12 original research and 3 review articles), most of which were presented at the MATRIB 2017 international conference. The full articles have not been published so far, and have been reviewed through our Paper Submission Tool (PST). Since both the authors and reviewers put in a great deal of effort, we have managed to complete this journal issue on time.

Our efforts to maintain the quality of published articles by publishing a double issue with fewer articles, obviously paid off - at the beginning of August this year we received a written notice from Clarivate Analytics (formerly IP & Science Business of Thomson Reuters) that since the beginning of 2017 our journal Tehnički Glasnik-Technical Journal has been indexed and abstracted in the Emerging Sources Citation Index (ESCI) under the Web of Science Core Collection (WoS). At the end of the written notice it said, "In the future Tehnički Glasnik-Technical Journal may be evaluated and included in additional Clarivate Analytics products to meet the needs of scientific and scholarly research community." In my opinion, it is a significant acknowledgment to the journal and to all those who have contributed to it. On the other hand, it is also a commitment to continue to maintain the quality and develop the journal to meet the high standards of the bases we want to be included in.

What is Emerging Sources Citation Index (ESCI)? Rapidly changing research fields and the rise of interdisciplinary scholarship calls for libraries to provide coverage of relevant titles in evolving disciplines. Emerging Sources Citation Index and its 10 year Archive provide an unmatched view of the global research landscape, covering scientific trends and developments beyond the high-impact literature. Emerging Sources Citation Index provides Web of Science Core Collection users with expanded options to discover new areas of research and relevant scholarly content. ESCI journals selected have been identified as important to key opinion leaders, funders, and evaluators worldwide and have passed an initial editorial evaluation and can continue to be considered for inclusion in products such as Science Citation Index Expanded, Social Science Citation Index, and Arts & Humanities Citation Index, which have rigorous evaluation processes and selection criteria. All ESCI journals are indexed according to the same data standards, including cover-to-cover indexing, cited reference indexing, subject category assignment, and indexing all authors and addresses.

In the end, as always, we welcome you, our dear readers, to use your input to contribute to our joint work and permanent endeavor to retain the quality of our joint journal.

Best wishes,

Full Professor Milan Kljajin, Ph.D.
Editor-in-Chief
Tehnički Glasnik-Technical Journal

ISSN 1846-6168 (Print), ISSN 1848-5588 (Online)
ID: TG-20170816162744

Original scientific paper

THE INFLUENCE OF CHLORIDE ION CONCENTRATION ON THE CORROSION BEHAVIOR OF THE CuAlNi ALLOY

Ladislav VRSALOVIĆ, Ivana IVANIĆ, Diana ČUDINA, Lea LOKAS, Stjepan KOŽUH, Mirko GOJIĆ

Abstract: The influence of different chloride ion concentration (0.1 %, 0.5 %, 0.9 % and 1.5 % NaCl solution) on the electrochemical behaviour of the cast CuAlNi alloy was examined with electrochemical techniques (open circuit potential measurements, linear and potentiodynamic polarization measurements and electrochemical impedance spectroscopy (EIS)). After polarization measurements, electrode surfaces were examined with an optical microscope and the SEM/EDS analysis. Polarization measurements revealed that an increase in chloride ion concentration leads to an increase of the corrosion current density values and a decrease of the polarization resistance values, which indicated a higher corrosion attack on the alloy. The examination of alloy surfaces with an optical microscope and the SEM/EDS analysis has shown that there is no indication of pitting corrosion in the 0.1% NaCl solution, but pits were clearly visible on the samples which were examined in the higher chloride concentration solutions. The EDS analysis has shown the existence of copper oxide on the electrode surface and a presence of a small percentage of aluminium in the form of aluminium oxide.

Keywords: corrosion; CuAlNi alloy; electrochemical methods; SEM/EDS analysis; shape memory alloy

1 INTRODUCTION

Copper and copper alloys are widely used in the applications that require the mechanical strength associated with high thermal and electrical conductivity and good corrosion resistance [1]. The addition of aluminium to the Cu-based alloys increases its corrosion resistance due to the formation of the protective layer of alumina, which builds up quickly on the surface after the exposure to the corrosive environment. The presence of nickel is important in the passivation of Cu–Ni alloys because of its incorporation in the Cu(I) oxide which is formed on the corroded surface of the alloy and which reduces the number of cation vacancies that normally exist in the Cu(I) oxide [2-5].

CuAlNi alloys are potentially very attractive materials because of their shape memory effect. The shape memory effect has been observed in the Cu alloys with aluminium content close to 14 wt. percent and with varying nickel content [6]. The shape memory alloy (SMA) is an alloy that remembers its original shape when returning to the pre-deformed shape upon heating [7]. The shape memory effect is related to the solid state transformation of martensite to austenite and vice versa [8]. Nitinol (NiTi) is the most commonly used SMA due to its superior thermomechanical and thermoelectrical properties, combined with the high corrosion resistance and biocompatibility, but this alloy is very costly [9-11]. Cu-Al-Ni alloys have low production cost, better machinability, better work/cost ratio, they are easier to manufacture, and have a higher range of potential transformation temperatures [5, 11, 12].

Copper based shape memory alloys have been intensively studied from the viewpoints of metallography, fracture behaviour, mechanical properties and activation energy of the precipitate grow process, but relatively little attention has been devoted to their electrochemical behaviour [6-8, 10, 12-15]. As the practical application of Cu-SMA is constantly increasing, these alloys are exposed to different corrosion media for a longer period of time and that could lead to the appearance of corrosion damage on their surface, jeopardise their structural integrity and cause immense consequences if the corrosion processes are not observed in time. Therefore it is important to evaluate the corrosion behaviour of Cu-based SMAs in different environments, and also to improve their corrosion resistance before their industrial applications.

2 RESULTS AND DISCUSSION

Fig. 1 presented the results of the open circuit potential (E_{OCP}) measurements for the CuAlNi alloy in different chloride solutions.

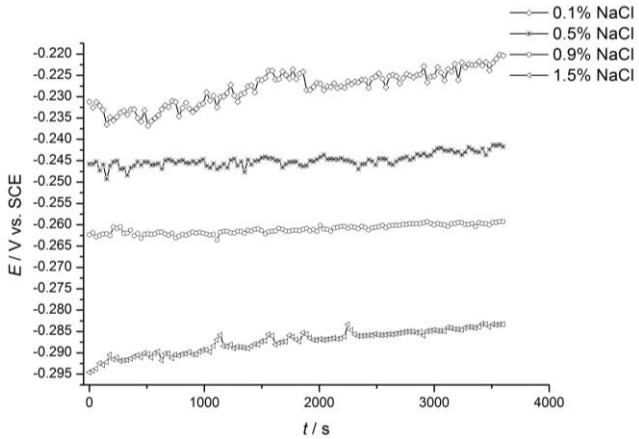

Figure 1 Open circuit potential vs. time curves for the CuAlNi alloy in chloride solutions

The open circuit potential is the potential of the working electrode relative to the reference electrode when no potential or current is being applied to the cell. The way in which a metal changes its potential upon immersion in

the solutions indicates the nature of the reaction which is taking place at its surface. Whilst a shift in potential towards more positive values denotes film formation and thickening, a shift in the negative direction signifies film destruction and the exposure of more of the bare metal to the aggressive solution [16].

From the Fig. 1 small changes in the potential of the CuAlNi alloy in a 60 minute period of time can be seen. The open circuit potentials of the CuAlNi electrodes have a tendency to shift towards the more negative values with increasing sodium chloride concentrations, so the highest difference between the E_{OCP} values for the CuAlNi alloy in the 0.1% NaCl solution and for the 1.5% NaCl solution was around 70 mV.

The electrochemical impedance spectra were taken after the E_{OCP} measurement and the results were shown in Fig.2 in the Nyquist and Bode complex plane.

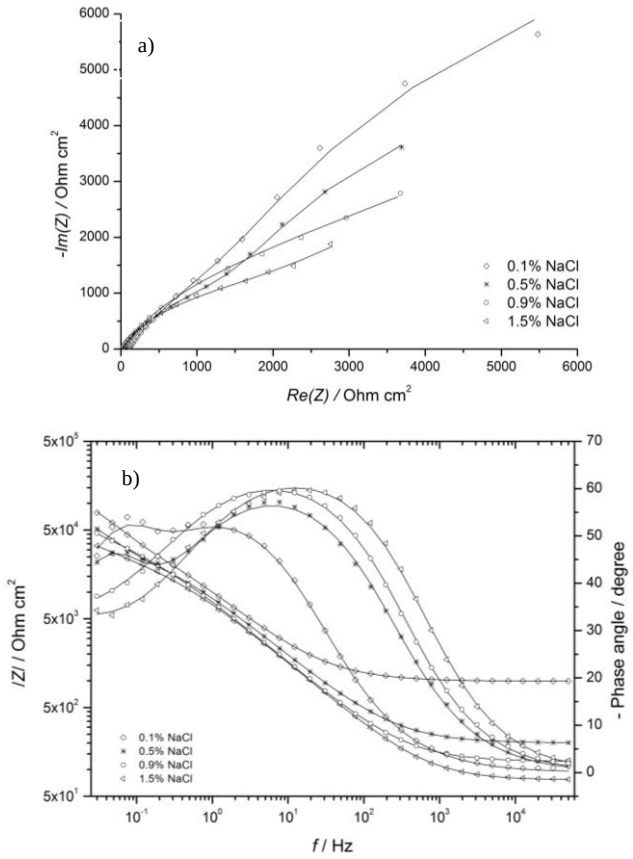

Figure 2 Nyquist a) and Bode b) plot of impedance spectra for the CuAlNi alloy in the 0.1% (-), 0.5% (-), 0.9% (-) i 1.5% (-) NaCl solution

The Nyquist plot, which represents the ratio of the imaginary (Z_{imag}) and real (Z_{real}) components of the impedance of the examined samples, shows fragments of a large incomplete semicircle. This is a typical impedance response for tin surface films. The observed time constants are partially overlapping and in such a graphic representation it is difficult to gain a clear insight into the results. From the Nyquist plot it is clearly visible that an increase in chloride concentration leads to a significant decrease of the diameter of the semicircle which indicates a lower corrosion resistance.

A more convenient method, which better shows the frequency dependence of the impedance data (and a clearer distinction between the individual time constants) is the so-called Bode diagram, i.e. the plots of the logarithm of impedance, Z, and the phase angle, respectively, *vs.* the logarithm of frequency, f. In this diagram (Fig. 2b), it is possible to observe three characteristic regions:

- In the high frequency region (f > 1 kHz), the log $|Z|$ values are low, tending towards the constant values, while the phase angle values fall rapidly towards 0°. This is a classic resistive response, corresponding to the electrolyte resistance.
- In the medium frequency region (f < 10 kHz), the linear log $|Z|$ *vs.* the log f relationship with a slope close to −1 and a phase angle of ≈ −70° mirror the capacitive behaviour of the system.
- At the lowest frequencies (f < 1 kHz), the phase angle of ≈ −20° and the slope of the log $|Z|$ vs. the log f close to −0.5 point towards the presence of a slow diffusion process.

The proposed equivalent circuit for the modelling of the impedance data is shown in Fig. 3. It consists of electrolyte resistance (R_{el}) connected with two time constants. The model is based on the circuits mostly used in literature for the simulation of the kinetics of the copper and copper alloy corrosion process and the protective properties of the surface corrosion product layer [3, 17-20].

The first time constant, observed in the high frequency region, is the result of the fast charge transfer process in the alloy dissolution reaction. In this case, R_1 represents the charge transfer resistance, and Q_1 represents the constant phase element and replaces the capacitance of the electrochemical double layer.

To account for the surface layer and the diffusion process in the low frequency range, additional equivalent circuit parameters were introduced, such as R_2 for the surface layer resistance, Q_2 for the constant phase element of the surface layer (Q_2 replaces the capacitance of the surface layer) and Warburg impedance, W, for the diffusion process.

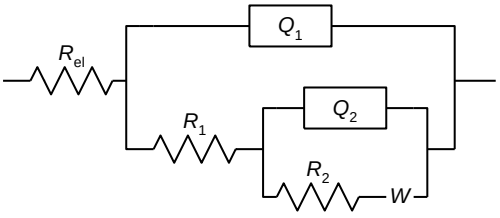

Figure 3 Proposed equivalent circuit for the modelling of the impedance data

The calculated equivalent circuit parameters for the CuAlNi alloy in a different chloride solution are presented in Tab. 1.

Table 1 Impedance parameters for the CuAlNi electrode in a different concentration of the NaCl solution

NaCl (%)	R_{el} (Ω)	$Q_1\times10^3$ ($F\times s^{n-1}$)	n_1	R_1 (Ω)	$Q_2\times10^3$ ($F\times s^{n-1}$)	n_2	R_2 (Ω)	W ($\Omega^{-1}s^{-1/2}$)
0.1	197.5	137.20	0.69	15238	101.30	1	32869	24.73
0.5	39.74	140.10	0.71	7293	301.30	0.99	13825	1491
0.9	24.54	153.50	0.73	6368	181.30	0.39	6113	7783
1.5	15.10	151.30	0.74	4653	431.60	0.50	1532	10339

After the impedance measurements, the linear polarization measurements were performed in the potential region of ±20 mV around E_{OCP}, and the results are shown in Fig. 4.

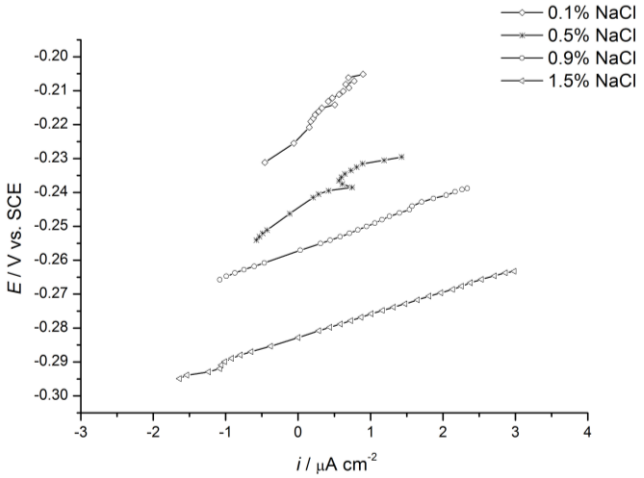

Figure 4 Linear polarization curves for the CuAlNi alloy in NaCl solutions

Polarization resistance (R_p) represents the resistance of metal to corrosion, and is defined by the slope of the polarization curve near the corrosion potential, by the Eq. (1):

$$R_p = \frac{\Delta E}{\Delta i}. \quad (1)$$

The values of corrosion resistance for the CuAlNi samples were shown in Tab. 2.

From Fig. 4 it can be seen that an increase in chloride concentration leads to a decrease of the slopes of the polarization curves, resulting in the lower values of R_p, which includes a lower resistance of the CuAlNi alloy to corrosion.

After the linear polarization measurements, potentiodynamic measurements were carried out in a wide range of potentials starting at −0.250 V from an open circuit potential and finishing at 1.100 V (Fig. 5).

The potentiodynamic polarization curve is composed of two branches: cathodic branch, which is the result of an occurring cathodic reaction and the anode part, which is the result of an occurring anodic reaction, in this case the alloy dissolution. The cathodic parts of polarization curves should reflect the hydrogen evolution reaction due to the deaeration of the solution with nitrogen, 20 minutes before the immersion of the electrode in electrolyte, as well as due to the slow deaeration during the examination.

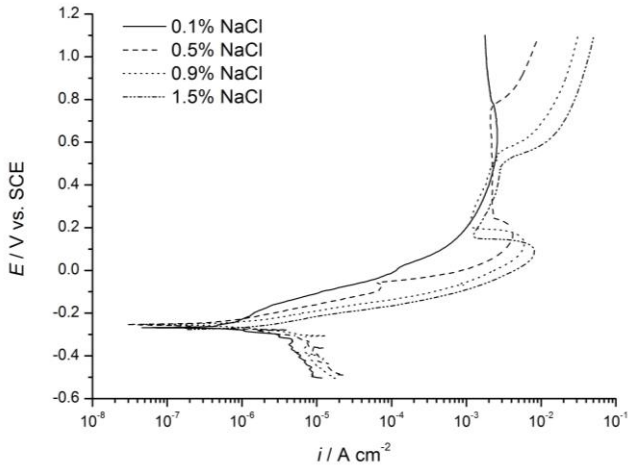

Figure 5 Potentiodynamic polarization curves for the CuAlNi alloy in NaCl solutions

Changes in the cathodic part of the polarization curves for the CuAlNi alloy in the NaCl solutions probably indicate the existence of a small concentration of oxygen in the solution, and therefore both cathodic reactions are possible: the oxygen reduction and hydrogen evolution reaction. The anodic parts of the curve describe the corrosion of the CuAlNi alloy. The anodic part of the polarization curve for the CuAlNi alloy in the 0.1% NaCl solution differs from the anodic parts of the polarization curves obtained by the CuAlNi alloy examinations in the higher concentrations of the NaCl solutions. This is probably due to the low concentration of chloride ions, which is why the anodic current density is significantly lower, indicating a weaker dissolution of the CuAlNi alloy. The anodic part of the polarization curves for the CuAlNi alloy in the 0.5, 0.9 and 1.5% NaCl solutions have three distinctive visible areas: the active dissolution region (apparent Tafel region), the active-passive transition region, and the third region in which the current density rises again with the positive potential changes due to the formation of Cu(II) species [21-23]. It is also clear that the values of the anode currents increase with the increase of the chloride ion concentration. The largest width of the pseudo-passive area was observed for the examinations of the CuAlNi alloys in the 0.5% NaCl solution, and the lowest width of the pseudo-passive area was noticed in the 1.5% NaCl solution. Moreover, after the dissolution of the corrosion products from the surface, the anodic current density increases in the following order: 0.5 % < 0.9 % < 1.5 % (area III in the anodic polarization curve).

The corrosion parameters obtained from the polarization measurements were shown in Tab. 2.

Table 2 Corrosion parameters obtained from the polarization measurements

NaCl (%)	R_p ($k\Omega\ cm^2$)	i_{corr} ($\mu A\ cm^{-2}$)	E_{corr} (V)
0.1	39.318	0.317	-0.220
0.5	29.000	0.551	-0.242
0.9	14.756	1.211	-0.259
1.5	12.886	2.041	-0.283

The data from Tab. 2 shows that an increased concentration of chloride ions leads to an increase in the corrosion current densities and a decrease in polarization resistance which indicates a higher corrosion of the CuAlNi alloy. It is also worthwhile mentioning that the recorded corrosion potential also decreased with an increase in chloride concentration.

After the polarization measurements, the corroded CuAlNi alloy surfaces were examined with an optical microscope with the magnification of 200 times. The results of the examinations were shown in Fig. 6 for the CuAlNi measurements in the 0.1, 0.9 and 1.5% NaCl solution.

It is interesting to note that at the lowest concentration of the NaCl solution, the presence of the pitting corrosion on the surface of the electrode was not observed, while in the examinations at the 0.9% and 1.5% NaCl solution, the pits were clearly visible on the surface of the CuAlNi electrodes. After the potentiodynamic polarization measurement in the 0.9% NaCl solution, a large number of smaller pits (Fig. 6b) were observed on the CuAlNi alloy surface, while in the 1.5% solution, a lower number of pits with a much larger diameter were noticed (Fig. 6c).

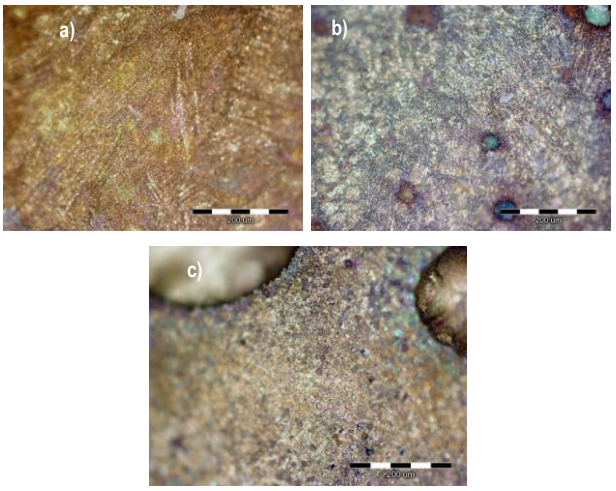

Figure 6 Optical micrographs of the CuAlNi alloy surfaces after the potentiodynamic polarization in the 0.1% a), 0.9% b) and 1.5% NaCl solution c)

The morphology of the alloy surfaces was examined by the SEM and EDS analysis and the results were presented in Fig. 7 for the CuAlNi alloy after the polarization measurements in the 0.9% NaCl solution.

The SEM/EDS surface analysis confirmed the observations obtained by examining the surface with an optical microscope. Pitting corrosion was not detected on the CuAlNi alloy surfaces which were examined in the 0.1% NaCl solution, while polarization examination in the higher chloride concentration leads to a pitting corrosion on the CuAlNi alloy.

In Fig.7 small pits are clearly visible, as is the rough surface of the corrosion products around them. The EDS analysis of the surface outside the pits revealed an elementary composition of the corrosion products on the surface of the CuAlNi electrodes. On the corrosion surface layer, the dominant elements were Cu and Cl, with small amounts of O, Al, and Ni, which confirms the observations of Benedetti and associates [21] on the formation of the aluminium oxide surface layer during the corrosion process of the Cu-Al alloys.

The analysis of the surface inside the pit showed a significantly higher percentage of chlorine relative to the surface around the pit, indicating that the corrosion inside the pits occurred by the formation of a soluble corrosive products of the copper chloride.

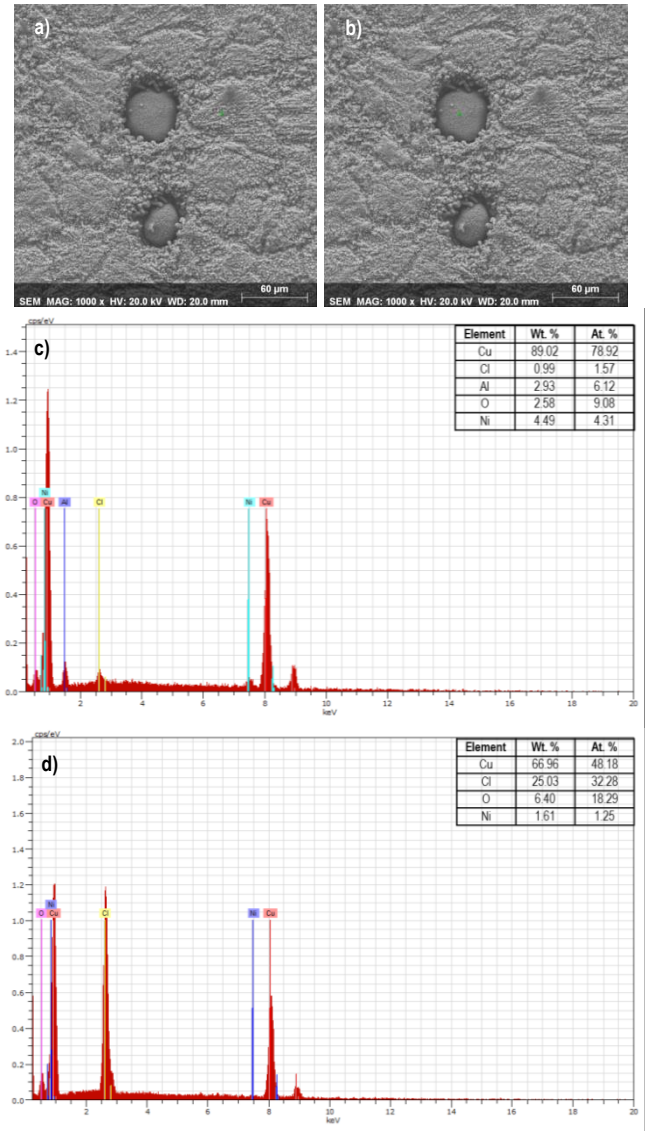

Figure 7 SEM micrograph with a marked position for the EDS analysis outside the pit a), inside the pit b), EDS results outside the pit c) and inside the pit d) for the CuAlNi alloy after the polarization measurements in the 0.9% NaCl solution

3 CONCLUSION

The open circuit potential for the CuAlNi alloy shifts to a negative direction with an increase in the concentration of chloride ions in the solution.

The results of the electrochemical impedance spectroscopy examinations showed that the overall

impedance of the system was reduced by increasing the chloride ion concentration.

A higher concentration of chloride ions leads to a lowering polarization resistance values and an increase in the corrosion current values, which indicates a more intense corrosion process.

The optical microscopy analysis of the electrode surfaces has shown the appearance of the pitting corrosion on the CuAlNi alloy after the polarization examinations in the 0.5%, 0.9% and 1.5% NaCl solutions.

The morphology examination of the alloy surfaces with SEM has confirmed the observations obtained by examining the electrode surfaces with an optical microscope. The largest number of pits is visible on the CuAlNi alloy surface after the corrosion examination in a 0.9% NaCl solution, while the largest diameter pits were recorded after the polarization in the 1.5% NaCl solution

The EDS surface analysis has shown the dominant percentage of copper and oxygen on the CuAlNi surface indicating the existence of copper oxide on the surface. The presence of a small percentage of aluminium indicates its distribution in the form of aluminium oxide on the surface layer.

Acknowledgements

This work has been fully supported by the Croatian Science Foundation under the project IP-2014-09-3405.

Note: Part of this research was presented at the International Conference MATRIB 2017 (29 June - 2 July 2017, Vela Luka, Croatia).

4 REFERENCES

[1] Liberto, R. C. N.; Magnabosco, R.; Alonso-Falleiros, N. Selective Corrosion in Sodium Chloride Aqueous Solution of Cupronickel Alloys with Aluminum and Iron Additions. // Corrosion. 63, (2007), pp. 211-219.

[2] Schussler, A.; Exner, H. E. The corrosion of nickel-aluminium bronzes in seawater—II. The corrosion mechanism in the presence of sulphide pollution. // Corrosion Science. 34, 11(1993), pp. 1803-1811.

[3] Badawy, W. A.; El-Sherif, R. M.; Shehata H. Electrochemical stability of Cu-10Al-5Ni alloy in chloride-sulphate electrolytes. // Electrochimica Acta. 54, 19(2009), pp. 4501-4505.

[4] Nady, H.; Helal N. H.; Rabiee, M. M.; Badawy, W. A. The role of Ni content on the stability of Cu-Al-Ni ternary alloy in neutral chloride solutions. // Materials Chemistry and Physics. 134, 2-3(2012), pp. 945-950.

[5] Gojić, M.; Vrsalović, L.; Kožuh, S.; Kneissl, A.; Anžel, I.; Gudić, S.; Kosec, B.; Kliškić, M. Electrochemical and microstructural study of Cu-Al-Ni shape memory alloy. // Journal of Alloys and Compounds. 509, 41(2011), pp. 9782-9790.

[6] Husain, S. W.; Clapp, P. C. The effect of aging on the fracture behavior of Cu-Al-Ni β phase alloys. // Metallurgical transactions A. 19A, (1988), pp. 1761-1766.

[7] Sathish, S.; Mallik, U. S.; Raju, T. N. Microstructure and shape memory effect of Cu-Zn_Ni shape memory alloys. // Journal of Minerals and Materials Characterization and Engineering. 2, (2014), pp. 71-77.

[8] Raju, T. N.; Sampath, V. Influence of aluminium and iron contents on the transformation temperatures of Cu-Al-Fe shape memory alloys. // Transactions of the Indian Institute of Metals. 64, 1-2(2011), pp. 165-168.

[9] Cai, W.; Meng, X. L.; Zhao, L. C. Recent development of TiNi-based shape memory alloys. // Current Opinion in Solid State and Material Science. 9, 9(2005), pp. 296-302.

[10] Kneissl, A. C.; Unterweger, E.; Bruncko, M.; Lojen, G.; Mehrabi, K.; Scherngell, H. Microstructure and properties of NiTi and CuAlNi Shape memory alloys. // Metallurgical & Materials Engineering. 14, 2(2008), pp. 89-100.

[11] Ivanić, I.; Gojić, M.; Kožuh, S. Shape Memory Alloys (Part II): Classification, Production and Application. // Kemija u industriji. 63, 9-10(2014), pp. 331-344.

[12] Čolić, M.; Rudolf, R.; Stamenković, D.; Anžel, I.; Vučević, D.; Jenko, M.; Lazić, V.; Lojen, G. Relationship between microstructure, cytotoxicity and corrosion properties of Cu-Al-Ni shape memory alloy. // Acta Biomaterialia. 6, 1(2010), pp. 308-317.

[13] Živković, D.; Holjevac Grgurić, T.; Gojić, M.; Čubela, D.; Stanojević Šimšić, Z.; Kostov, A.; Kožuh, S. Calcualtion of thermodynamic properties of Cu-Al-(Ag,Au) shape memory alloy systems. // Transactions of the Indian Institute of Metals. 67, 2(2014), pp. 285-289.

[14] Kumar Jain, A.; Hussain, S.; Kumar, P.; Pandey, A.; Dasgupta, R. Effect of varying Al/Mn ratio on phase transformation in Cu-Al-Mn shape memory alloys. // Transactions of the Indian Institute of Metals. 69, 6(2016), pp. 1289-1295.

[15] Ivanić, I.; Kožuh, S.; Kosel, F.; Kosec, B.; Anžel, I; Bizjak, M.; Gojić M. The influence of heat treatment on fracture surface morphology of the CuAlNi shape memory alloy. // Engineering Failure Analysis. 77, (2017), pp. 85-92.

[16] El Desouky, H.; Aboeldahab, H. A.: Effect of Chloride Concentration on the Corrosion Rate of Maraging Steel. // Open Journal of Physical Chemistry. 4, (2014), pp. 147-165.

[17] Cicileo, G.; Rosales, B.; Varela, F.; Vilche, J.: Comparative study of organic inhibitors of copper corrosion. // Corrosion Science. 41, 7(1999), pp. 1359-1375.

[18] Zhang, D.; Gao, L.; Zhou, G. Inhibition of copper corrosion by bis-(1-benzotriazolymethylene)-(2,5-thiadiazoly)-disulfide in chloride media. // Applied Surface Science. 225, 1-4(2004), pp. 287-293.

[19] Srivastava, A.; Balasubramaniam, R. Electrochemical Impedance Spectroscopy Study of Surface Films Formed on Copper in Aqueous Environments. // Materials and Corrosion. 56, 9(2005), pp. 611-618.

[20]Badawy, W. A.; Ismail, K. M.; Fathi, A. M. Effect of Ni content on the corrosion behavior of Cu–Ni alloys in neutral chloride solutions. // Electrochimica Acta. 50, 18(2005), pp. 3603-3608.
[21]Benedetti, A. V.; Sumodjo, P. T. A.; Nobe, K.; Cabot, P. L.; Proud, W. G. Electrochemical studies of copper, coper-aluminium and copper-aluminium-silver alloys: Impedance results in 0.5 M NaCl. // Electrochimica Acta. 40, 6(1995), pp. 2657-2668.
[22]Rosatto, S. S.; Cabot, P. L.; Sumodjo, P. T. A.; Benedetti, A. V. Electrochemical studies of coper-aluminium-silver alloys in 0.5 M H_2SO_4. // Electrochimica Acta. 46, 7(2001), pp. 1043-1051.
[23] Kear, G; Barker, B. D.; Walsh, F. C. Electrochemical corrosion of unalloyed copper in chloride media – a critical review. // Corrosion Science. 46, 1(2004), pp. 109-135.

Authors' contacts:

Dr. Sc. Ladislav VRSALOVIĆ, Associate Professor
University of Split, Faculty of Chemistry and Technology
Ruđera Boškovića 35, 21000 Split, Croatia
Tel. 021 329 444, Fax. 021 329 461, e-mail: ladislav@ktf-split.hr

Dr. Sc. Ivana IVANIĆ,
University of Zagreb, Faculty of Metallurgy,
Aleja narodnih heroja 3, 44103 Sisak, Croatia

Diana ČUDINA, M. Ch. E.
University of Split, Faculty of Chemistry and Technology
Ruđera Boškovića 35, 21000 Split, Croatia
Tel. 021 329 444, Fax. 021 329 461,
e-mail: diana.cudina@gmail.com

Lea LOKAS, M. Ch. E., Senior Associate
Development-Innovation Center AluTech,
Velimira Škorpika 6, 22000 Šibenik, Croatia

Dr. Sc. Stjepan KOŽUH, Associate Professor
University of Zagreb, Faculty of Metallurgy,
Aleja narodnih heroja 3, 44103 Sisak, Croatia

Dr. Sc. Mirko GOJIĆ, Full Professor
University of Zagreb, Faculty of Metallurgy,
Aleja narodnih heroja 3, 44103 Sisak, Croatia

ISSN 1846-6168 (Print), ISSN 1848-5588 (Online)
ID: TG-20170816161804

Original scientific paper

THE INFLUENCE OF PRINTING SUBSTRATE PROPERTIES ON COLOR CHARACTERIZATION IN FLEXOGRAPHY ACCORDING TO THE ISO SPECIFICATIONS

Dean VALDEC, Petar MILJKOVIĆ, Borko AUGUŠTIN

Abstract: Flexography is widely used in the packaging industry due to the fact that print can be adapted into various printing substrates, whose surface characteristics substantially affect the reproduction quality. Accordingly, this research comprises the comparison of the most important quality parameters of graphic reproduction in accordance with the ISO 12647-6 standard for three types of printing substrates: uncoated and coated paper and OPP film. The main goal is to examine the effect of the printing process in combination with various printing substrates on the color characteristics on the print. After the printing of a color-test form, the characterization of prints was carried out. The obtained results serve as the guidelines and recommendations for an easier and simpler control of reproduction. It has been concluded that the existing standard provides only basic recommendations. Accordingly, the characterization of the process should be adjusted to the customers' expectations.

Keywords: flexography; ISO specifications; print quality; printing substrate

1 INTRODUCTION

Flexography is a printing technique which uses photopolymer plates with elevated printing elements that leave a direct print on the substrate. The printing technique is very sensitive, and the printing plate is easily adjusted to all printing substrates. Due to its flexibility and softness, the substrate can cause, under pressure and low viscosity color, an extremely high Tone Value Increase (TVI). The printing plate makes a significant segment of the entire process which gives the flexography certain advantages. Due to the elastic printing elements, this printing technique enables printing in different absorbing and non-absorbing printing substrates such as: thin films, flexible and hard foils, all kinds of paper, cardboard of different thickness and strenghts, packaging material of corrugated surface and similar [1].

The surface characteristics of the printing substrate have a significant influece on the printing quality. On paper, the surface is additionally enriched by the finishing processes (coating, impregnating, parchmentization and laminating). The most common procedure of paper finishing is coating; therefore, the papers are divided into uncoated (raw) and coated papers [2].

The flexography process enables a high quality graphic reproduction which almost has a photo level quality. In the printing process, there have to be goal values and tolerances for the entire process, including the composition and ink viscosity, plate thickness and dot consistency, the self-adhering mounting tape and printing conditions (settings for printing pressure and speed) for the consistency in achieving the production goals [3].

The entire process of flexography consists of a large number of influential parameters that need to be standardized for specific printing conditions (Fig. 1). The concept of standardizing the reproduction process includes all the factors present in the production process which also influence the quality of the final printed product. Graphic prepress, printing platemaking, print and printing substrates used in the process have to be mutually aligned and optimized in order to get the best quality of the flexography reproduction. Therefore, all the phases of the technological process within a unique working order have to be characterized, which is the basic precondition for the standardization of the entire process.

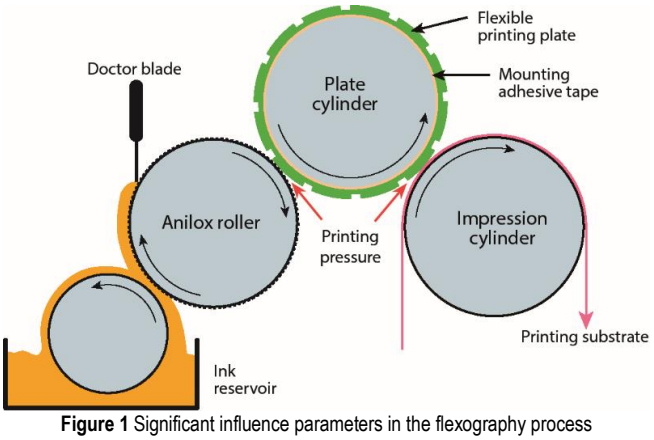

Figure 1 Significant influence parameters in the flexography process

The most common and at the same time the most efficient mode of achieving top print quality is coordination with the goal values in the ISO 12647-6 standard. However, many printing houses set their own standards by combining different line screens and volumes of the anilox roller, which in turn characterize specific printing processes in accordance with specific printing substrate classes [4].

2 METHODOLOGY

The following chapter describes the research methodology of the influence of the printing substrate on the characteristics of colour reproduction in three types of printing substrates with the objective of comparing the quality of reproduction and optimization of the production

process. The research framework describing the research purpose and process is shown in Fig. 2.

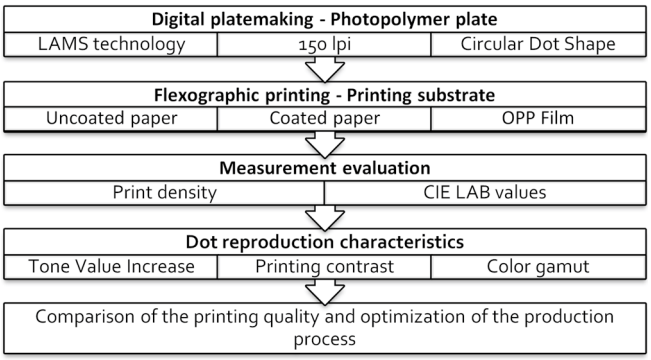

Figure 2 Research framework

2.1 Photopolymer platemaking

The experimental part of this paper begins with the design of the test form set up in a way which enables the evaluation of a quality dot reproduction by applying acceptable and established methods and research techniques. The test form used in the experiment is shown in Fig. 3.

Figure 3 Layout of the test form for printing

The color test form consists of the following elements:

- measuring patches with cascading transition in the range from 0 – 100 %,
- Ugra / Fogra test wedge for the evaluation of all the important color-reproduction characteristics,
- *flexo iO chart* for determining the print out colour gamut,
- elements for the evaluation of the text size (from 2 – 12 pt) and line thickness (from 0.05 – 0.50 mm),
- color-image for visual print evaluation.

The photopolymer plate was made by using the LAMS digital technology with the following settings defined: line screen 150 lpi, conventional AM round dot shape, screen angles (7.5°; 37.5°; 67.5° and 82.5°) and 2540 dpi resolution.

2.2 Printing

The polymer plate is mounted on the plate cylinder of a commercial, six-color flexography machine Nilpeter FB4200. The printing is performed by the principle "roll to roll" printing in the 60 m/min speed. In the course of the printing process, the printing substrate passes through the plate cylinder and impression cylinder. For an appropriate printing pressure, the distance between the two cylinders needs to be optimal. Light pressure is crucial for a good quality of reproduction since it prevents the halo effect and optimizes the Tone Value Increase [5]. It is often not easy to print when using light pressure, namely due to the characteristics of the printing substrate surface, the uneven height of the printing elements or the type of task which is being printed (full color printing, combined printing or process printing). Light pressure is the smallest needed pressure for the ink to transfer from the anilox roller to the printing plate and from the plate to the printing substrate [6].

Printing specifications:

- Flexo printing machine: Nilpeter FB4200
- Flexo ink: PULSE SLM UV Process CMYK
- Printing width: 330 mm
- Printing length: 490,00 mm
- Anilox line count: 405 lpi
- Anilox cell volume: 3.1 BCM
- Printing substrate: uncoated paper, coated paper, film.

The printing experiment is envisaged in a way that the test plate is printed by using the process CMYK UV ink on three different printing substrates, while other parameters are kept constant, including the speed and pressure in print, as well as the characteristics of the self-adhesive mounting tape and anilox roller. The chosen printing substrates are from different quality classes with different physical and optical characteristics (porosity, gloss, surface gloss, opacity, grammage).

Specification of the three selected printing substrates:

- Uncoated, white, machine-finished label paper HERMAwhite (601), grammage 72 g/m^2, opacity 83%.
- White label paper, semi-gloss coated on one side HERMAextracoat (242) grammage 80 g/m^2, opacity 86%, surface gloss 30%.
- White, high gloss, opaque OPP label film Treofan DECOR – LWD, thickness 38 μm, unit weight 23.5 g/m^2, opacity 82%, gloss 65%.

Films and foils are usually defined as a thin synthetic polymer layer. Therefore, it is necessary to prepare in advance the films and foils which have a significant influence on their surface tension and enable the ink to connect with the printing substrate which then decreases the level of difficulties in printing.

2.3 Printing evaluation

In order to compare the research results, it is important for the printing experiment to be set in controlled conditions. Each of the chosen types of printing substrates belongs to a separate qualitative group. The measured CIELCH values of process colors on prints must be matched with the goal values according to the ISO 12647-6 standard, i.e. within the limits of an acceptable deviation.

Densitometric and colorimetric values on printings are measured by using the spectrophotometer X-Rite Exact (geometry 45°/0°, standard type of lighting D50, neutral filter (No), measuring angle 2°, aperture size 2 mm). As a result of measuring, the mean value of the three measurements is taken in each patch for every basic print color.

The Tone Value Increase as the first indicator for the quality of reproduction is a difference between the measured area coverage on the print in relation to the nominal value of the coresponding test patch. The Tonal Value Increase is never completely compensated because color reproduction will be overly light. The Controlled Tone Value Increase in accordance with the standard is an entirely acceptable occurence.

The Print Contrast, as the second examined indicator of the reproduction quality, measures the ability of the printing process to reproduce shadow tones. The goal is to achieve a larger color gamut by using the optimal color density for a specific printing process [7].

3 RESULTS AND DISCUSSION

3.1 Color difference

Based on the measured CIELCH values for solid patch of primary CMY and secondary RGB colors on three types of printing substrates and the goal value defined according to ISO 12647-6:2012(E) standard [8], the hue difference is calculated and compared with the acceptable deviations in hue color (Tab. 1). The acceptable deviation for solid tone of the process colors according to the mentioned standard amounts to $\Delta h_{ab} < 6°$.

Results show that hue differences for all the process colors in all three types of printing substrates are within the acceptable tolerances, except for the *magenta* in OPP films where the value of hue differences is above the upper limit and amounts to $\Delta h_{ab,M} = 6{,}56°$. The mean value of hue differences for process colors in all three types of printing substrates is significantly under the upper acceptable limits ($\Delta h_{ab} < 6°$) and for the uncoated paper it amounts to 1,93°, for the coated paper 2,12° and for OPP film 2,73°. Such values indicate to precisely the opposite from the hypothesis that the highest deviations would be those in uncoated paper due to its relatively poor surface characteristics in relation to other printing substrates. Generally speaking, the minimal values in hue differences are seen in *cyan*, and maximal values are seen in *magenta*. The values in hue differences for secondary colors are not listed in the calculation of average value and are shown only for informative purpose.

Table 1 Hue differences (Δh_{ab}) for CMY and RGB colors in line with the ISO 12647-6:2012(E) standard

DeltaH / Lch													
	h (ISO 12647-6)	Uncoated paper				Coated paper				OPP film			
		L (%)	C_{ab} (%)	h_{ab} (°)	Δh_{ab}	*L* (%)	C_{ab} (%)	h_{ab} (°)	Δh_{ab}	*L* (%)	C_{ab} (%)	h_{ab} (°)	Δh_{ab}
C	233.00	58.43	46.12	234.51	1.51	53.77	61.37	231.36	1.64	56.46	62.06	233.16	0.16
M	357.00	51.74	60.69	359.47	2.47	46.18	75.63	0.17	3.17	48.47	70.28	350.44	6.56
Y	93.00	87.11	74.64	91.20	1.80	88.03	96.04	91.46	1.54	87.38	84.19	94.46	1.46
R	36.00	50.19	69.78	31.92	4.08	45.25	89.35	36.37	0.37	45.91	80.69	33.47	2.53
G	160.00	54.14	49.06	150.47	9.53	47.67	72.14	157.01	2.99	50.24	71.49	155.68	4.32
B	296.00	32.19	36.01	296.60	0.60	18.84	50.51	298.49	2.49	22.97	55.62	294.56	1.44
		avg_{CMY} = 1.93°				avg_{CMY} = 2.12°				avg_{CMY} = 2.73°			

Table 2 CIE LAB values of the tested printing substrate and the recommended values according to the standard

Printing substrate	*L** (%)	*a**	*b**
Uncoated paper	91.55	1.48	2.80
Coated paper	93.55	0.76	3.25
OPP film	91.01	0.21	−4.44
ISO 12647-6	>88	–3 to +3	–5 to +5

According to the mentioned standard, ISO 12647-6, the recommended CIE *L*a*b** values for the printing substrate are defined in the following gamut: for *L** (>88), for *a** (from –3 to +3) and for *b** (from –5 to +5). In Tab. 2, it is shown that all the examined printing substrates meet the mentioned criteria. The lightness value in all printing substrates is higher than 91%. Accordingly, it was to be expected that the reproduction of the process colors would be within the tolerance limits.

3.2 Color gamut

The comparison of color reproduction in the three tested printing substrates is presented by the color gamut of the print. Based on the measured CIELAB values of the primiary and secondary colors, three hexagones were constructed within the ab diagram that show the gamut of the reproduced colors for a specific type of printing substrates (Fig. 4).

The smallest color gamut was quite expectedly seen in the uncoated paper and it is significantly smaller than in the other two types of the printing substrates. Furthermore, the color gamut of the coated paper is higher than in the OPP film, which proved to be completely opposite from the set hypothesis. A larger gamut in the coated paper in relation to the OPP film was seen in the red and yellow area of the ab diagram, while in the green and blue area there are no significant deviations. Such gamut results in the coated

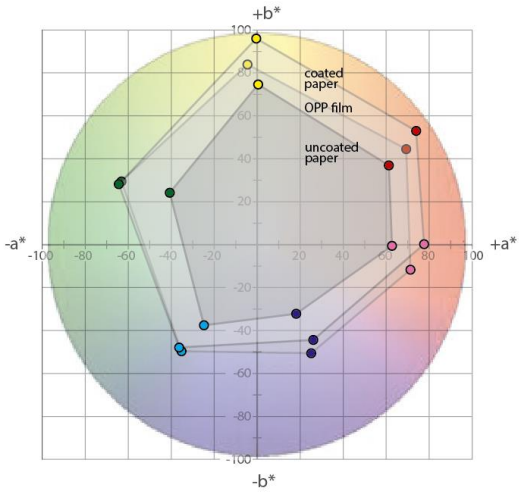

Figure 4 Overview of the color gamut in the ab diagram for three chosen printing substrates

paper and OPP film can be seen in the LAB values for the printing substrates.The difference in the coordinate *b* (Δ*b*) between the mentioned printing substrates amounts to 7.69, which indicates a shift from the blue to the yellow area of the ab diagram (Fig. 4).

3.3 Tone Value Increase

The printing quality in modern graphical technology is related to the quality of dot reproduction, and by applying the densitometric method, all the significant characteristics of dot printing can be determined.

One of the key factors influencing the quality and accuracy of dot reproduction is the change of dot size which can result in tone and color shifts. Therefore, the definition of Tone Value Increase is a significant parameter in the characterization of production processes. Tab. 3 shows the Tone Value Increase of process colors measured in two characteristic measuring fields (40% and 80%) for all three types of printing substrates. Tab. 3 also shows recommended values in accordance with the ISO specifications serving as a point of comparison.

Table 3 Tone Value Increase in the process color for the three chosen printing substrates

Tone Value Increase CMYK@40% / 80%						
	Uncoated		Coated		OPP label film	
	40%	80%	40%	80%	40%	80%
C	22.50	10.20	21.00	11.30	20.30	13.10
M	23.30	10.40	22.20	13.10	21.60	12.10
Y	23.60	12.60	19.40	12.00	19.20	12.90
K	24.70	10.70	21.50	11.90	22.50	13.00
ISO 12647-6	18.2	11.0	18.2	11.0	18.2	11.0

The Tone Value Increase results in all the tested printing substrates show somewhat higher values from the recommended ones. The Tone Value Increase in the middle tones for the process colors (at 40%) is the highest in the uncoated papers (4-6% higher than the ISO recommendation), while in the coated papers and OPP film, it is expectedly lower (1-2% higher than the ISO recommendation). In shadow tones (at 80%), the values are higher for 1-2% in all printing substrates than in the ISO recommendation.

3.4 Relative printing contrast

As a rule, prints should have the highest possible printing contrast. In order to achieve this, solid tones should have a high color density, while the halftone screen is still open. By increasing the ink film, the printing contrast is increased only up to a certain limit. By further increasing the ink film, halftone dots are filled and the printing contrast falls down again. The optimal color density for a certain printing process can be determined by using the relative printing contrast based on measuring the three quarter halftone dot patch. In the process of CMY colors, it is measured at the 70% tone value, while for the color black it is measured at the 80% tone value.

The obtained results for the printing contrast indisputably show that the printing substrates with poorer substrate characteristics result in a lower printing contrast. Although unexpectedly, the highest printing contrast can be seen in the coated paper print (in *cyan* it amounts to 46.20%). A significantly lower printing contrast in relation to the coated paper, for 9-13%, was measured in the uncoated paper, while in the OPP film it is lower for 5-10%. This indicates that despite the better substrate characteristics as a key parameter for the quality of reproduction, the quality parameters in the OPP film show lower values in relation to the coated paper, which can also be seen in Tab. 4. Such results in the OPP film can be ascribed to the influence of surface tension between the ink and the printing substrate.

Table 4 Printing contrast of the process colors for the three chosen printing substrates

Print Contrast CMY@70%, K@80%			
	Uncoated	Coated	OPP film
C	34.50	46.20	36.10
M	35.7	41.40	36.10
Y	26.70	40.20	30.90
K	23.60	32.80	24.20

4 CONCLUSION

The purpose of characterizing the entire reproduction process is in the programmed printing mode, i.e. managing the process from one point with a predictable and repeatable quality product level. This point is a graphical prepress which is connected to the overall process by the application of the color managing system. In the graphical prepress, corrections are done in certain work phases in line with the obtained results of the specific measurable parameters of the reproduction quality. These adjustments depend on the different characteristics of the photopolymer plates, different characteristics of the printing substrates, different ink types and different anilox roller specifications. The design process has to be matched with the standard, i.e. it should be implemented within the framework of the prescribed tolerances. It is therefore crucial to understand the entire production process.

The ISO 12647-6 standard contains in its specification only certain values of the qualitative color reproduction parameter which serve only as a starting reference. The reason behind it is that the characterization of the production process depends on a certain combination of ink, anilox roller, printing plates, printing substrates and printing machine. Therefore, there are no appropriate modes of implementing characterization which would take all these parameters into account and define the specific values for all possible combinations. Hence, it is important for the group of qualitative data, i.e. the process characterization, to be aligned with the customers' expectations. The second reason for the inability to design an appropriate standard is the fast development of the flexographying industry and the application of advanced technological solutions in all the production process areas.

Hue differences (Δh_{ab}) are a basic parameter in the process colors defined by the ISO specifications. Hue difference values are in this research completely matched with the mentioned standard, which is a basic precondition for further characterization. Therefore, the values of the qualitative parameters in the three types of printing substrates, based on this research, can be taken as framework values in order to further specify the mentioned production processes.

The evaluation of qualitative reproduction parameters under the influence of different printing substrate characteristics showed significant indicators which can give a serious contribution to the advancement of production process and can also result in an increased quality. The definition of repeatable and exact parameters within the process results in a constancy of the reproduction quality. This presents the first step towards standardization.

Note: This research was presented at the International Conference MATRIB 2017 (29 June - 2 July 2017, Vela Luka, Croatia).

5 REFERENCES

[1] Kipphan H., Handbook of Print Media: Technologies and Production Methods, New York: Springer, (2001).
[2] Bolčević N., Modrić D., Ivančić Valenko S., Keček D., Analiza otisaka kod pojave toniranja na različitim tiskovnim podlogama, International conference on materials, tribology, recycling, MATRIB 2014, Vela Luka, pp. 60-67, (2014).
[3] James A., Correlating anilox-roll specifications to flexographic print targets and tolerances, Converting Quarterly, vol. 2, no. 3, pp. 52-57, (2011).
[4] Teachout P., Process Standardization, Flexo, pp. 28-32, (2009).
[5] Flexographic Technical Association (FTA). Flexographic Image Reproduction Specifications and Tolerances (FIRST) Book (3rd ed.). Ronkonkoma, NY: FTA., (2003).
[6] Valdec, D.; Zjakić, I.; Milković, M., The influence of variable parameters of flexographic printing on dot geometry of pre-printed printing substrate, Tehnički vjesnik 20 (2013), 4, pp. 659-667.
[7] Flexographic Technical Association (FTA), Flexography: Principles & Practices, New York: Foundation of Flexographic Technical Association, Inc., (1999).
[8] ISO 2012, International standard ISO 12647-6, Graphic technology — Process control for the production of half-tone colour separations, proofs and production prints — Part 6: Flexographic printing, ISO, Geneva, (2012).

Authors' contacts:

Dean VALDEC, PhD, Assistant Professor
University North
Trg dr. Žarka Dolinara 1
48000 Koprivnica, Croatia
E-mail: dean.valdec@unin.hr

Petar MILJKOVIĆ, PhD, Assistant Professor
University North
Trg dr. Žarka Dolinara 1
48000 Koprivnica, Croatia
E-mail: petar.miljkovic@unin.hr

Borko AUGUŠTIN
ABS 95 d.o.o.
Jazbina 157, 10000 Zagreb, Croatia

ISSN 1846-6168 (Print), ISSN 1848-5588 (Online)
ID: TG-20170816160928

Original scientific paper

THE IMPACT OF THE TEXT AND BACKGROUND COLOR ON THE SCREEN READING EXPERIENCE

Anja ZORKO, Snježana IVANČIĆ VALENKO, Mario TOMIŠA, Damira KEČEK, Darijo ČEREPINKO

Abstract: Everyday use of modern technologies implies the need for an optimization of readability and legibility parameters used for the reading of text on screen. A lot of research on readability and legibility in printed materials and digital media has been conducted. It has been noted that the rules for the optimal readability and legibility do not apply equally to both mediums. The choice of proper typeface and font size, foreground and background colour, line spacing, sentence length, and text difficulty have the biggest role in text legibility. There is a tendency in our speaking area to read black text on a white background, which is a standard colour combination in printed materials. Furthermore, many studies have concluded that the above mentioned colour combination is one of the best when it comes to achieving optimal text readability and legibility. The purpose of this study was to test the readability and legibility of text on a computer screen by taking into consideration the different colour combinations of text and background. The factors listed above were used to define the text sample. In this research, for each of the five groups tested, the colour of the text and background were varied, while the content and other parameters of the text sample were constant.

Keywords: colour; eye tracking; legibility; readability; reading speed; text

1 INTRODUCTION

Colour has been studied for many years in many aspects, such as physics, psychology, art and graphic design. The term colour, when referred to as a physically measurable stimulus defines colour as the dominant light wavelength of the visible part of the spectrum which causes colour perception. Colour can also be defined by its abstract nature as a sensory experience that is generated by the stimulation of the visual system with specific electromagnetic radiation. [1]

The human perception of colour begins when electromagnetic radiation stimulates the cones present in the eyes. A different stimulation of red, green and blue cones generates the experience and perception of different colours. The digital, on-screen display, uses the additive colour mixing technique and RGB colour space. The RGB colour space is very much like the human colour perception; it also uses three components for colour building. In the RGB colour space, colour is defined by a red, green and blue component and each of them can be defined in the range from 0 to 255, which means in 256 different values. Colour can also be written in a hexadecimal system. The first two digits define the value of red; the next two value of green and the last two values define the blue colour component. [2]

Regardless of the aspect in which colour is studied, it is ubiquitous and indispensable in everyday life. The current lifestyle, ever-present technology and the existence of the Internet greatly affect our way of spending time. Either for work or leisure, most of that time is spent in front of a screen, computer, mobile or tablet. Therefore, for overall health perseverance, it is important to know what effect colour can have on text readability and legibility, as well as whether it affects the eye strain.

Previous research shows that specific text and background colour combinations can affect text readability and legibility. The readability of printed materials has been thoroughly examined and documented; research shows that a combination of black text on a white background (positive text) is more readable than a combination of white text on a black background (negative text). Previous research also show that a slightly coloured paper does not affect text readability, but the brightness contrast between the foreground and background colours do affect it; the greater the contrast, the better the readability. [3]

Beside the general guidelines, previous research has given specific colour combinations that are now considered optimal for readability enhancement (black text on white background and black text on yellow background) and some which are not recommended for use (as shown in Fig. 1, green text on an orange background and red text on a green background). [1] [3]

Figure 1 Best and worst foreground and background colour combinations for printed materials

2 READABILITY AND LEGIBILITY

Čerepinko [4] defines legibility as an optical and visual characteristic of character and readability as an optical and visual characteristic of blocks of text and its defining of how difficult a character is for reading. The readability of text refers to its content and represents the objective difficulty of reading which can be measured with various formulas. The ease of reading also depends on the competence and reading abilities of the reader itself.

While analysing the readability research, Dillon [5] states that the speed of reading, accuracy of reading, fatigue,

understanding of the read text and personal preferences can be researched. According to Dillon, measuring the speed of reading to define text readability is one of the most common methods. It can be carried out in two ways. The first way is by defining the length of text that is going to be read and then measure the time required to read it for every subject. Other option is to limit the time of reading and measure the length of read text in a limited time. The process of reading depends on many factors of which the most significant are the content suitability of the text, age and readers' education [6]. An average reader, in a text that is suitable for his or her age and education level, fixates on 1.2 words in one gaze. For a more complex text and less known topics, a number of fixated words drops down below 1 and vice versa, while a simpler text generates a greater number of fixated words. [7]

Previous research show that the readability of a text depends on a number of factors, the appearance and size of the typeface, proper character combining, the medium on which it is printed and the method with which the text is printed. Thereby, the optimal amount of characters in a line (60 to 70 characters in printed materials and 40 for the digital screen) has been previously defined. [8] The influence of contrast on readability and legibility has also been previously researched [9]. The serif typefaces proved to be more readable for printed materials, while the sans serif fonts proved to be more readable for the technologies that display text on digital screens (tablet, personal computer) [10], and they are preferred by the majority of readers.

3 W3C CONSORTIUM AND WEB CONTENT ACCESSIBILITY GUIDELINES

The World Wide Web Consortium (W3C) guidelines are often used while preparing materials for digital devices. "W3C is international community whose mission is to define open standards to ensure the long-term growth of the Web." [11]

W3C has defined some web content accessibility guidelines (WCAG 2.0). Those guidelines contain recommendations on how to arrange web content so that it is accessible and equivalent to a greater number of users. Guidelines are separated by categories such as visibility, usability, intelligibility, robustness. That clear difference between the foreground and background colour can help improve readability, and it is mentioned under the visibility guidelines. To get a better overall content accessibility, it is recommended to have a greater colour contrast.

Minimal contrast is defined in two categories:

- Level AA - contrast ratio at least 4.5:1
- Level AAA - contrast ratio at least 7:1 [12]

The colour and brightness contrast can be used to define the colour of text and colour of the background. The brightness contrast or reflection can be defined as a ratio of the amount of light reflected from the object in contrast to the light shining on the object. [13] W3C defines brightness contrast as a difference of value between the brightness values of text according to the brightness values of the background. The values 125 and greater are defined as positive and acceptable. The colour contrast is defined as a physical value of the colour, the difference between colours in a defined colour space. According to the W3C guidelines, the difference between two colours should be 500 or more. [3][12]

4 RESEARCH METHODOLOGY

The purpose of this study was to examine the influence of different foreground and background colour combinations on the screen reading experience. At the beginning of the research, it was necessary to define the textual sample, typeface, and colour combinations. 100 students from the University North, the Multimedia, Design and Application Department were tested.

4.1 Sample definition

According to Brangan's research of readability formulas, for the purpose of this experiment, a textual sample of a difficult (LIX=46; bordering medium) reading difficulty was used. The text reading difficulty was measured by using the LIX formula (1) adjusted for the Croatian language:

$$LIX = A/B + (C \times 100)/A + 2 \quad (1)$$

where A is the number of words, B is the number of sentences and C represents the number of long words (eight or more characters). According to the LIX formula, the text reading difficulty is measured by the following scale: <24 very easy, 25-34 easy, 35-44 medium, 45-54 difficult, >55 very difficult. [14]

Sheedy et al. have been researching the typeface influence on the legibility of textual characters and words on a digital screen, and according to that research, Arial and Verdana are the most legible, and Times New Roman and Franklin the least [15]. For this reason, the typeface used for the sample in this research is a sans serif typeface Verdana, font size 27 pt, arranged in one column.

Fig. 2 shows the sample used in this research. The sample is copied from the "Grafički dizajn i komunikacija" book by the authors Tomiša and Milković, and it is a segment from the chapter about colour spaces. [16]

Pri radu s bojama na ekranu važno je pravilno izabrati pozadinsku boju jer je to uglavnom najveća površina gdje je prisutna jedna boja. Treba uzeti u obzir kriterije poput karaktera boje, svjetline i ostalih elemenata boje. Važno je znati unaprijed koji se efekti žele postići. Pozadinska boja rijetko je jedina boja na ekranu. Obično se kombinira sa slovnim znacima, simbolima, slikama i logotipima. Takvi različiti elementi međusobno djeluju i omogućuju jedni drugima kontraste u kvaliteti i kvantiteti.

Figure 2 Textual sample used in this research

For research purposes, two best and two worst colour combinations were chosen, as defined by the previously mentioned research (Fig. 1). A black text on a white background and a black text on a yellow background were chosen as the best colour combinations, and a green text on an orange background and a red text on a green background as the worst. For the fifth test group, a black text on a cream background was chosen because that is the colour combination that imitates the colours of printed books. [3][1][17]

Since those colours have generally been defined in the CMYK colour space (research was done for printed materials), for the needs of this research, precise colour tones have been selected from the web safe colour palette. The web safe colour palette defines colours which should be used for web designated materials. The usage of safe colours should ensure that the same colour looks identical on most digital devices independent of the device characteristics and applications that are used. [1]

The enclosed Tab. 1 shows an overview of the chosen colours and their RGB and hexadecimal values.

Table 1 Overview of the chosen colour values

Colour	RGB colour code			Hexadecimal colour code
	Red	Green	Blue	
white	255	255	255	FFFFFF
cream	255	255	204	FFFFCC
yellow	255	255	0	FFFF00
orange	255	153	0	FF9900
red	255	0	0	FF0000
green	0	128	0	008000
black	0	0	0	000000

Tab. 2 shows samples used in this research, as well as the colour contrast, brightness contrast and tone difference values. Values have been calculated with an application available on the snook.ca1 website. The application uses the WCAG 2.0 formula for contrast calculations. It is possible to precisely define the wanted colours of the text and background, and the application then calculates the contrast values and verifies whether those values are acceptable considering the W3C guidelines. [12]

Table 2 Samples and their colour contrast, brightness contrast and tone difference values

Colour of text	Colour of background	Sample	Colour contrast	Brightness contrast: (>= 125)	Tone difference: (>= 500)
black	white	SAMPLE	21	255	765
black	cream	SAMPLE	20.43	249.18	714
black	yellow	SAMPLE	19.56	225.93	510
green	orange	SAMPLE	2.4	90.92	280
red	green	SAMPLE	1.28	1.11	383

After reading the sample, the reading habits on digital screens and the subjective reading difficulty were tested by using the prepared survey. The reading difficulty was evaluated by using the Likert scale from 1 to 5, where 1 defined hard to read and 5 easy to read.

4.2 Devices used in research

The textual samples used for this research were shown on a Samsung LCD screen, S22A350H model. The screen size was 21.5 inches and the aspect ratio was 16:9. The subject's distance from the screen was in the range from 50 to 80 centimetres, which is the distance suggested as the most favourable for longer viewing and reading on a digital screen. The specified distance was optimal according to the eye tracking device specifications and the monitor visual angle which was 170°/160°. [18][19]

The subject reading measuring was accompanied by the eye tracking technology which allows us to measure the point of gaze and fixation points while watching the screen. The device used was the Gazepoint GP3 Desktop eye tracking device and the accompanying Gazepoint Analaysis 3.5.0 software.

5 RESULTS AND ANALYSIS OF THE RESEARCH

The empirical analysis of this research was based on the results obtained from the measurement conducted among the students of the University North, the undergraduate interdisciplinary professional study of the "Multimedia, Design and Application" Department. The descriptive and inference statistic methods have been used in the data analysis. Students have been analysed based on gender, age and year of enrolment.

Of a total of 100 subjects, 52 were male and 48 female. On the basis of age, subjects were separated into three age groups. The first group included students younger than 21, the second included students from the age 21 to 25 and the third included students aged 26 and older. The first group was more numerous than the other two (58% of the examinees), while the third group consisted of only 7% of examinees. A bit more than half of the interviewed students were enrolled in first year (52%), while only two students were enrolled in their third year of college.

Within the inferential statistic, the distribution of the reading time data obtained by the research was examined. The distribution of the reading time data, which was tested with the Kolmogorov–Smirnov test, statistically significantly differs from the normal distribution. Therefore, for the testing of the statistically significant differences between the samples, a nonparametric Kruskal–Wallis test was used. In the cases of the statistically significant differences between the samples, multiple comparisons test was used to determine the statistically significantly different samples. The differences confirmed at $p<0.05$ were considered statistically significant. For the graphical representation of the reading time data distribution, the Box and Whisker Plots were used. The statistical analysis was performed by using the Matlab 7.0 mathematical software.

In Tab. 3 the descriptive statistics of the text reading time and the results of the Kruskal–Wallis test are shown.

Table 3 Descriptive statistics and results of the Kruskal-Wallis test for the text reading time

GROUP	Mean (s)	Median (s)	Kruskal-Wallis test	
			H	*p*
G1	31.60	32	11.53	0.02
G2	29.35	28		
G3	31.40	32		
G4	29.55	29.50		
G5	29.20	28		

As shown in Tab. 3 and Fig. 3, the shortest average reading time was determined for the group G5, 29.20 seconds. Group G1 had the longest average reading time of 31.60 seconds. The biggest mean value of 32 seconds was identified for the groups G1 and G3, while the lowest mean value was identified for the groups G2 and G5. From Tab. 3 it can be seen that there is a statistically significant difference in times of reading (p=0.02). By using the multiple comparisons test, it has been confirmed that the groups G1 and G5 are statistically significantly different.

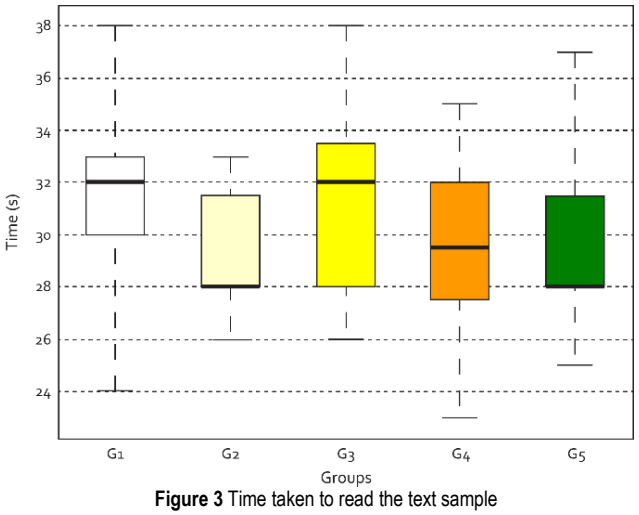

Figure 3 Time taken to read the text sample

The ratio of the number of mistakes was tested for all five groups. From a total of 100 students that were included in the research, 43 of them read the textual sample without a mistake. Group G4 had the largest percentage of students that read the sample without a mistake (55%). That percentage was just slightly lower in group 1, where 50% of the students read the text without a mistake. Group G3 was the group where the least number of students read the text without a mistake, only 30%. In 37% of the readings, there was one mistake, two mistakes in 33%, three mistakes in 12%, four in 11% and five mistakes occurred in 7% of the readings. Group G3 had the largest number of students that made one mistake during the reading (six students), and in group G4 only two students made one mistake.

Tab. 4 shows the results of the tests, the longest, shortest and average time of reading, as well as the total number of mistakes for every group of examinees. From the results shown, it can be concluded that the combination of the black text on a white background is the most readable combination of colours. The mentioned colour combination was shown to the group G1 and that group also had the least number of total mistakes.

The sample shown to the group G3 (a black text on a yellow background) stands out as the worst colour combination for text readability. Group G3 had the largest mean value of reading time (Tab. 3) and the biggest total number of mistakes (Tab. 4). Fig. 4 also shows the deviation in the heat map of the group 4 in relation to the other four.

Groups G4 and G5, which had combinations of colour defined as the worst for readability, produced unexpected results. [17] The total number of mistakes in the mentioned groups was lower (Table 4) than the total number of mistakes for the groups G2 and G3 which had the best colour combinations. Group G5 also had the shortest average time of reading.

Table 4 Results of measurement, times of reading and a total number of mistakes

	G1 black text white background	G2 black text cream background	G3 black text yellow background	G4 green text orange background	G5 red text green background
longest time of reading (s)	38	33	38	35	37
shortest time of reading (s)	24	26	26	23	25
average time of reading (s)	31.5	29.6	31.2	29.6	29.2
total number of mistakes	18	28	31	23	24

Since measurements were recorded by an eye tracking camera, the results of the research are also visible with the help of heat maps that show the points of interest for the subjects. The areas at which the subjects looked the most are coloured in warm colours and the least viewed areas are coloured in blue.

As it is visible from the examples in Fig. 4, heat maps of all five samples were similar, only the group G3 showed some deviation. The sample 3 had a black text on a yellow background. The results of the measurements show that the group G3 also had the most number of total mistakes. It can be assumed that the above mentioned colour combination is the most tiring and there is no tendency of fixation as there is on the other four maps.

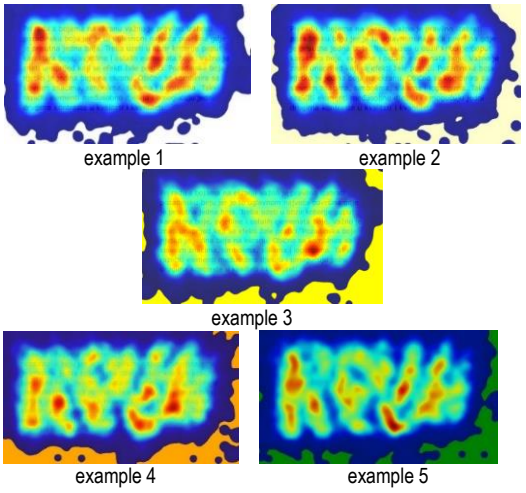

Figure 4 Overview of heat maps

6 CONCLUSION

According to previous research about the influence of colour on the readability of printed materials, it was confirmed that the combination of a black text and white background is one of the most readable and a combination of a red text on a green background is the least readable [17].

The purpose of this research was to determine the foreground and background colour influence on the readability on a digital screen. The results obtained in this research are similar to those obtained for the readability on printed materials. A black text on a white background came out as the most readable colour combination. The group that read above the mentioned sample had the least total number of mistakes, although the average time of reading was the longest, 31.5 seconds. That does not mean that the mentioned combination is not a good colour combination because the average time of reading for all groups was between 29.2 and 31.5 seconds. In a survey that was carried out just after testing, the respondents also declared that the black foreground-white background colour combination is the least stressful for the eyes.

A black text on a yellow foreground has proven to be the least readable colour combination. The results of these colour combination readings have the biggest total number of mistakes and the least percent of students (30%) read this sample without mistakes.

Unsuspected results were obtained for the fourth and fifth sample, a green text on an orange background and a red text on a green background. Even though on printed materials those combinations have proven to be the least readable, this research shows they are good for reading on a digital screen. It is interesting that the total number of mistakes was lower for those samples than for the second and third (black-cream, black-yellow) samples. It can be assumed that it is due to the fact that those samples had a lower colour contrast which can be seen in Tab. 2.

Given the fact that this is only the start of a possibly large field of research, a recommendation for future experiments would be to increase the amount of colour combinations and the number of respondents tested in order to determine if there is (and what it would be) any specific effect causing the differences between the same combinations of colours in the different media (screen and print).

Note: This research was presented at the International Conference MATRIB 2017 (29 June - 2 July 2017, Vela Luka, Croatia).

7 REFERENCES

[1] Žufić, J.; Kalpić, D.: Boja i efikasnije e-poučavanje, Metodički obzori: časopis za odgojno-obrazovnu teoriju i praksu, Vol. 4 (2009)1-2 No. 7-8 (2009) 57-72
[2] Kodner, J.; Nonaka, A.; Wilson, J.; Brajnard, D.; Ungar, L.: Determining the Readability of Colored Text, Univ. of Pennsylvania Philadelphia
[3] Tinker, M. A.: Experimental Studies on the Legibility of Print: An Annotated Bibliography, Reading Research Quarterly, Vol. 1, No. 4 (1966) 67-118
[4] Čerepinko, D.: Optimizacija grafičkih parametara korisničkoga sučelja za 'tablet novine', Doktorska disertacija, Grafički fakultet Sveučilišta u Zagrebu, 2014.
[5] Dillon, A.: Reading from paper versus screens: a critical review of the empirical literature, Ergonomics, Vol. 35, No. 10 (1992) 1297-1326
[6] Just, M. A.; Carpenter, P. A.: A theory of reading: From eye fixations to comprehension, Psychological Review, Vol. 87, No. 4 (1980) 329-355
[7] Furlan, I.: Čitanje u svjetlosti teorije informacije, Pedagogija, Vol. 4 (1963) 596-612
[8] Rabinowitz, T.: Exploring Typography, Clifton Park, NY: Thomson/Delmar Learning, 2006
[9] Legge, G.: Psychophysics of Reading, Mahwah, NJ: Lawrence Erlbaum Associates, 2006
[10] Čerepinko, D.; Keček, D.; Periša, M.: Text Readability and Legibility on iPad with comparison to Paper and Computer Screen, Tehnički vjesnik Vol. 24, No. 4 (2017) 1197-1201
[11] https://www.w3.org/ (Accessed: 4.04.2017)
[12] https://www.w3.org/TR/WCAG/#visual-audio-contrast (Accessed: 4.04.2017)
[13] York, J.: Legibility and Large-Scale Digitization, Hathi Trust Digital Library, 2008.
[14] Brangan, S.: Razvoj formula čitkosti za zdravstvenu komunikaciju na hrvatskom jeziku, doktorska disertacija, Zagreb, Medicinski fakultet Sveučilišta u Zagrebu, 2011
[15] Sheedy, J. E.; Subbaram, M. V.; Zimmerman, A. B.; Hayes, J. R.: Text legibility and the letter superiority effect, Human Factors: The Journal of the Human Factors and Ergonomics Society, Vol. 47, No. 4 (2005) 797-815
[16] Tomiša, M.; Milković, M.: Grafički dizajn i komunikacija, Veleučilište u Varaždinu, 2013., ISBN 978-953-7809-19-5
[17] Zjakić, I.; Milković, M.: Psihologija boja, Veleučilište u Varaždinu, 2010., ISBN 978-953-95000-1-4
[18] http://www.samsung.com/us/computer/monitors/LS22A350HS/ZA-specs (Accessed: 27 April 2017.)
[19] http://narodnenovine.nn.hr/clanci/sluzbeni/2005_06_69_1354.html (Accessed: 6 April 2017.)

Authors' contacts:

Anja ZORKO, Teaching Assistant
Snježana IVANČIĆ VALENKO, Lecturer
Mario TOMIŠA, Ph.D, Associate Professor
Damira KEČEK, Senior Lecturer
Darijo ČEREPINKO, Ph.D, Assistant Professor

University North,
104. brigade 3, 42000 Varaždin, Croatia
anja.zorko@unin.hr,
snjezana.ivancic@unin.hr,
mario.tomisa@unin.hr
damira.kecek@unin.hr
darijo.cerepinko@unin.hr

ISSN 1846-6168 (Print), ISSN 1848-5588 (Online)
ID: TG-20170815202822

Original scientific paper

BANKNOTE CHARACTERIZATION USING THE FTIR SPECTROSCOPY

Katarina ITRIĆ, **Damir MODRIĆ**

Abstract: Counterfeit methods are more sophisticated than ever before, so it is necessary to implement as many different methods as possible to get reliable information on the origin of the banknotes. The FTIR spectroscopy provides exactly this, a different approach to the identification of different banknote components, from the paper itself to the characterization of the inks, holograms and watermarks. This paper examines the similarities and differences in the composition of the paper used for making banknotes in six different currencies, and at the same time deals with the characterization of the unique features of a particular currency. Moreover, the consistency within the particular currency is examined by comparing multiple banknotes of the same denomination.

Keywords: banknote; FTIR spectroscopy; counterfeit.

1 INTRODUCTION

Counterfeiting money is one of the oldest criminal activities; it dates back all the way to the 5th century AD, and it got more and more sophisticated during the centuries.

Every year approximately 600 000 euro notes are removed from the circulation [1]. As for Croatia, a total of 353 counterfeit kuna banknotes were withdrawn from circulation in the first six months of 2016, which is an increase of 64.2 % relative to the number of counterfeit kuna banknotes registered in the same period in 2015 [2]. In the same period, 72 counterfeit US dollar banknotes were registered, as well as 206 counterfeit euro banknotes.

The authentication of the detected counterfeit banknotes has shown that counterfeiters often imitate some security features, such as the security thread, watermark, hologram and optical variable ink element.

In order to prevent banknote counterfeiting, every new edition increases the number of security elements of the banknotes, from adding security threads that react to UV light, 3-D security ribbons woven into paper, watermarks and colour shifting inks, in addition to the microprinting and raised printing elements. Of course, paper itself contains additional security fibres. Naturally, the number of counterfeit elements depends on the denomination of the banknote.

Nearly all modern banknotes incorporate multiple anti-counterfeiting devices. Some notes, especially the high-denomination ones, may have as many as fifty such elements, some obvious, some secret. This ranges from multiple alphabetical fonts and differing sizes and shapes for letters and digits in serial numbers to special inks that can only be seen under ultra-violet or infrared light. Heat transfers of optical variable devices (OVD) and/or holograms are also favoured on modern banknotes

Throughout history, cotton paper was used for hundreds of years as a basis for the major currencies, and it is still widely spread due to its customizing ability during the production process with security threads, embedded watermarks and machine-readable elements, while at the same time it offers unlimited opportunities for attractive banknote design due to its high print quality. Eventhough most of the generally used banknotes around the world are made of paper, different plastic materials are emerging and proving themselves useful.

2 MATERIALS AND METHODS

Since it is much easier to forge a banknote with a similar visual characteristic as the original banknote than to produce a banknote with the identical chemical composition as the original, the FTIR spectroscopy is a great solution for genuine validation.

The FTIR spectra of samples were recorded in the ATR mode, as the method is suitable for determining the composition of organic binder materials, and in some respect the identification of pigments. Regarding the inorganic pigments, many of them have characteristic absorption bands in the mid-IR region, but at the same time there are many that either do not absorb in that region at all, or have absorptions that have their peaks at the low wave number end and are not characteristic enough [3]. The penetration depth (d_p) of the IR radiation into the sample depends on the wavelength (λ) of the IR radiation, the angle of the incidence of the radiation (θ), the refractive index of the ATR crystal (n_c) and the refractive index of the sample (n_s), Eq. (1):

$$d_p = \frac{\lambda}{2\pi} \cdot n_c \cdot \left[\sin^2\theta - \left(\frac{n_s}{n_c} \right)^2 \right]^{\frac{1}{2}}. \quad (1)$$

The FTIR spectra were recorded by the FTIR IRAffinity-21 spectrometer with the Specac Silver Gate Evolution as a single reflection ATR sampling accessory with the angle of incidence at 45° and a ZnSe flat crystal plate (index of refraction 2.4). A total of 15 cumulative scans were taken for each sample with the resolution of 4 cm^{-1} in the spectral range of 600÷3700 cm^{-1}.

Table 1 Currencies used in the study

Currency	Denomniation	Number of banknotes	Denomniation	Number of banknotes
Croatian kunas	50	7	20	5
US Dollars	100	1	1	1
Russian ruble	500	1	50	1
Indonesian rupiah	5000	1	1000	1
euro	50	1	10	1
Romanian leu	10	1	1	1

3 RESULTS

The results of the measurements are given in Figs. 1÷16. The spectra of the paper used for the printing of 50 kuna notes for all seven samples are shown in Fig. 1. The kuna banknotes are printed on a multicolour paper made of 100% cotton fibre [4]. Since the same spectra were obtained for the both of the examined denominations, 50 kunas and 20 kunas, only the spectra of 50 kuna notes will be given.

All seven spectra of the 50 kuna notes, regardless of their date of issue or their current condition, show almost an identical paper composition, which implies a great reproducibility within the same denomination notes. Same can be said for the spectra of the hologram within the same samples (Fig. 2). In the Fig. 1, a clear evidence of the cellulose substrate is given with the peaks from 1160÷998 cm^{-1} and at 898 cm^{-1}.

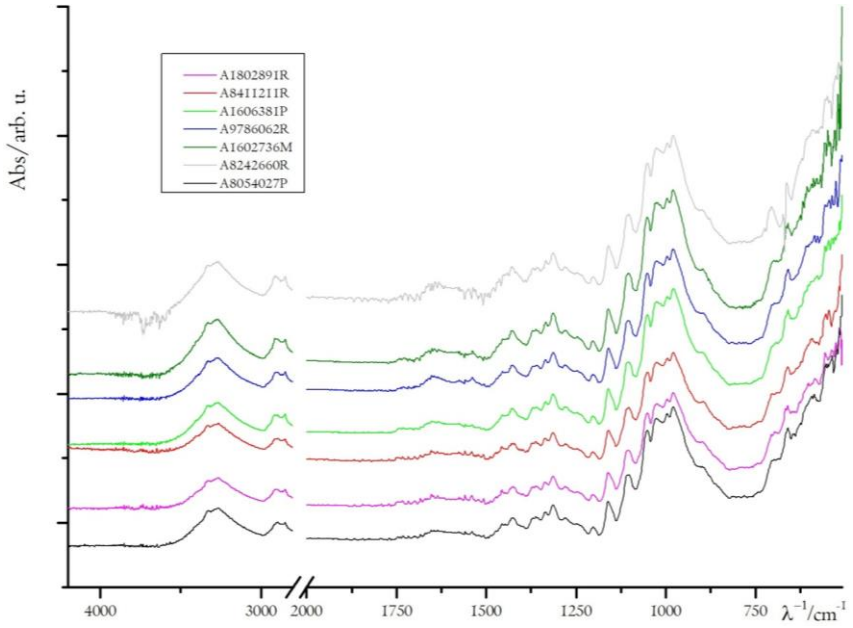

Figure 1 FTIR spectra of the paper used for the 50 kuna notes

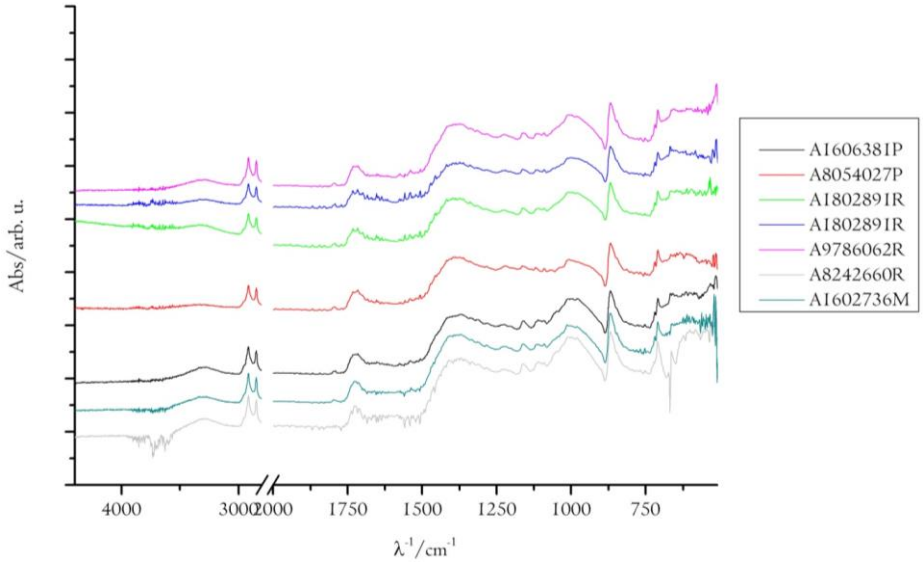

Figure 2 FTIR spectra of holograms printed on the 50 kuna notes

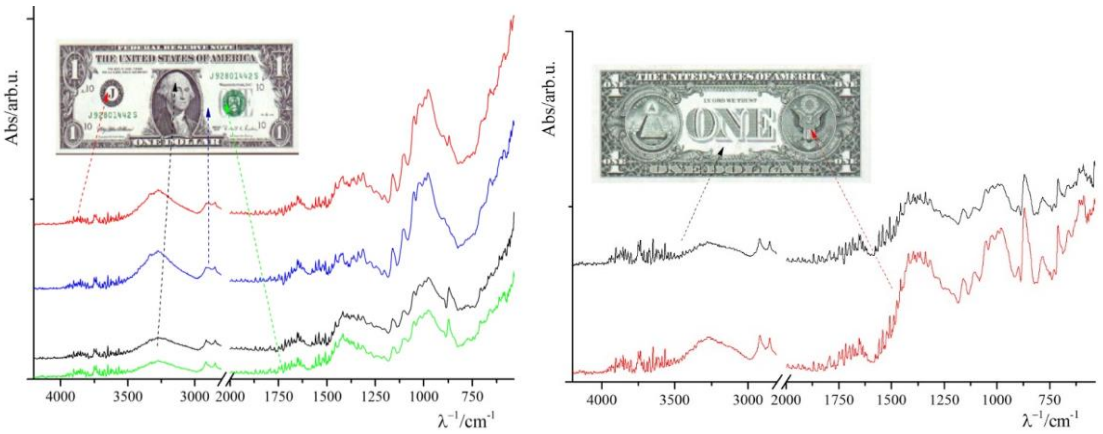

Figure 3 FTIR spectra of a one dollar note: front side (left) and back side (right)

The FTIR spectra of a one dollar note (Fig. 3) again shows the characteristic peaks of the cellulose substrate with the peaks from 1160÷998 cm^{-1} and at 898 cm^{-1}, and additionally, the spectra of the treasury seal and the portrait of George Washington show an extra band at 870 cm^{-1} which can be attributed to $CaCO_3$ responsible for the relief appearance. The intensity of the cellulose peaks is influenced by the composition of the paper, which is 25% linen and 75% cotton. The spectra from the backside show the same peaks, with different intensities.

The backside of the 100 dollar note (Fig. 4) again confirms the equality, while the front side gives different spectra for the characteristic areas (Fig. 4), the 3D security ribbon includes strong absorption peaks at 1700, 1280, 825 and 750 cm^{-1}, the treasury seal and the Benjamin Franklin portrait spectra show the additional peak characteristic of $CaCO_3$ connected with the raised printing, while the federal reserve seal, watermark and the suptrat itself show the characteristic cellullose bands mentioned already.

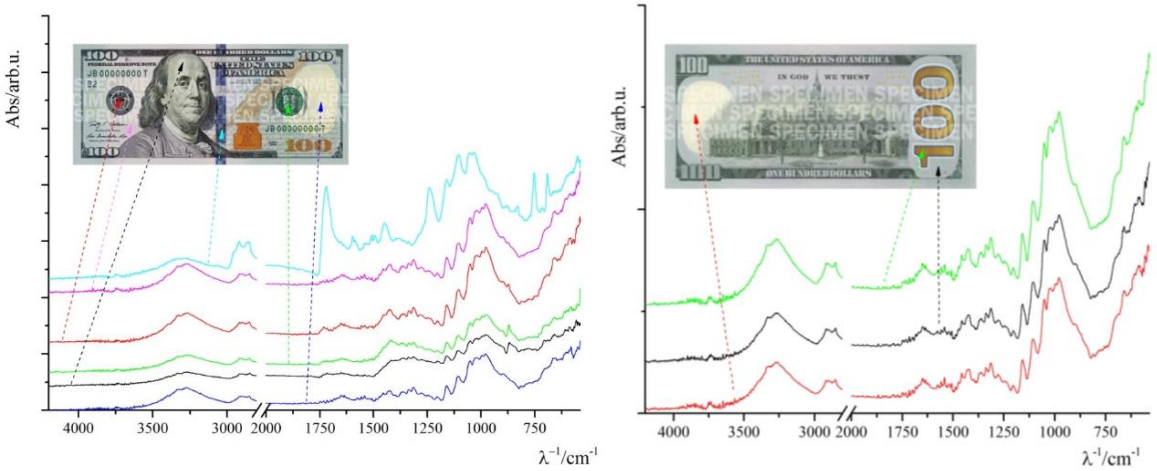

Figure 4 FTIR spectra of a 100 dollar note: front side (left) and back side (right)

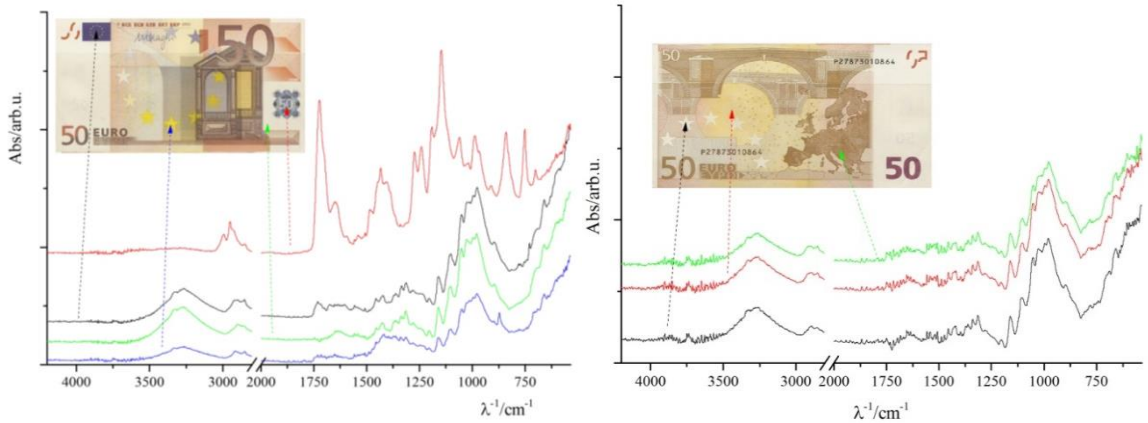

Figure 5 FTIR spectra of a 50 euro note: front side (left) and back side (right)

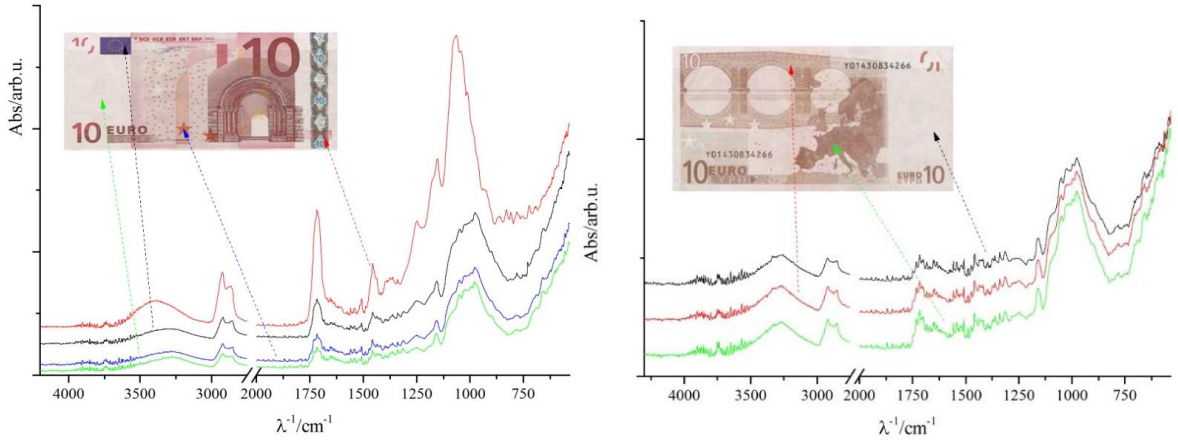

Figure 6 FTIR spectra of a 10 euro note: front side (left) and back side (right)

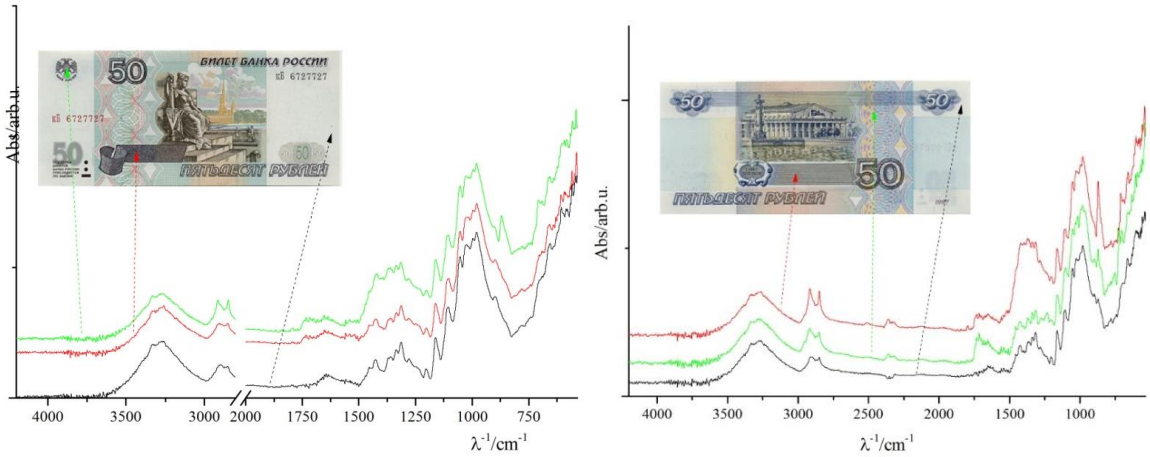

Figure 7 FTIR spectra of a 50 ruble note: front side (left) and back side (right)

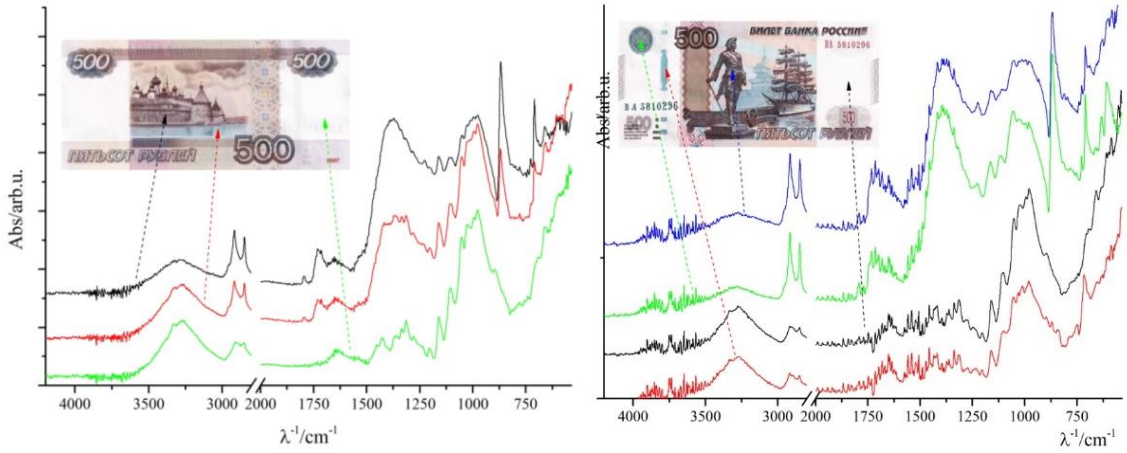

Figure 8 FTIR spectra of a 500 ruble note: front side (left) and back side (right)

Euro banknotes are made of 100% cotton fibre, so their spectra is similar to the Croatian kuna banknotes. The hologram spectra of a 50 euro note includes characteristic peaks at 1725, 1645, 1434, 1271, 1242, 1186, 1146, 1067, 991, 838, 757 cm^{-1}, which are characteristic to the plastic film that covers the hologram. The hologram spectra of a 10 euro note (Fig. 6) includes a lower number of peaks than in the spectra obtained in the 50 euro note; the characteristic peaks are at 1725, 1434, 1271, 1242, 1186 and 1146 cm^{-1}.

The difference might arise in the origin of the banknotes, since a 50 euro note was made in Germany, while the 10 euro note was made in Spain. From Fig. 5 it is clear that the spectra from the back side of the 50 euro banknote show an identical compposition, regardless of the position from which the spectra was obtained. The same thing can also be said for the back side of a 10 euro note (Fig. 6).

The 50 and 500 ruble banknotes are printed on high quality cotton paper (50 ruble notes on light-blue paper, and 500 ruble notes on light purple paper) (Fig. 7 and Fig. 8).

The Romanian leu notes are unlike most other currencies which are cotton based; they are made of composed polymer. One leu note (Fig. 9) can be identified by its spectra with characteristic peaks at 1050, 1130, 1250, 1600÷1500 and 1700 cm^{-1}. The spectra are the same from both sides with the exception of an eagle shaped window, and an extra peak at 890 cm^{-1} in the spectra of the monastery at the backside.

The transparent window of a 10 leu note (Fig. 10) has the same spectra as the transparent window of one leu note.

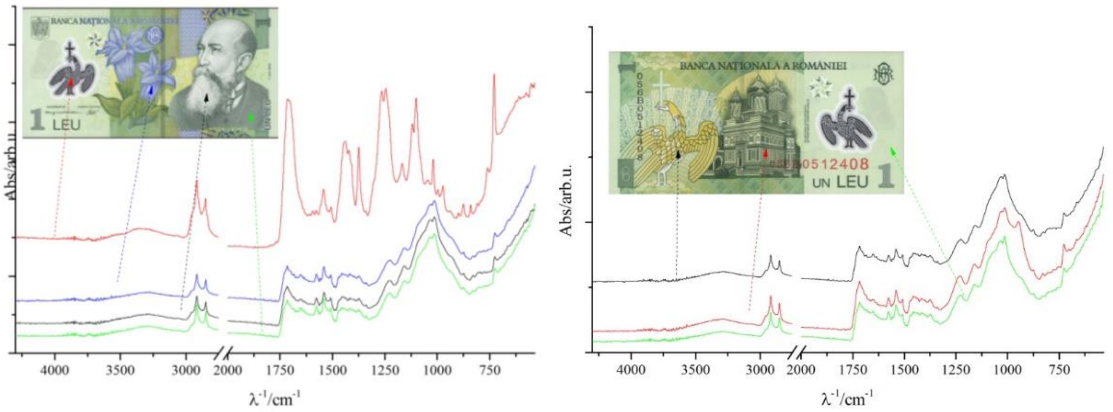

Figure 9 FTIR spectra of a one leu note: front side (left) and back side (right)

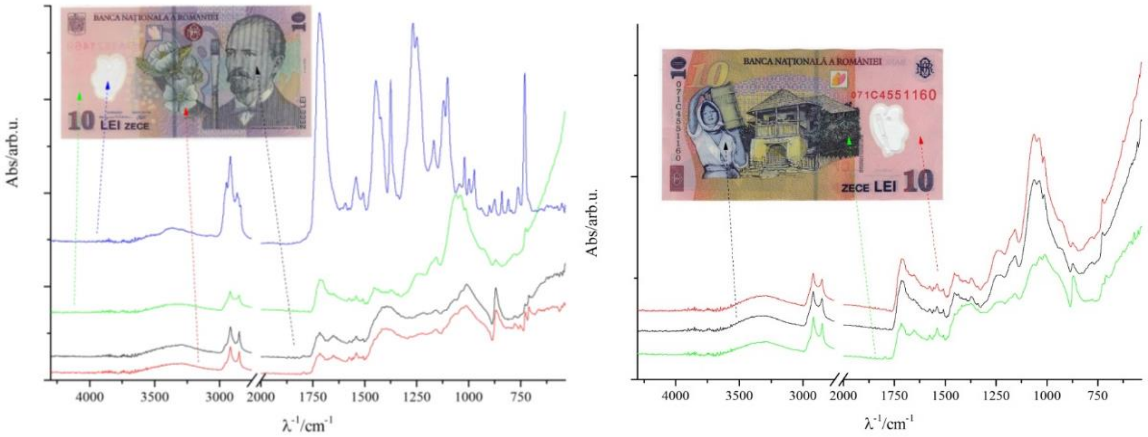

Figure 10 FTIR spectra of a 10 leu note: front side (left) and back side (right)

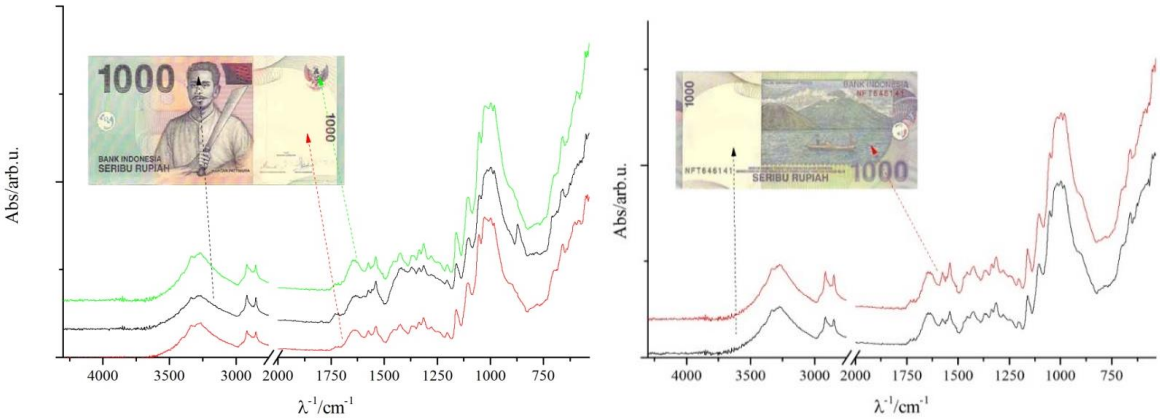

Figure 11 FTIR spectra of a 1000 rupiah note: front side (left) and back side (right)

Indonesian rupiahs are made of long fibers from any kind of wood, or a mix of different types of wood, with the abacá fiber used as a preferable material. The cellulose based material (Fig. 11) is confirmed with the peaks in the region from 1160÷998 cm^{-1}, again with the clear evidence of $CaCO_3$ at 877cm^{-1} associated with the relief elements. The same reasoning and conclusion can be applied while analysing the 5000 rupiah note (Fig. 12).

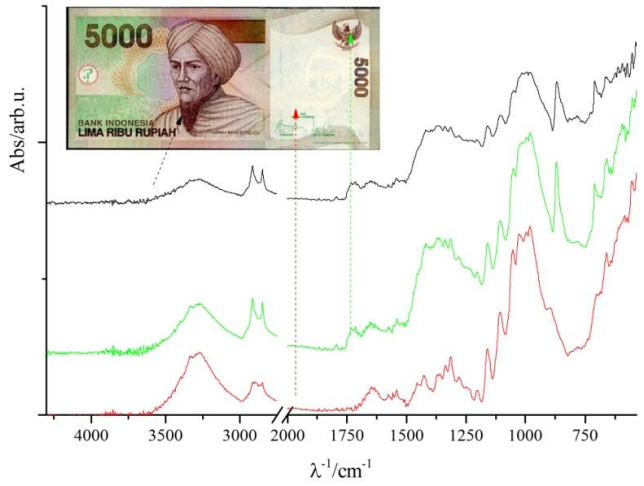

Figure 12 FTIR spectra of a 5000 rupiah note (front side)

4 CONCLUSION

Our measurements confirmed that the production of banknotes, and especially inks, varies from country to country, which is clearly seen in the obtained FTIR spectra.

The spectra consistency was confirmed within the same denomination of the currency, regardless of the condition of the banknote itself.

Since the high quality forged notes can possess fluorescent inks, holograms and metal strips, the process of identifying counterfeit notes is becoming extremely challenging. Once the FTIR spectra of the genuine notes are obtained, it is quite easy, even for a non-scientist, to compare the main peaks of the forged and genuine banknotes. It also allows us to group fake notes according to the similarities of their spectra, which is beneficial in the process of investigating their origin.

With an increase in the measuring of different areas of banknotes, what is obtained is a larger data set which then results in a higher probability of discrimining between the original banknote and a counterfeit note.

Note: This research was presented at the International Conference MATRIB 2017 (29 June - 2 July 2017, Vela Luka, Croatia).

5 REFERENCES

[1] European Central Bank News Release, 10 January 2013 - Biannual information on euro banknote counterfeiting
[2] https://www.hnb.hr/documents/20182/855655/e-statistika-krivotvorina1-6-2016.pdf/0a5fccf0-e766-4086-80c5-352625ee53f9 (Accesed on 1 June 2017).
[3] Willis, H. A.; van der Maas, J. H.; Miller, R. G. J.: Laboratory Methods in Vibrational Spectroscopy, London: John Wiley and Sons, 1987.
[4] http://old.hnb.hr/novcan/eobljnov.htm (Accesed on 1 June 2017).

Authors' contacts:

Katarina ITRIĆ
University of Zagreb, Faculty of Graphic Arts,
Getaldićeva 2, 10000 Zagreb, Croatia
katarina.itric@grf.hr

Damir MODRIĆ
University of Zagreb, Faculty of Graphic Arts,
Getaldićeva 2, 10000 Zagreb, Croatia

ISSN 1846-6168 (Print), ISSN 1848-5588 (Online)
ID: TG-20170328162304

Original scientific paper

COST OPTIMIZATION AND WORK QUALITY IMPROVEMENT OF SMALL AND MEDIUM ENTERPRISES IN SERVICE ACTIVITIES BY USING A WEB APPLICATION

Bruno JAMAN, Dominika CRNJAC MILIĆ, Krešimir NENADIĆ

Abstract: The aim of this paper is the development of a web application for ordering in the service sector of small and medium enterprises with the purpose of optimizing the opportunity costs. A special focus is placed on the amount of services rendered, which increases with the minimization of cancelled orders that are not timely replaced with new ones, but also on the quality control of the performed services that reflects on the motivation of employees or their replacement with new ones in order to improve the business. The following web technologies were used while developing the web application: HTML, CSS, JavaScript, PHP and MySQL. An insight into the technologies used to create web applications is given and some of the basic concepts used in the web application are explained. The paper describes the functionality and design of the web application. The analysis of cost effectiveness through managerial control, management systems, digitization of businesses and employees evaluation is given. The functionality of this web application is aimed at small and medium enterprises engaged in the service industry.

Keywords: database; digitization of business; service sector; small and medium business enterprises; web application

1 INTRODUCTION

The idea to write this article derived from the hypothesis that there is a need for more control and evaluation of employees of small and medium enterprises (SME) in the service sector in order to achieve competitiveness in the increasingly complex market competition in a time of economic crisis. Furthermore, another reason lies behind the fact that the ICT technologies can be of great importance without the company management having to make significant investments. As a result of the research and writing a master's degree thesis, a web application was designed in order to allow the persons in charge of controlling the employees to quickly and easily, without any particular knowledge of ICT, perform the function of controlling the operation of the company, employee evaluation and quality control of the performed work, which today are some of the factors that the survival of SMEs depends on.

The main function of a web application is to optimize time and resources in the work of employees in order to reduce the opportunity costs, i.e. the missed revenue resulting from poor employees operating the time distribution system and services that are provided with a certain quality.

The main goal is to minimize the number of cancelled orders by reminding users of their appointments, but also by offering an alternative service operator within the same enterprise.

On the technical side, the challenge is the database structure that will contain information about the contracted period in which the job should be performed, customers, employees and their working schedule, and a system that will manage the data and distribution of the upcoming requirements (events).

1.1 Technologies used to develop a web application

HyperText Markup Language (HTML) is the base in developing web applications [1]. HTML is not a programming language but a descriptive language used to organize webpage content. The web browser communicates with the web service and receives content as a list of elements to be presented to the user. The presentation of elements is organized by using CSS.

Cascading Style Sheets (CSS) is a descriptive language used to influence the presentation of the HTML elements [2]. It can be used to define different rules for a different kind of HTML document elements, such as: text and background colours, background images, fonts, text presentation and many more rules. The advantage of CSS is that it can be written in a separate file and then applied to any HTML document. This results in the reusability of the CSS code for any target HTML document. CSS can also be used to format the design of an HTML file depending on the type of the medium where the content is displayed [3].

PHP: Hypertext PreProcessor (PHP) is an object-oriented script language used to write the server script code. Such a code is executed on the server side and the result is shown on the client side (web browser). It was designed by Rasmus Lerdorf and the first version was published in 1995. The use of PHP scripts results in dynamic webpages. Server script can generate some output that depends on the user input from the forms in web documents [4]. PHP scripts in this paper are used for database communication and management.

In order to use database functionality, a database management system service, in this case the Relational Database Management System (RDMS), has to be installed on the server. The most common and most widespread open source database system is MySQL (*My Structured Query Language*), developed by Oracle. A database is a structured

set of data consisting of at least one table. The MySQL databases usually consist of more than one table [5].

The database is relational, which means that there are some rules for relations and interactions between the tables. The data from one table can point to some data in the other table (one-to-one relation) or they can point to several different data in more than one table (one-to-many relation). In the database designing process, the rules and data types that are in certain columns of the tables are created in order to allow the writing of only the defined data types in the tables. The database is well-designed if the database structure and rules are well-defined by the designer (programmer). The number of columns in a table is limited to 4096 and the row size to 65535 bytes [6].

In addition to HTML and CSS, JavaScript is one of the three key technologies of the client side Internet programming. It is used in the vast majority of webpages and is supported in all web browsers. It first appeared in 1995 as the Netscape Navigator browser functionality. Although it is named like Java, the two languages are quite different in their functionality. JavaScript provides additional dynamic functionality for webpages. The JavaScript library jQuery was used to facilitate the webpage functionality development. JavaScript has access to all objects that are part of the document and it thus enables an easy access to all parts of the document.

XAMPP (eXtensible Apache MariaDB/MySQL PHP Perl) is an open source, multiplatform application developed by Apache Friends. It consists of the Apache web server emulator and PHP, Perl and MySQL (or MariaDB in the newer versions) modules [7]. It is used as a server emulator to test the server side functionality of the developed web application.

1.2 Goals of the developed system

The system was developed to meet several goals. It has to be applicable to the service sector of the SMEs and it has to be easy to use without much knowledge or additional training in the field of ICT. In addition to that, the system has to be easily adaptable to various service activities. The result should be a system ready for use in companies engaged in the service sector with the potentially minimal changes with respect to the type of services provided to customers. In order to achieve this, it was necessary to include a content management system in the application.

2 APPLICATION FUNCTIONALITY

The application functionally is divided into two parts. One part of the application is available to the customers and the other part is available to the administrator, but also to the employees if the company wants it so. The access to the client part or the administrator part of the system is determined by the value of *authority* variable from the database table *'users'* for every single user.

The administrator has the privilege to change the type of services, add or delete employees and to make any changes to the system. By performing such modifications, changes are instantly visible throughout the whole system.

Before one can use the system, it is necessary to register and create a user profile. After the registration is completed, the customer can log into the system and choose one of the two tasks: to schedule a new appointment or to browse through the existing appointments.

A new schedule for the client is requested through an interactive web form. The client first chooses the type of the required service and after that, all available employees that support the required service are dynamically added to the form so the client can choose one of the available employees. The next feature that the client has to choose is one of the available dates for the requested employee and service. As the last part of scheduling appointment, the client has to confirm the requested service, employee and date by clicking on the confirm button. The client also has the ability to browse through the requested appointments and cancel them through the web form.

There is an administrator panel accessible only to the users with administrator privileges. The administrator panel consists of features used to manage the employees and their working hours, but it also gives an insight into the analysis and statistics of the provided services and employees who perform those services. The emphasis is placed on the simplicity and intuitiveness of the administrator's part of the web application so that no additional training concerning ICT is necessary to manage the application or to adapt the application performance to the needs of the company. The only skill necessary to work with the web application administrative panel is the basic knowledge needed to work on a computer and the knowledge of the use of the Internet (web browser).

One of the features is to manage the activities (services). Along with the overview of activities, it is possible to delete an existing activity or change the previously given service price. It is possible to add a new service and to set its price.

The employees' management gives insight into the total number of employees, their scheduled appointments, service management supported by the current employees, deleting employees and scheduling the employees' working shifts. Adding new employees to the services that they are trained to provide is available through the administrator panel. It is available to mark a scheduled appointment as finished (held) and finished appointments are not listed in the scheduled appointments overview, but they are kept in the database in order to keep track of all the finished appointments when analysing the employees and services.

The timetable provides insight into the free and reserved employees' periods of time for the selected month.

The last administrator panel feature is the display of statistics for the individual or overall staff and for the service analysis. The displayed information include the total number of scheduled appointments for a specific service or employee along with the total income realized from one or all services of one or all employees together.

2.1 Application and database structure

Bootstrap was used to design the application's layout with some modifications in the CSS files. Web application content (HTML code) is dynamically generated by using PHP, JavaScript (jQuery) and data from the database. Any change in the employees' data, services or working hours by the administrator is momentarily recorded in the database and used in code generation in the following requests for services.

Database operations are realized through PHP/MySQL and the majority of web forms are dynamically generated with the help of jQuery.

The MySQL database is the main and most complicated part of this web application. The database consists of five tables: users, employees, services, timetable and scheduled appointments.

The table *users* contains information about the registered users who use the provided services and other users of the application such as the administrator and employees. Each user is identified by the unique ID in the *users* table and other tables that reference any application user. The table *users* also contains the following information: e-mail, first name, last name, phone number, hashed password and user privileges.

The next table is called *employees*. It contains relevant information about the employees such as the ID, first name, last name and the most important list of supported services by the employee.

The table *activities* contains information about the provided services names and price for every provided service.

The table *dates* contains information about all scheduled appointments: date and time, the employee responsible for that appointment, the client that requested that appointment and information on whether the scheduled appointment is held.

Each employee has an individual table that contains the working dates and times for the whole year. This table contains records for the holidays, free days, working shifts layouts and vacation day layouts.

2.2 Advantages and disadvantages of the application

The main advantage of this application is the very simple use of the administrator's panel and the application's adaptability to the company services requested by the clients. The processes of publishing a web application on the web server and setting up application parameters are performed in several minutes. In order to adjust the application's parameters to the company's needs, the administrator has to insert services that the company offers and add employees and services they support into the database. After the working hours for each employee are set, clients are able to schedule appointments for the supported services through an interactive web form. The first testing prototype of the web application was for consulting services, but possible varieties of the application can be for a car workshop, spa centre or any similar small enterprise. It is performed without any necessary programing skills and without changing the application's source code.

The application's main disadvantage is its realization to be universally applicable for companies that offer some services. Any other type of company or business would require a change in the application's source code. The first functional application's prototype does not have the notification functionality for the changes in the requested services scheduled terms or for the cancelling of services. This type of functionality could be achieved with sending e-mails or SMSs in the future web application's prototypes or versions.

3 APPLICATION'S PROFITABILITY

Today, the big entrepreneurs and enterprises are already expected to have the support of digital systems which help them in the business processes or even in the management of the whole enterprises. Such digital systems provide a large possibility for improvements and gaining an advantage over the competitors. Companies that partially or fully implement digital business solutions gain advantage over the companies that do not implement it. Information technologies require special training for employees and the return on invested capital is long-term and it is often difficult to accurately determine or predict it [8].

Consumers are used to web applications where they can get services or full access to the information they require in a matter of several mouse clicks, and they expect that the service industry and small enterprises already follow those trends. Consumers require Internet access services, an overview of the current and past activities and a possibility to change future services. If those expectations are not met on time, it opens up a space for someone to provide and take over a part or the entirety of a company's business. Digital systems that provide maximum profitability are the ones with intuitive management, full accessibility at any time and without errors. In addition to attracting a larger part of the market, this type of service gives companies better control over the activities and lowers the risk of the loss of opportunity cost due to an automatic management of appointments, and the consequence is that the company can offer more competitive prices.

Digitalization reduces the number of required documents in paper form, provides automatic determination of available free terms and their distribution, and it also accelerates the overall company performance.

Efficient use of the digitalization of business processes is reflected in the reduction of the manual data entry on paper, information is concentrated in one place and thus, there is a much better understanding of business costs and risks. Obtaining various pieces of information and statistics at the right time allows managers and company owners to get insight into the problems before it is too late and it gives them the possibility to correct the errors and guide their business towards the desired path. It is very difficult for large companies to reverse engineering and digitalize all their processes, which is why company management often

decides to completely change their processes by adapting them to digitalization. For small and medium-sized enterprises, this does not happen even though they have other problems related to the digitalization process.

In the example of a small company with the aim of reducing the opportunity cost when ordering and bringing closer its activities to as many consumers as possible, digitalization will open up new possibilities and provide numerous advantages. The automated scheduling of terms eliminates any opportunity for human error in booking, and at the same time it gives user the access to the agreed terms and any changes related to them. Scheduling the terms of services over the Internet is provided in the negligible trade service industry, and it is a safe way of getting a large number of new users. User access and the convergence of its work to a computer or mobile phone is a trend, and certainly will be the default way of doing business in the future of these companies.

In addition to the advantages in terms of getting new customers and a better business in this way, the digital system opens up numerous opportunities for the employees, management and owners of companies. Access to information in one place opens up opportunities for an easier evaluation of employees and jobs that the company deals with for the manager; and for employees, that insight builds confidence in the integrity and objectivity of such an evaluation. With the help of the obtained information, the employer may terminate activities that are visibly unprofitable or unused. An examination of the work of employees can result in moving employees to positions that suit them better or referring them to a better education about the activities they are weaker in.

In practice, SMEs in commercial establishments mostly have web shops (e.g. *zelda.hr*), but such systems do not have the application or the managerial control similar to the introduced system. The digitalization of systems that offer some services is very rare and it usually comes down to one web form that the company provides to see if there is any interest from the client side for the services, but all further scheduling of appointments is performed orally.

3.1 Application applicability in management control

Henry Fayol was among the first to define management control as something that consists of the monitoring of the overall performance according to the agreed plan, given commands and agreed principles to draw attention to errors in order to correct them and prevent their recurrence. The philosophy and application of managerial control were subjected to a constant and critical analysis [9]. Another definition of management control is that it is the process by which managers influence other members of the organization to implement the strategy of the organization [10].

The systems for management control are defined as systems that include mainly the accounting area of control and planning, the monitoring of activities, performance measurement and separate management control of the strategic and operating control. Such systems are described more as a process of influencing behaviour. Systems for management control also represent a way to achieve the collective cooperation of individuals or organizational units that may not completely share their goals, but use this cooperation for their progress toward specific organizational goals [11].

The possibility of using these applications as a tool to aid management control allows access to information in one place. What we can get from the application is useful information on activities such as the frequency of the used services and the income rendered from those services. If the service is very rarely used, it is probably a good move to stop providing the service or to reduce the price of that service if the manager chooses to make such a decision. If they notice that the service has a sufficient number of terms but is still not profitable, the price of this service should be increased.

Apart from the information about services, this application can provide information about the work of employees. An overview of the services provided, the number of terms of services they have done and their income could be provided. From that information we can draw conclusions that are useful for management employees and their evaluation. Employees who provide certain services may be further educated in the field related to the provision of those services to clients, all in order to provide them to do their work the best they can or to give the employee some other task to do if he or she is better at it. If a certain service is used only once or twice, it might be a problem for an employee who provides it, and the customers will not come back to schedule new terms. If one of the services is very often used, but all clients choose the same employee to provide the service, it would be good to explore the mode of that employee and try to teach other employees to work in the same or similar manner. Some services could have a very large number of wanted terms and only a few employees with the expertise needed to provide this service, and the logical step would then be to educate current employees or recruit new experts to provide customers with those services. All of those changes would be easily incorporated into the system of the application considering its dynamic generation.

From these examples it is clear that this application can serve as a tool for management control, as part of the management control systems or the systems for the evaluation of employees.

4 CONCLUSION

This paper points to the functionality of the system for ordering in the service sector of small and medium enterprises which use ICT technology in the form of an application whose design is composed in a very simple way so that the person with the basic knowledge in the use of computers and the Internet can adapt the application to the needs of his/hers business.

The results of the paper can be easily implemented in practice, in the daily work of small and medium enterprises engaged in the service industry because the application is

easy to use and there is no need for any additional education of users. The aim is to organize work and make the application a part of the management control systems, evaluation and worker motivation.

The proposal for further research and work in this direction is to improve the system by issuing Internet accounts or to enable the use of the system by giving the customers via an SMS and e-mail the necessary information related to the requested service.

5 REFERENCES

[1] Flanegan, D.: JavaScript - The definitive guide (6th ed.), O'Reilly Media, 2011.
[2] Pouncey, I.; York, R.: Beginning CSS: Cascading Style Sheets for Web Design, Wiley / Wrox, 2011.
[3] http://www.w3schools.com/css/css_intro.asp (Accessed: 1 December 2016)
[4] Nixon, R.: Learning PHP, MySQL, JavaScript, CSS & HTML5, Third Edition, O'Reilly Media, 2014.
[5] www.mysql.com, MySQL 5.7 Reference Manual, What is MySQL? (Accessed: 1 December 2016)
[6] www.mysql.com - C.10.4 Limits on Table Column Count and Row Size – reference manual (Accessed: 1.12.2016)
[7] https://www.apachefriends.org/about.html (Accessed: 1.12.2016)
[8] Salo, J.; Alajoutsijarvi, K.; Karjaluoto, H.: Digitalization and the Changing Structure of Business Networks, University of Oulu, 2003.
[9] Fayol, H.: General and Industrial Management, Pitman Publishing, New York, 1949.
[10] Newton, A. R.: The Management Control Function, Harvard Business School Press, Boston, 1970.
[11] Langfield-Smith, K.: Management Control Systems and Strategy: A Critical Review, Monash University, Australia, 1997.

Authors' contacts:

Dominika CRNJAC MILIĆ, Associate Professor
Josip Juraj Strossmayer University of Osijek
Faculty of Electrical Engineering, Computer Science and Information Technology Osijek
Kneza Trpimira 2B, 31000 Osijek, Croatia
+385 31 224 681 / dominika.crnjac@etfos.hr

Krešimir NENADIĆ, Associate Professor
Josip Juraj Strossmayer University of Osijek
Faculty of Electrical Engineering, Computer Science and Information Technology Osijek
Kneza Trpimira 2B, 31000 Osijek, Croatia
+385 31 495 429 / kresimir.nenadic@etfos.hr

APPENDIX

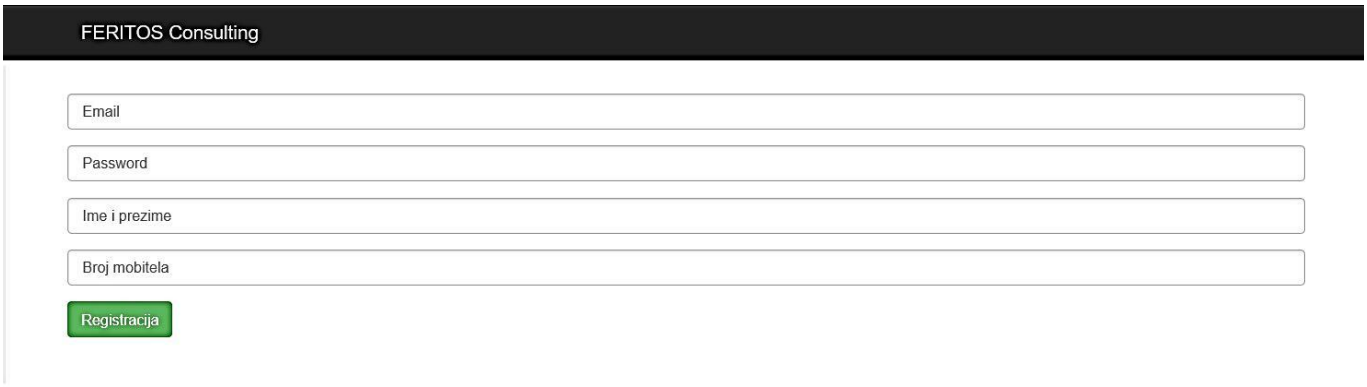

a) Registration form

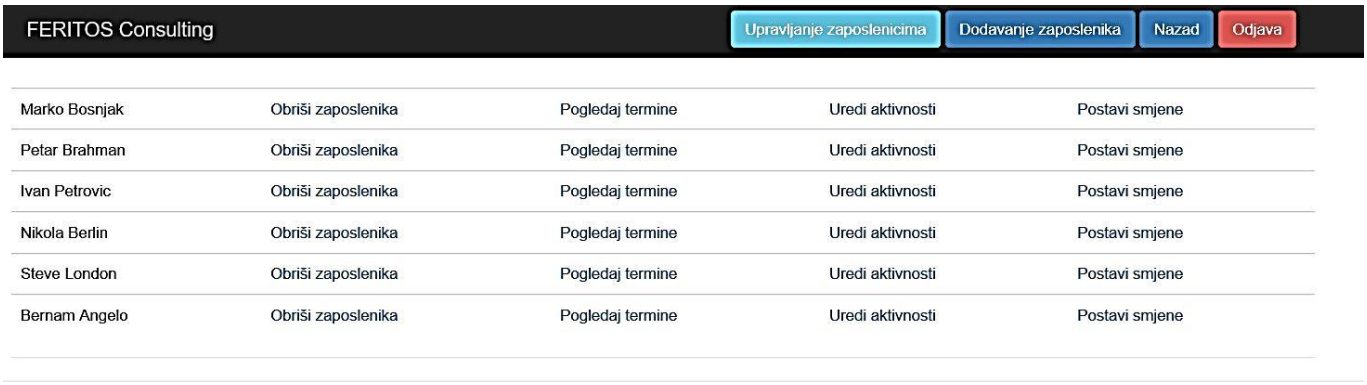

b) Employee management

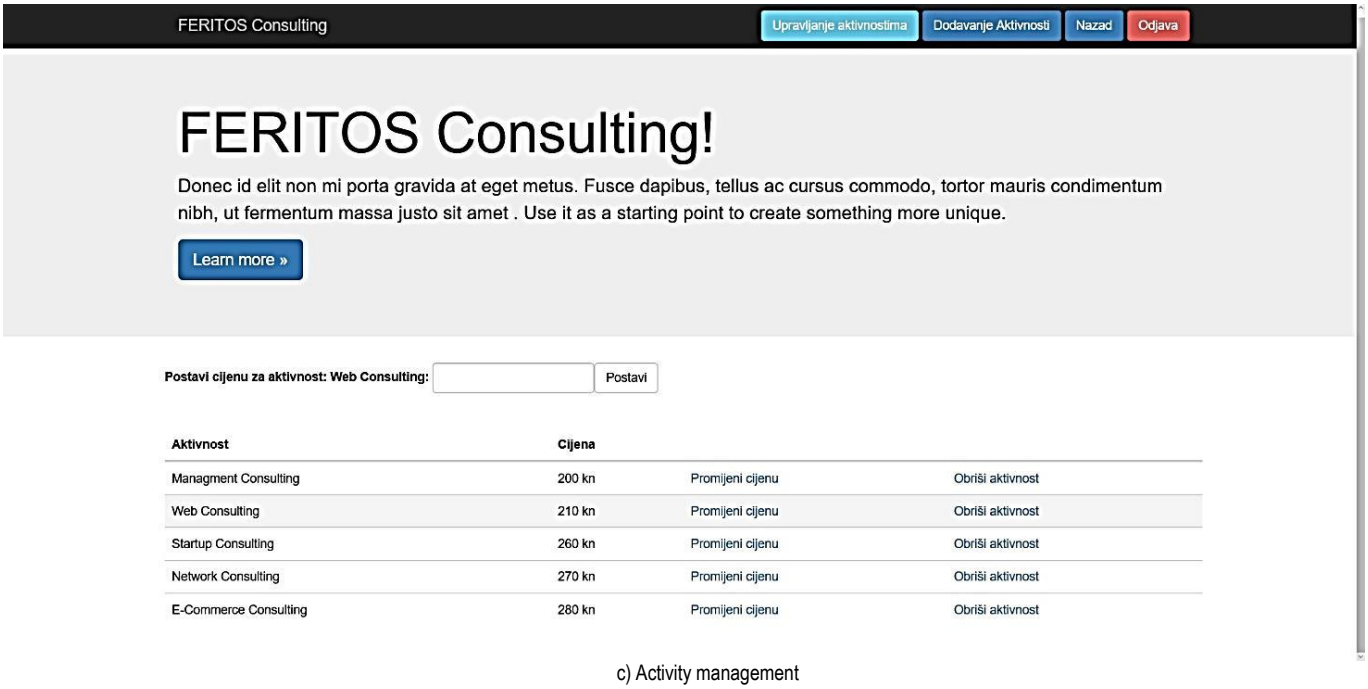

c) Activity management

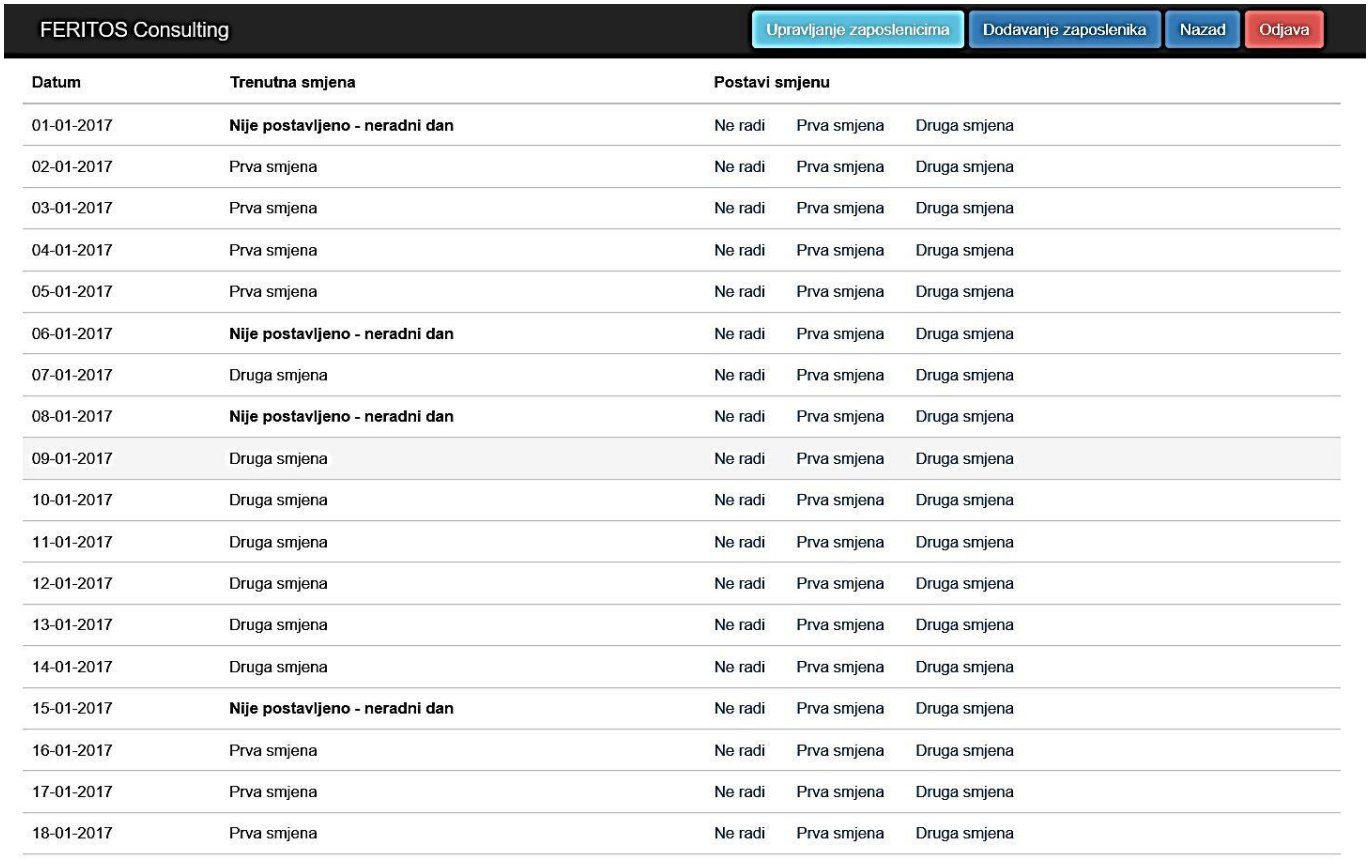

Datum	Trenutna smjena	Postavi smjenu		
01-01-2017	**Nije postavljeno - neradni dan**	Ne radi	Prva smjena	Druga smjena
02-01-2017	Prva smjena	Ne radi	Prva smjena	Druga smjena
03-01-2017	Prva smjena	Ne radi	Prva smjena	Druga smjena
04-01-2017	Prva smjena	Ne radi	Prva smjena	Druga smjena
05-01-2017	Prva smjena	Ne radi	Prva smjena	Druga smjena
06-01-2017	**Nije postavljeno - neradni dan**	Ne radi	Prva smjena	Druga smjena
07-01-2017	Druga smjena	Ne radi	Prva smjena	Druga smjena
08-01-2017	**Nije postavljeno - neradni dan**	Ne radi	Prva smjena	Druga smjena
09-01-2017	Druga smjena	Ne radi	Prva smjena	Druga smjena
10-01-2017	Druga smjena	Ne radi	Prva smjena	Druga smjena
11-01-2017	Druga smjena	Ne radi	Prva smjena	Druga smjena
12-01-2017	Druga smjena	Ne radi	Prva smjena	Druga smjena
13-01-2017	Druga smjena	Ne radi	Prva smjena	Druga smjena
14-01-2017	Druga smjena	Ne radi	Prva smjena	Druga smjena
15-01-2017	**Nije postavljeno - neradni dan**	Ne radi	Prva smjena	Druga smjena
16-01-2017	Prva smjena	Ne radi	Prva smjena	Druga smjena
17-01-2017	Prva smjena	Ne radi	Prva smjena	Druga smjena
18-01-2017	Prva smjena	Ne radi	Prva smjena	Druga smjena

d) Work shift management

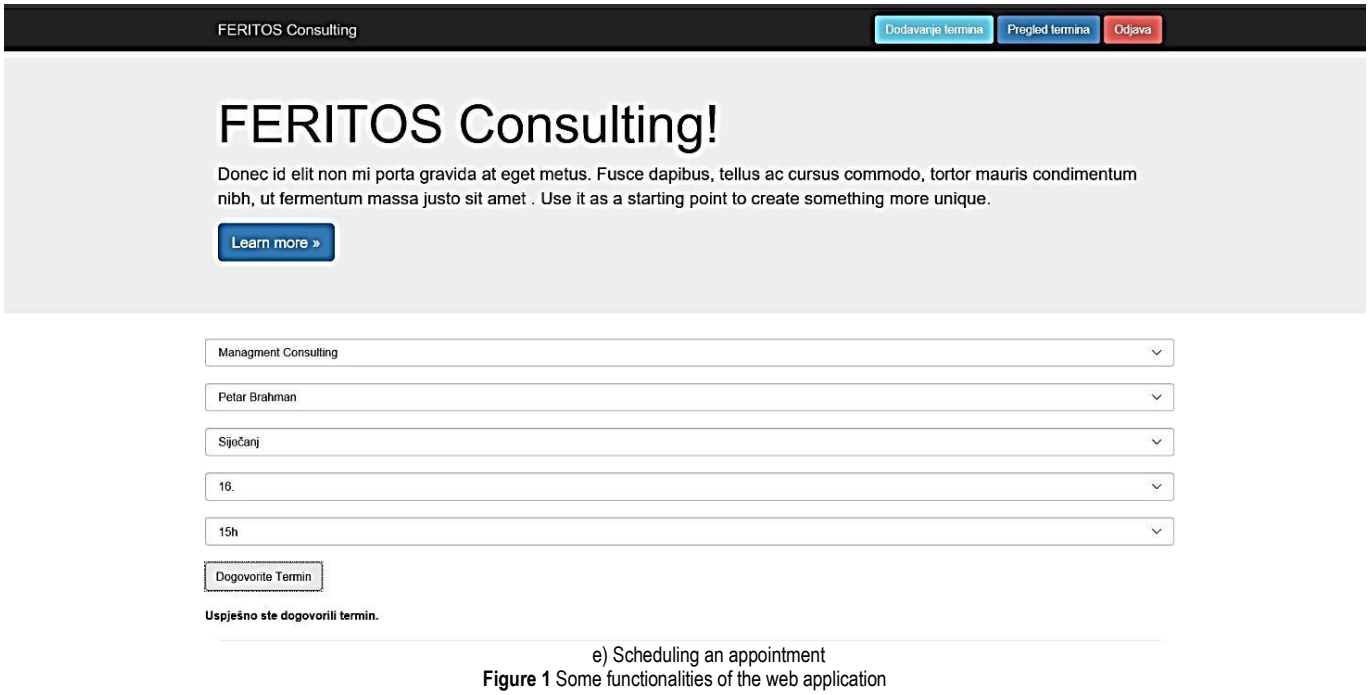

e) Scheduling an appointment

Figure 1 Some functionalities of the web application

ISSN 1846-6168 (Print), ISSN 1848-5588 (Online)
ID: TG-20170816134819

Original scientific paper

INFLUENCE OF SI/AL RATIOS ON THE PROPERTIES OF COPPER BEARING ZEOLITES WITH DIFFERENT FRAMEWORK TYPES

Karolina MADUNA, Narendra KUMAR, Dmitry Yu. MURZIN

Abstract: Several copper containing zeolite based catalysts with different initial Si/Al and different zeolite support (types MCM-22, FAU, BETA) were synthesized or prepared from commercial precursors in a powdered and pelleted form via a direct hydrothermal synthesis and ion exchange method, and then subsequently characterized for the evaluation of their chemical, surface and catalytic properties. The characterization of the zeolites, which included the analysis of their morphological and acid-base properties, was performed by using various techniques such as the N2 physisorption, Pyridine-FTIR, XRD, SEM-EDAX and TEM. The activity and stability of the prepared catalysts were tested in the catalytic screening in a catalytic wet peroxide oxidation of the model polyphenolic wastewater. The obtained results provided an insight into the cause-and-effect relationship between the silica to alumina ratio and its direct effect on the acidity and basicity of the prepared zeolites, as well as the indirect one on their morphology, textural and surface properties of both the parent zeolite and active metal component. The use of active catalysts resulted in successfully operating the process under mild conditions with low energy consumption. It was found that the copper and iron containing catalysts showed promising activity, while the stability of the active metal component still is and remains a challenge to obtain.

Keywords: acidity; catalytic wet peroxide oxidation; morphology; phenolic wastewater; surface properties; transition metals; zeolites

1 INTRODUCTION

Zeolitic metal aluminosilicate solids are successfully used as catalysts in many industrial fine and bulk chemicals processes such as pharmaceuticals manufacture, petroleum refining and basic petrochemistry due to their microporous three-dimensional framework structures and high activity coupled with good stability [1, 2]. Apart from their proven applicability in manufacturing and processing, zeolites have also shown a potential for use in a variety of other fields. One such area, wastewater treatment, strongly gains in importance due to the contemporary environmental concerns and the growing need for a high quality freshwater supply. The potential application of metal modified zeolites as catalysts in wastewater treatment processes such as advanced oxidation (AOP) and catalytic wet oxidation (CWO) has been vastly studied in the past decades. Such studies are only intensifying with the discovery of new zeolitic structures [3-6].

Among them, large pore zeolites such as FAU, BETA or MCM-22 have peeked interest for the use in the processes that deal with large organic molecules that can be found in environmental catalysis and applications such as the CWPO of organic compounds. Although the reports on the catalytic properties of zeolite and zeolite based catalysts in the CWPO of the industrial olive oil mill effluents are scarce [7-9], there are numerous studies of the model OOMW wastewater or single compounds aqueous solutions. As it was reported by Liotta et al. [5], transition metal exchanged (mostly iron and copper) zeolites of the FAU or MFI morphology exhibit promising results. However, there are still some open issues in connection to their stability such as resistance to the leaching of the active metal during the reaction. The leaching of the active metal components from redox molecular sieves catalysts in the liquid phase oxidation catalysis is considered to be the consequence of the strong complexing and solvolytic properties of oxidants (e.g. H_2O_2) and/or products (e.g. H_2O, ROH, RCO_2H). This leads to the deactivation and secondary contamination of the effluent both undesirable from the economic and ecological point of view. To have a utility on an industrial scale, the heterogeneous catalyst should be very robust with no or negligible leaching of the active components, therefore turning the focus in the catalyst development for the use in the CWPO on not only active but also stable catalysts, is a necessity.

Additionally, apart from a few recent reports [10, 11], most of the studies in the field are concentrating on the examination of the catalytic properties of the powdered catalysts for which mass transfer limitations can be neglected. However, in order to move from a laboratory scale to the development of a commercial CWPO process, more detailed studies with the pelletized or beaded catalysts should be conducted. In this case, mass transfer and diffusion processes in the boundary layer surrounding the catalyst pellet and in the pores of the catalyst, with the latter being more probable, should be considered.

Therefore, in the current research study, several zeolite based catalysts with different initial Si/Al ratios containing copper as an active metal component and different zeolite support (types MCM-22, FAU, BETA) were synthesized or prepared from commercial precoursors in a powdered and pelleted form via direct hydrothermal synthesis and ion exchange method, and then subsequently characterized for an evaluation of their chemical, surface and catalytic properties.

2 MATERIALS AND METHODS

2.1 Zeolite preparation

In the first two cases, a series of proton forms of Na-BETA and Na-MCM-22 zeolites with varying Si/Al ratios were prepared by means of the thermal treatment of the ammonium form of commercial zeolite (BETA, Si/Al of 25,

150 and 300) and direct hydrothermal synthesis (MCM-22, Si/Al of 30, 50 and 100) according to the previously described procedures [12, 13]. The copper bearing zeolite based catalysts were prepared by means of ion exchange from metal salt aqueous solutions in order to obtain a low loading/high dispersion of copper over the parent zeolite. In the third case, a commercial pelleted zeolite catalyst of the FAU type (13X, pellet size ~0.63 mm) with high aluminium content (Si/Al ratio of 2.6) was used as a support during the preparation of the copper bearing 13X catalyst by using the same method of incorporation of the active metal cation incorporation: ion exchange.

2.2 Characterization methods

The textural characterization of the catalysts was performed by nitrogen physisorption at 77 K by using the Sorptomatic 1900 Carlo Erba instrument. Prior to the measurements, the samples were outgassed at 423 K for 3 h at a reduced pressure below 0.1 mbar. The specific surface area and pore volume calculations were performed by using the Dubinin's equation for microporous and the B.E.T. equation for mesoporous samples. The pore size distributions were acquired by using the Horvath-Kawazoe method.

The strength of the Brønsted and Lewis acid sites of the catalysts was measured with infrared spectroscopy (ATI Mattson FTIR) by using the pellet technique working in the range of wavenumbers of 4000–400 cm^{-1} with pyridine as a probe molecule [14]. The temperature programed desorption of pyridine was conducted by evacuation at three different temperatures (523, 623 and 723 K) to obtain a distribution of acid site strength. The spectral bands at 1545 and 1540 cm-1 were used for the identification and quantification of the Brønsted (BAS) and Lewis (LAS) acid sites by using the corresponding bands intensities and molar extinction coefficients proposed in [15, 16].

The morphology of the prepared material was studied by using the scanning electron microscopy (SEM) and transmission electron microscopy (TEM). The SEM analysis was performed on a carbon coated samples by using a LEO Gemini 1530 instrument equipped with a Thermo Scientific UltraDry Silicon Drift Detector (SDD). The transmission electron microphotographs were taken by the JEM-1400 Plus transmission electron microscope (TEM) operated at a 120 kV acceleration voltage. The powdered samples were suspended in 100% ethanol under ultrasonic treatment for 10 min. For each sample, a drop of ethanol suspension was deposited on a Cu fiber carbon grid (200 Mesh) and evaporated, thereafter the images were recorded.

The copper content in the catalysts was determined by UV/VIS (UV1600PC, Shimadzu) at 270 nm from the copper acetate solutions used during an ion exchange and by the SEM-EDAX analysis during the SEM morphological studies of the powdered samples analysing the multiple section areas of the spread sample across the sample holder cell.

2.3 Catalytic screenings

The catalytic screening of the synthesized zeolites was evaluated in a model test reaction: catalytic oxidation of model polyphenol (tyrosol or phenol) with hydrogen peroxide in aqueous solutions.The catalytic experiments were carried out in a 200 cm^3 glass batch reactor equipped with a pH electrode and a temperature sensor at the atmospheric pressure at 363 K with the catalyst loading of 0.5 g/L and the initial concentrations of hydrogen peroxide and model phenolic coumpounds of up to 0.1 mol dm^{-3} and 1000 ppm, respectively, according to the reactor setup presented in Fig. 1.

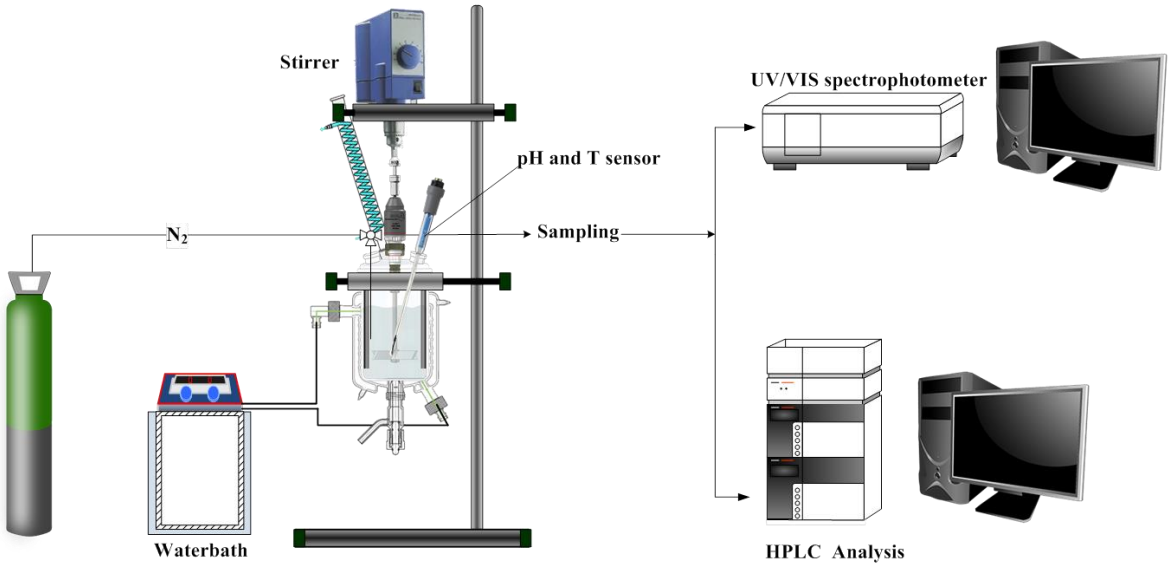

Figure 1 Process scheme of the reactor setup for catalytic screenings

To avoid the influence of the interphase mass transfer limitations on the observed kinetics, a high stirring speed (N=800 rpm) was employed and powder catalysts with particles sizes <125 μm were used during the runs. At regular time intervals, liquid samples were taken out of the reactor and analysed for monitoring the concentrations of tyrosol and hydrogen peroxide. For the quantification of the tyrosol content, Agilent Technologies Series 1100 HPLC was used equipped with an Ultra Techsphere ODS 5u analytical column (250×4.6 mm) connected to a diode array (DAD) detector. A mixture of 0.5 wt. % of H_3PO_4 in water and methanol (70:30=v:v) was used as a mobile phase for the isocratic analysis at a flow rate of 0.8 ml min^{-1} and temperature of 308 K at λ=280 nm. The ammonium metavanadate UV-VIS spectrophotometric method at 450 nm adopted from Nogueira et al. [16] was used for the measurement of hydrogen peroxide concentrations. The copper content in the reaction mixture was measured by ICP-OES from the diluted reaction mixture solutions on a PerkinElmer, Optima 5300 DV instrument.

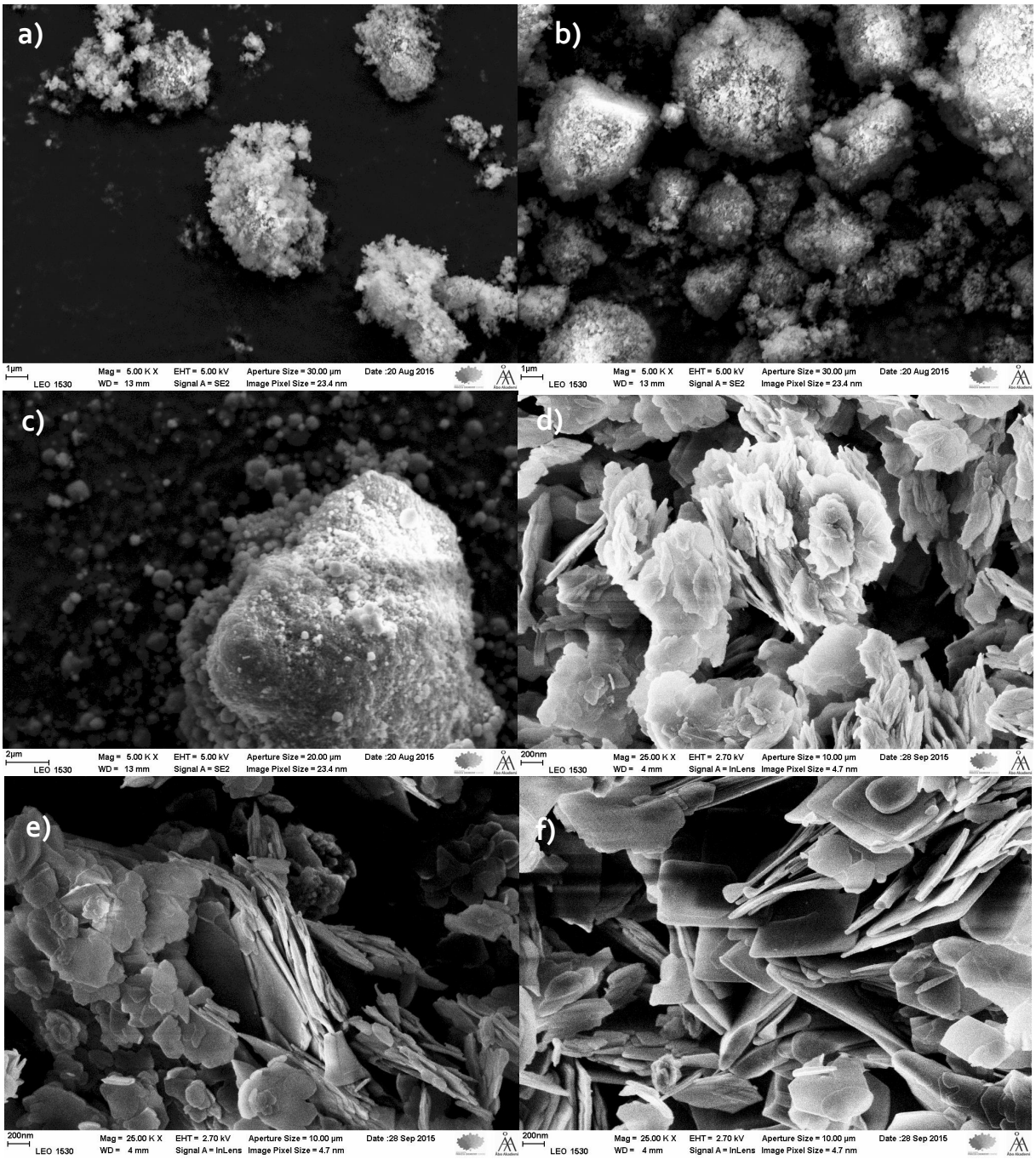

Figure 2 SEM images of Cu-BETA-25, Cu-BETA-150, Cu-BETA-300 (a-c) and Cu-MCM-22-30, Cu-CM-22-50, Cu-MCM-22-100 (d-f)

3 RESULTS AND DISCUSSION

The textural properties and respective active metal loadings of the prepared catalysts are presented in Tab. 1. All the catalysts exhibited similar textural properties, with high surface areas and large pore volumes. The active metal content of the catalysts was kept low except in the case of 13X zeolite which was several times higher due to the significantly higher acidity of the FAU zeolite type.

Table 1 Textural properties and respective active metal loadings of synthesized zeolites

Zeolite	Si/Al	Specific surface area $m^2\ g^{-1}$	Pore volume max $cm^3\ g^{-1}$	Copper content wt. %
Cu-H-BETA-25	25	705	0.59	1.1
Cu-H-BETA-150	150	649	0.68	1.3
Cu-H-BETA-300	300	783	0.40	0.9
Cu-H-MCM-22-30	30	612	0.41	1.03
Cu-H-MCM-22-50	50	522	0.30	0.90
Cu-H-MCM-22-100	100	270	0.17	0.25
Cu-13X pellet	2.6	618	0.34	8.0

The silica to alumina ratio significantly influenced textural properties, showing that both the pore volume and specific surface area decrease as the aluminium content in the parent zeolite gets lower due to the decrease in the presence of large opening cavities in the zeolites, and this can be observed both for BETA and MCM-22 zeolites. Similarly, the copper content decreased with the lower aluminium content in the zeolites indicating strongly that the active metal cation centres are directly dependant on the occurrence of aluminium 3+ sites in the zeolite framework.

The morphological studies of selected catalysts presented in Fig. 2 revealed typical crystallites structures for the BETA (round shaped), MCM-22 (layered leaflets) and FAU (needle shaped, not presented here) zeolite types. It can be observed that a slight decrease in the crystallite size occurs with the decrease of aluminium content in the zeolite of the specific framework type, which is specially pronounced for the MCM-22 zeolite whose particles decrease in average size from 0.9 μm for Si/Al=30 to 0.5 μm for Si/Al=100. Similarly, the copper particle size analysis by using the TEM images (not presented here) that was preformed on the Cu-MCM-22 zeolites showed that the active metal particles decrease in size with increasing Si/Al ratios. The Cu particle size distributions are decreasing in the range and size with the decrease in aluminium content having the average particle size of 6.3, 3.6 and 2.7 nm, respectively.

Table 2 Acidity of the prepared zeolite catalysts as the measured TPD pyridine desorption

Zeolite	Si/Al	Brønsted acidity, μmol/g			Lewis acidity, μmol/g		
		250 °C	350 °C	450 °C	250 °C	350 °C	450 °C
Cu-H-BETA-25	25	136	211	64	180	35	3
Cu-H-BETA-150	150	153	170	113	179	46	2
Cu-H-BETA-300	300	37	41	2	74	27	2
Cu-H-MCM-22-30	30	157	163	123	126	44	1
Cu-H-MCM-22-50	50	102	113	20	124	47	0
Cu-H-MCM-22-100	100	43	41	10	78	32	2

The Brønsted and Lewis acidities of the synthesized Cu-BETA and Cu-MCM-22 zeolites, as determined by the pyridine adsorption (FTIR), are presented in Tab. 2. As expected, the zeolite with the highest amount of aluminium showed to be the most acidic in terms of weak (523 K), medium (623 K) and strong (723 K) Brønsted acid sites. The total and the Brønsted acidity drop with the decrease in the aluminium content in the zeolites, while the Lewis acidity remains less pronounced and less affected by the change in the Si/Al ratios. The zeolites with the lowest aluminium content (Cu-H-BETA-300 and Cu-MCM-22-100) displayed the lowest total and Brønsted acidity, while the amount of the Lewis acid sites slightly increased when compared to the other samples.

The catalytic screening results are shortly summarized in Table 3. As it can be seen, the extent of the polyphenolic compound removal, as well as the decomposition of hydrogen peroxide over the catalyst surface during which the hydroxyl radicals are formed, strongly depend on the copper content of the catalyst, but also on the zeolite framework type, acidity and particle sizes of both the zeolites and active metal compound.

Table 3 Catalytic activity and copper leaching in the CWPO reactions with the Cu-MCM-22 and Cu-MCM-36 catalysts (T=60 °C, $c_{PPh,0}$= 500 mg/L, $c_{HP,0}$= 0.07 mol/L, m_{cat}=100 mg, N=800 rpm)

Zeolite	Si/Al	X_{PPh}, %	X_{HP}, %	γ_{Cu}, mg dm^{-3}
Cu-H-BETA-25	25	95	45	3
Cu-H-BETA-150	150	100	50	4
Cu-H-BETA-300	300	84	21	2
Cu-H-MCM-22-30	30	23	4	1
Cu-H-MCM-22-50	50	93	28	2
Cu-H-MCM-22-100	100	70	10	1
Cu-13X pellet	2.6	90	60	16

The stability of the catalysts showed to strongly depend on the yield of the reaction in terms of the conversion of polyphenol compounds. The more reaction progressed, the more of polyphenol was converted to low-molecular carboxylic acids that caused the decrease of the pH of the reaction mixtures, what is considered to be the main cause of the leaching of the active metal component of the catalyst, i.e. the copper particles. The leaching extent was also dependent on the acidity of the parent zeolite, showing that the catalysts that were more acidic in nature were also proved to be less stable.

4 CONCLUSIONS

The obtained results provided an insight into the cause-and-effect relationship between the silica to alumina ratio and its direct effect on the acidity and basicity of the prepared zeolites, as well as the indirect one on their morphology, textural and surface properties of both the parent zeolite and active metal component. As expected, the increase of the alumina content in the zeolite results in higher acidities of the material, which in turn affects the morphology and size of both the zeolite and active metal particles.

The use of active catalysts resulted in successfully operating the process under mild conditions with low energy consumption. It was found that copper and iron containing catalysts showed promising activity, while the stability of the active metal component still is and remains a challenge to obtain and further studies are required in order to understand the mechanisms of the deactivation process, as well as the development of the applicable stabilization techniques such as the postyinthesis chemical or thermal treatment. The catalyst pellet/particle size plays an important role in the activity in the CWPO showing that a decreasing of it occurs with the increase of the pellet size.

Acknowledgement(s)

The work of Karolina Maduna Valkaj is supported under the European Commission and the Croatian Ministry of Science, Education and Sports Co-Financing Agreement No. 291823. In particular, Karolina Maduna Valkaj acknowledges the project financed from The Marie Curie FP7-PEOPLE-2011-COFUND program NEWFELPRO: Grant Agreement No. 33 – "Preparation and Characterization of Zeolite Based Catalysts for Phenolic Wastewater Treatment (ZCat4Water)."

Note: This research was presented at the International Conference MATRIB 2017 (29 June - 2 July 2017, Vela Luka, Croatia).

5 REFERENCES

[1] Čejka, J.; Centi, G.; Perez-Pariente, J.; Roth, W. Zeolite-based materials for novel catalytic applications: Opportunities, perspectives and open problems, J. Catal. Today 179 (2012) 2–15.
[2] Weitkamp, J. Zeolites and catalysis, Solid State Ionics 131 (2000) 175–188.
[3] Wang, N.; Zheng, T.; Zhang, G.; Wang, P. A review on Fenton-like processes for organic wastewater treatment, J. Environ. Chem. Eng. 4 (2015) 762–787.
[4] Navalon, S.; Alvaro, M.; Garcia, H. Heterogeneous Fenton catalysts based on clays, silicas and zeolites, Appl. Catal. B Environ. 99 (2010) 1–26.
[5] Liotta, L. F.; Gruttadauria, M.; Di Carlo, G.; Perrini, G.; Librando, V. Heterogeneous catalytic degradation of phenolic substrates: catalysts activity, J. Hazard. Mater. 162 (2009) 588–606.
[6] Busca, G.; Berardinelli, S.; Resini, C.; Arrighi, L. Technologies for the removal of phenol from fluid streams: a short review of recent developments, J. Hazard. Mater. 160 (2008) 265–288.
[7] Giordano, G.; Perathoner, S.; Centi, G.; De Rosa, S.; Granato, T.; Katovic, A.; Tagarelli, A.; Tripicchio, F. Wet hydrogen peroxide catalytic oxidation of olive oil mill wastewaters using Cu-zeolite and Cu-pillared clay catalysts, Catal. Today. 124 (2007) 240–246.
[8] Najjar, W.; Azabou, S.; Sayadi, S.; Ghorbel, A. Screening of Fe–BEA catalysts for wet hydrogen peroxide oxidation of crude olive mill wastewater under mild conditions, Appl. Catal. B Environ. 88 (2009) 299–304.
[9] Perathoner, S.; Centi, G. Wet hydrogen peroxide catalytic oxidation (WHPCO) of organic waste in agro-food and industrial streams, Top. Catal. 33 (2005) 207–224.
[10] Taran, O. P.; Zagoruiko, A. N.; Ayusheev, A. B.; Yashnik, S. A.; Prihod'ko, R. V.; Ismagilov, Z. R.; Goncharuk, V. V.; Valentin, N. Wet peroxide oxidation of phenol over Cu-ZSM-5 catalyst in a flow reactor. Kinetics and diffusion study, Chem. Eng. J. (2015), in press.
[11] Yan, Y.; Jiang, S.; Zhang, H. Efficient catalytic wet peroxide oxidation of phenol over Fe-ZSM-5 catalyst in a fixed bed reactor, Sep. Purif. Technol. 133 (2014) 365–374.
[12] Kumar, N.; Leino, E.; Mäki-Arvela, P.; Aho, A.; Käldström, M.; Tuominen, M.; Laukkanen, P.; Eränen, K.; Mikkola, J.-P.; Salmi, T.; Murzin, D. Y. Synthesis and characterization of solid base mesoporous and microporous catalysts: Influence of the support, structure and type of base metal, Microporous Mesoporous Mater. 152 (2012) 71–77.
[13] Käldström, M.; Kumar, N.; Heikkilä, T.; Yu. Murzin, D. Pillared H-MCM-36 mesoporous and H-MCM-22 microporous materials for conversion of levoglucosan: influence of varying acidity, Applied Catalysis A. General, 2011, 397, 13-21.
[14] Aho, A.; Kumar, N.; Eränen, K.; Salmi, T.; Hupa, M.; Yu. Murzin, D. Catalytic pyrolysis of biomass in a fluidized bed reactor: influence of acidity of H-beta zeolite, IChemE, part B, Process Safety and Environmental Protection, 2007, 85, 473-480.
[15] Emeis, C. A. Determination of Integrated Molar Extinction Coefficients for Infrared Absorption Bands of Pyridine Adsorbed on Solid Acid Catalysts, J. Catal. 141 (1993) 347–354.
[16] Nogueira, R.; Oliveira, M.; Paterlini, W. Simple and fast spectrophotometric determination of H(2)O(2) in photo-Fenton reactions using metavanadate, Talanta 66 (2005) 86–91.

Authors' contacts:

Karolina MADUNA
Faculty of Chemical Engineering and Technology,
Department of Reaction Engineering and Catalysis,
Marulićev trg 19, 10000 Zagreb, Croatia
kmaduna@fkit.hr

Åbo Akademi University, Department of Industrial Catalysis and Recation Engineering, Biskopsgatan 8, FI-20500 Turku, Finland

Narendra KUMAR
Dmitry Yu. MURZIN
Åbo Akademi University, Department of Industrial Catalysis and Recation Engineering, Biskopsgatan 8, FI-20500 Turku, Finland

ISSN 1846-6168 (Print), ISSN 1848-5588 (Online)
ID: TG-20170816142553

Original scientific paper

INFLUENCE KINDS OF MATERIALS ON THE POISSON'S RATIO OF WOVEN FABRICS

Željko PENAVA, **Diana ŠIMIĆ PENAVA**, **Željko KNEZIĆ**

Abstract: Poisson's ratio is one of the fundamental properties of any structural material including woven fabrics and textile materials. This coefficient determines important mechanical characteristics of fabrics in many applications, including a variety of composite systems containing textiles as a structural element. Due to the anisotropy of woven fabrics, Poisson's ratio changes over the fabric sample stretching. In this paper, the practical application of the uniaxial testing of woven fabrics for determining its breaking properties and Poisson's ratio is presented. Experimental testing was carried out on two different fabrics of a different raw material composition (cotton, wool) and of the same weave (plain weave). Samples were stretched with tensile force in the weft and warp direction, and based on the different measured values of the fabric stretching, warp and weft, Poisson's ratio is calculated. The influence of the raw material composition on the values of Poisson's ratio was examined.

Keywords: anisotropy; elongation at break; Poisson's ratio; warp; weft; woven fabric

1 INTRODUCTION

Nowadays, the use of textile materials in different industrial branches is on the rise. Anisotropy is a characteristic of most materials, especially woven fabrics. The impact of the direction of action of the external load (tensile force) on the properties of the fabric is enormous, and is frequently examined [1]. The mechanical properties of fabrics under the influence of the tensile load began to be studied in 1937 [2]. Kilby defined the Poisson's ratio and measured the tensile properties of fabrics in an arbitrary direction of the tensile force. He noted that there is a connection between the Poisson's ratio, shear modulus and modulus of the elasticity of the fabric [3]. The Poisson's ratio affects certain mechanical properties of the fabric such as the draping and shear. The researchers determined Poisson's ratio in the warp and weft based on the geometric model of fabric and without the impact of the Poisson's ratio of the yarn. The Poisson's ratio in fabrics comes out of the interaction between the warp and weft, and can be expressed in terms of structural and mechanical system parameters [4]. Due to the woven fabric anisotropy, the analysis of the impact of the physical parameters of fabric on the value of the Poisson's ratio is useful and provides a better explanation for certain woven fabric behavior. Because of the inherent nature of textile, an accurate and reliable measurement of the Poisson's ratio is a difficult task. This engineering property is studied by many scientists.

Bao and colleagues [5] were examining why in the measurements of the Poisson's ratio, when uniaxial tensile load is put on the fabric, errors occur. The previously measured experimental values were compared with the theoretical results. He also studied the influence of the yarn and fabric structural parameters of the Poisson's ratio. An accurate measurement of the Poisson's ratio of woven fabric is quite difficult to obtain due to the lack of reliable experimental techniques [6]. Uniaxial testing is most commonly performed in woven fabrics by using either the commercial or custom designed instruments [7] and analyzing the physical and mechanical properties of textile products [8]. The Poisson's ratio of textile materials used in the non-woven geotextile was analyzed by Giroud [9]. He set the theoretical equation to calculate the Poisson coefficient, as a function of strain.

Experiments on the extension of the woven fabric sample under the static load will are discussed in this paper. The influence of the raw material composition on the values of the Poisson's ratio has been researched, too.

2 THEORETICAL OVERVIEW

The Poisson's ratio, which expresses the change in the volume of a solid undergoing deformation, is an important characteristic, along with the initial modulus of elasticity and shear, of the behavior of a material under a tension load; and can be used in the calculations of the true stresses (from the actual cross-sectional area) coming into being in the textile fibers and yarns subjected to the extension, and can serve, moreover, as an indirect characteristic of the structure of the material and of the mechanism of its deformation. It is well known that when a solid having the shape of a rectangular parallelepiped, Fig. 1a, is subjected to tension forces in the direction of its axes *x, y* and *z*, the change in its volume equals:

$$\frac{\mathrm{d}V}{V} = \frac{y \cdot z \cdot d_x + x \cdot z \cdot d_y + x \cdot y \cdot d_z}{x \cdot y \cdot z} = \\ = \frac{d_x}{x} + \frac{d_y}{y} + \frac{d_z}{z} = \varepsilon_x + \varepsilon_y + \varepsilon_z \tag{1}$$

where ε_x, ε_y and ε_z are the relative tensile deformations in the direction of the *x, y* and *z* axes of the parallelepiped.

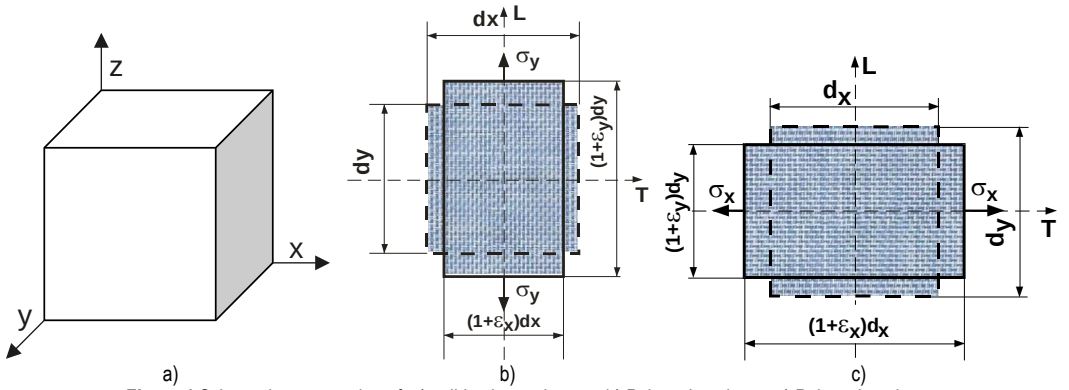

Figure 1 Schematic presentation of: a) solid volume element, b) Poisson's ratio v_{xy}, c) Poisson's ratio v_{yx}

In the tensile deformation in the direction of the *x* axis, the solid will be subjected to compression in the direction of the *y* and *z* axes (i.e, laterally to the *x* axis):

$$\frac{\mathrm{d}V}{V} = \varepsilon_x - 2\cdot\varepsilon = \varepsilon_x \cdot \left(1 - 2\cdot\frac{\varepsilon}{\varepsilon_x}\right) = \varepsilon_x \cdot (1 - 2\cdot\nu) \tag{2}$$

where ε is the relative compressive deformation and ν is the Poisson's ratio.

It is obvious that for $\nu = 0.5$ the volume of a material subjected to tensile forces will not change ($\mathrm{d}V = 0$), for $\nu < 0.5$ the volume will increase ($\mathrm{d}V > 0$), while for $\nu > 0.5$ it will decrease ($\mathrm{d}V < 0$).

When a fabric is stretched in one direction, it tends to contract in the direction perpendicular to the direction of the stretch, Fig. 1b, 1c. The yarns in the direction of the tensile force are flattened out (extended), and in the orthogonal or non-loading direction, the yarns have a longer geometrical path to 'curve around'. Because there is no limiting force, the waviness (amplitude) of the yarn in the vertical direction of the force increases. The consequence to this is the dimension reduction of the fabric width. This phenomenon is called the Poisson effect. The Poisson's ratio, a measure of the Poisson effect, is the ratio of the relative contraction strain *s* to the related extension strain ε in the direction of the applied load. To determine the Poisson's ratio of fabrics, devices for measuring the tensile strength are used, and the coefficient is determined in the linear part of the diagram of the Hooke's law [10]. During the testing of the fabric to stretch, the initial length of the tested sample l_0 is increased for Δl, and a final sample length of fabric is *l*. The initial width of the fabric sample b_0 is decreased for Δb and the final sample width is *b*. The physical meaning of the Poisson's ratio ν is shown by the Eq. (3). The Relative contraction and extension strains have an opposite sign.

$$\nu = \left|\frac{s}{\varepsilon}\right| = \left|\frac{l_0}{b_0}\cdot\frac{b-b_0}{l-l_0}\right|, \quad s = -\nu\cdot\varepsilon\,. \tag{3}$$

The relative longitudinal strain (relative extension strain) ε and transverse strain (relative contraction strain) *s* is defined in the Eq. (4).

$$\begin{aligned} \varepsilon &= \frac{\Delta l}{l_0}\cdot 100\% = \left(\frac{l}{l_0} - 1\right)\cdot 100\% \\ s &= \frac{\Delta b}{b_0}\cdot 100\% = \left(\frac{b}{b_0} - 1\right)\cdot 100\% \end{aligned}\,. \tag{4}$$

Due to the anisotropy of the fabric, the Poisson's ratio is being changed in the process of the extension of the fabric sample.

3 EXPERIMENTAL TESTING

The experimental study was carried out by measuring the extension of woven fabrics samples under the action of the tensile force till rupture [11]. The tensile force acts on the samples that are cut at warp and weft direction. The values of the tensile force in relation to the relative extension were measured. For the extensions and tensile forces which act in the warp and weft direction, the corresponding contraction strains of woven fabrics were scanned. The Poisson's ratio of woven fabrics was calculated by using the testing results. Two different fabrics of a different raw material composition (cotton, wool) and of the same weave (plain weave) were available. The raw material and the structural properties of the tested fabrics are shown in Tab. 1.

Table 1 Structural characteristics of the tested samples

	Warp direction			Weft direction				
Fabric structure	Fiber composition	Yarn count (tex)	Linera density (cm^{-1})	Fiber composition	Yarn count (tex)	Linera density (cm^{-1})	Mass per unit area (g/m^2)	Thickness, *t* (mm)
Plain	Cotton	32	22	Cotton	30	22	150.34	0.318
Plain	Wool	50.6	26	Wool	47	18	234.75	0.568

The yarn count was determined by the gravimetric method according to the standard ISO 2060:1994. The number of threads per unit length was tested according to the standard ISO 7211-2:1984. The standard ISO 5084:1996 describes a method for the determination of the thickness of the fabric. Before testing all samples were conditioned under the conditions of the standard atmosphere (relative air humidity 65 ± 2 %, at a temperature of 20 ± 2 °C). Standard samples with the dimensions of 300 × 50 mm were cut and clamped in clamps of the tensile tester at a distance of l_0=200 mm and subjected to a uniaxial tensile load till rupture. The pulling speed of clamps is 100 mm/min. The samples were cut in the weft direction (φ =0°) and warp direction (φ = 90°). Three tests were done on the tensile tester for each mentioned cutting direction of the sample. The tensile properties of all samples were tested in accordance with the standard ISO ISO13934-1:2008 by using the strip method for measuring the fabric strength on the tensile strength tester Textechno Statimat M. This tensile tester is an automatic, microprocessor-controlled instrument operating on the principle of constant deformation speed, Fig. 2.

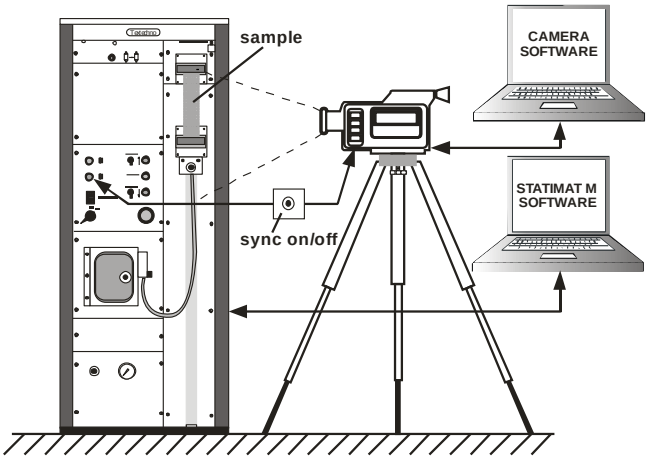

Figure 2 Schematic view of the experiment

For an accurate recording and measurement of the spatial deformation of fabric, a 1x1 grid pattern was mounted on the tensile tester immediately behind the test specimen; the whole process of drawing the specimen till rupture was recorded by the Panasonic NV-GS500 Digital Video Camera placed on a tripod in front of the device. The digital video camera had the resolution of 720 × 576 pixels, and a recording speed of N_{sl}=25 frames/s, and was connected to the computer via an IEEE 1394 (FireWire) interface. The horizontal distance between the camera and the sample was such that 1 mm on the grid amounted to 10 pixels on the picture. Two sources of white light which mutually closed the angle of 90° were used for measuring. The number of images N at a certain extension is:

$$N = \frac{\varepsilon \cdot l_0}{100} \cdot \frac{60}{\mathrm{v}} \cdot N_{\mathrm{sl}} \,. \tag{5}$$

The tensile tester and the camera were connected to a special assembly with a simultaneous on/off which fully ensured the exactness of the video recording of the entire process of stretching the fabric to rupture. The width of each sample was measured in three spots (1/4, 2/4 and 3/4 of the length and width of the sample). The transverse strain was obtained after all samples were recorded by camera, and the mentioned grid pattern enabled a fast and accurate editing of the footage processed by the software package Adobe Premiere created for this purpose which specified the spatial deformation of samples on the basis of shifting in the direction of the x- and y-axis.

3.1 Overview of testing results

The diagrams (F-ε) of mean values of the test results of the action of the tensile force F and the corresponding longitudinal strain (extension) ε for the samples that are cut in the weft and warp direction are shown in Fig. 3.

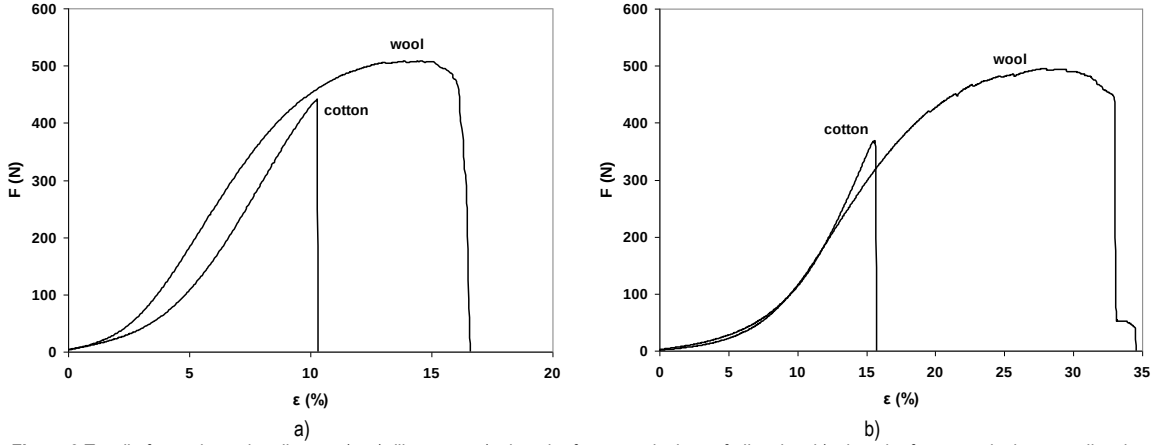

Figure 3 Tensile force-elongation diagram (F-ε) till rupture: a) when the force acts in the weft direction, b) when the force acts in the warp direction

3.2 Determination of Poisson's ratio

The fabric sample width is b_0 = 500 pixels, which is equivalent to b_0 = 50 mm. When reading the value of the fabric width, after the effect of the force, the relative transverse strain is calculated by using the Eq. (4). The contraction of fabric occurs in the transverse direction, i.e. in the direction which is perpendicular to the direction of stretching. Due to this phenomenon, there is a loss of the rectangular shape of the sample, i.e. there is a contraction of the fabric sample. The relation between the continuous change of the relative contraction s (%) of the sample and its relative extension ε (%) when a force acts on the samples that are cut in the weft direction is shown in Fig. 4a by a characteristic curve. Fig. 4b shows a characteristic curve of the relative contraction of the sample in relation to its relative extension when the force acts on samples that are cut in the warp direction. When a force acts on samples that are cut in the weft and warp direction, at the same relative extension ε, cotton fabric has a higher relative contraction s than wool fabric, Fig. 4. When the force acts in the weft direction, at a relative extension ε = 10%, the lateral contraction for the cotton fabric is s = 12.56% and for wool fabric s = 7.57 %. The lateral contraction of cotton fabric is 66% higher than the contraction of wool fabrics for ε = 10%. When force acts in the warp direction, at a relative extension ε = 15.5%, the lateral contraction for cotton fabric is s = 17.47% and for wool fabric s = 9.12%. The lateral contraction of cotton fabric is 92% higher than the contraction of wool fabric for ε = 15.5%. Both fabrics have a bigger extension and contraction when the force acts in the warp direction.

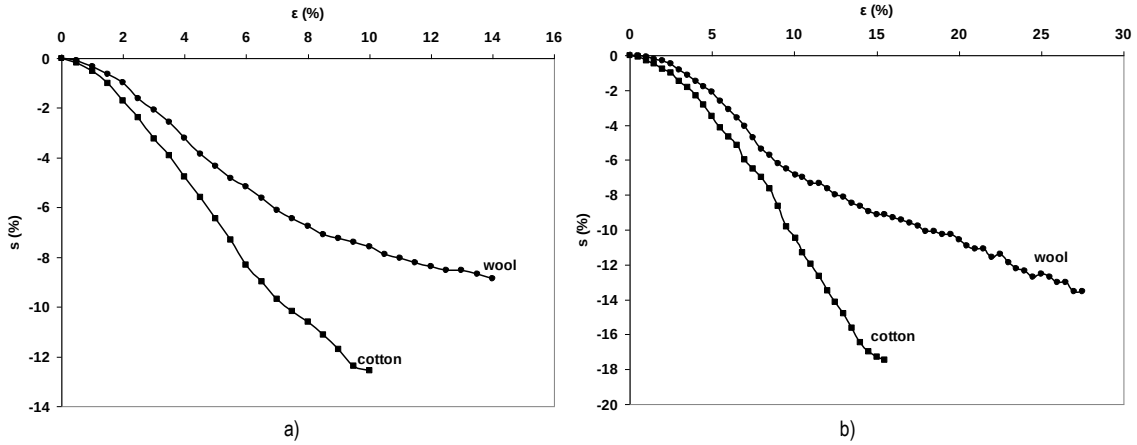

Figure 4 Diagram of the relative contraction of the fabric s (%): a) when the force acts in the weft direction, b) when the force acts in the warp direction

From the diagrams in Fig. 4 it is evident that fabric contractions are small at the beginning of stretching. After that, with the increase of stretching, the values of fabric contractions also increase.

According to the Eq. (3) and based on the experimental values of the relative contraction s and relative extension ε from Fig. 4, the values of the Poisson's ratio v are calculated when the force acts on the samples that are cut in the weft and warp direction. Fig. 5a shows a curve of the values of the Poisson's ratio v in relation to its relative extension when the force acts on the samples that are cut in the weft direction and Fig. 5b shows the values in the warp direction.

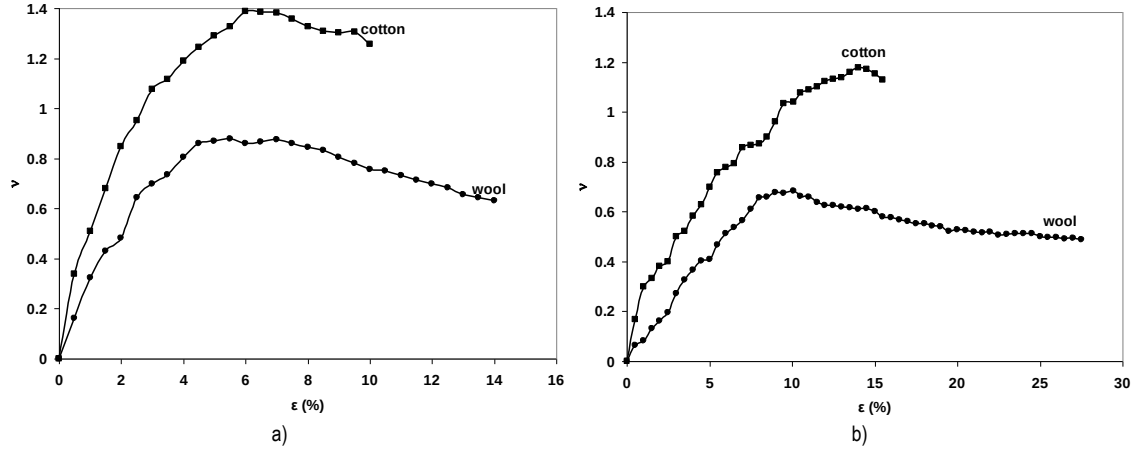

Figure 5 Poisson's ratio v of the fabric: a) when the force acts in the weft direction, b) when the force acts in the warp direction

The shape of the Poisson's ratio curve of the woven fabric is the result of the internal interactions in the fabric. The shape of the Poisson's ratio (Fig. 5) affected by the changes in the value of the relative contraction of the fabric are shown in Fig. 4. The Poisson's ratio curve consists of two zones. The first zone includes the area from the beginning to the highest peak of the curve. When a force acts in the weft direction, the highest value of the Poisson's ratio for the cotton fabric ν = 1.39 is where the relative extension ε is between 6 and 6.5%, and for wool fabric ν = 0.88 is where ε is between 5.5 and 6%, Fig. 5a. When a force acts in the warp direction, the highest value of the Poisson's ratio for the cotton fabric ν = 1.18 is where the relative extension ε is between 14 and 14.5%, and for wool fabric ν = 0.68 is where ε is between 9.5 and 10%, Fig. 5b. Both fabrics have a higher value of the Poisson's ratio when the force acts in the weft direction.

Cotton fabric has a higher value of the Poisson's ratio than wool fabric for each value of the extension. When the force acts in the weft direction, at a relative extension ε = 6 %, the value of the Poisson's ratio for cotton fabric is 62% higher than the Poisson's ratio for wool fabrics. When the force acts in the warp direction, at a relative extension ε = 6 %, the value of Poisson's ratio for cotton fabric is 52% higher than the Poisson's ratio for wool fabrics.

The second zone is from the highest peak of the curve to the end of stretching, i.e. it is interrupted. In this zone, the curve of the Poisson's ratio decreases and it represents the end of the lateral contraction despite the stretching of the fabric sample.

After considering the equation of the Poisson's ratio, the relative contraction becomes a constant when the lateral contraction of the woven fabric is completed. Furthermore, the sample is still stretching for the value ε. Therefore, the equation of the Poisson's ratio takes on a new form, which is the general form of the reciprocal function. Mathematically, the limit of this equation is zero. In practice, due to the break of the sample, this condition never occurs. However, taking into account the significance of the Poisson's ratio that represents the ratio between the transverse and longitudinal deformation of the material, if the transverse deformation does not take place in this ratio, the Poisson's ratio has no practical significance.

The ending of the lateral contraction of a woven fabric can occur for two reasons. Firstly, due to the termination of the flattening crimp of yarn in the direction of the stretching fabric and secondly, because of the structure of the fabric. If there is a possibility of a further contraction of fabric, it can not continue taking place because there is no continued existence of space between the neighboring threads in the fabric, so there can be no contraction of the fabric.

Note: This research was presented at the International Conference MATRIB 2017 (29 June - 2 July 2017, Vela Luka, Croatia).

4 CONCLUSION

Due to the anisotropy of woven fabrics, the Poisson's ratio is not constant, but varies with each fabric extension. The behavior and shape of the Poisson's ratio curve of the coated fabric that is subjected to the tensile force mostly depends on its behavior in a direction perpendicular to the extension. The Poisson's ratio values depend on the number of coatings applied to the raw fabric. The shape of the Poisson's ratio curve for woven fabrics is a result of the internal interactions in the coated and raw fabrics. A change in the values of the relative contraction of coated fabrics affects the shape of the Poisson's ratio curve. When the force acts on samples that are cut in the weft direction, the Poisson's ratio assumes the maximum value at a relative extension of cotton fabrics between 6 and 6.5%, and for wool fabrics between 5 and 5.5%. When the force acts on the samples that are cut in the warp direction, the Poisson's ratio assumes the maximum value at a relative extension of cotton fabrics between 14 and 14.5%, and between 9.5 and 10% for wool fabrics. In the weft and warp direction, the values of the Poisson's ratio of cotton fabrics are higher than the Poisson's ratio of wool fabrics at the same relative extension.

Because of the anisotropy of fabrics, the Poisson's ratio is not constant. It is changing with each elongation of the woven fabric. The behavior and form of the curve of the Poisson's ratio of the woven fabric which is exposed to tensile force, i.e. elongation, mainly depends on the behavior of the fabric in a direction perpendicular to the elongation. First, the Poisson's ratio increases nonlinearly and after having reached the peak value, it decreases. These two zones represent two different processes in the deformation of the fabric. The first zone represents the way of the lateral contraction because of the longitudinal stretching. The second zone shows the termination of the lateral contraction of the woven fabric and the fabric is stretching without any further contractions.

5 REFERENCES

[1] Kovar, R.; Gupta, B. S. Study of the Anisotropic Nature of the Rupture Properties of a Plain Woven Fabric. // Textile Research Journal, 79, 6(2009), pp. 506-516.

[2] Peirce, F. T. The geometry of cloth structure. // Journal of the Textile Institute, 28, (1937), T45-T96.

[3] Kilby, W. F. Planar Stress-strain Relationship in Woven Fabrics. // Journal of the Textile Institute, 54, (1963), pp. 9-27.

[4] Lloyd, D. W. et al. An Examination of a "Wide jaw" Test for the Determination of Fabric Poisson Ratio. // Journal of the Textile Institute, 68, 9(1977), pp. 299-302.

[5] Bao, L. et al. Error Evaluation in Measuring the Apparent Possion's Ratios of Textile Fabrics by Uniaxial Tensile Test. // Sen'i Gakkaishi, 53, 1(1997), pp. 20-26.

[6] Basset, R. J. et al. Experiment Methods for Measuring Fabric Mechanical Properties: a Review and Analysis. // Textile Research Journal, 69, 11(1999), pp. 866-875.
[7] Sun, H. On the Poisson's ratios of a woven fabric. // Composite Structures, 68, 4(2005), pp. 505-510.
[8] Zheng, J. Measuring Technology of the Anisotropic Tensile Properties of Woven Fabrics. // Textile Research Journal, 78, 12(2008), pp. 1116-1123.
[9] Giroud, J. P. Poisson's Ratio of Unreinforced Geomembranes and Nonwoven Geotextiles Subjected to Large Strains. // Geotextiles and Membrane, 22, (2004), pp. 297-305.
[10] Nazanin, E. S. et al. Effect of Fabric Structure and Weft Density on the Poisson's Ratio of Worsted Fabric. // Journal of Engineered Fibers and Fabrics, 8, 2(2013), pp. 63-71.
[11] Penava, Ž. et al. Investigation of warp and weft take-up influence on Poisson's ratio of woven fabric. // Tekstil, 63, 7-8(2014), pp. 217-227.

Authors' contacts:

Željko PENAVA
University of Zagreb,
Faculty of Textile Technology,
Prilaz B. Filipovića 28a, 10000 Zagreb, Croatia

Diana ŠIMIĆ PENAVA
University of Zagreb,
Faculty of Civil Engineering,
Kačićeva 26, 10000 Zagreb, Croatia
dianas@grad.hr

Željko KNEZIĆ
University of Zagreb,
Faculty of Textile Technology,
Prilaz B. Filipovića 28a, 10000 Zagreb, Croatia

ISSN 1846-6168 (Print), ISSN 1848-5588 (Online)
ID: TG-20170827194345

Original scientific paper

EFFECT OF HEAT TREATMENT PARAMETERS ON THE MECHANICAL PROPERTIES AND MICROSTRUCTURE OF ALUMINIUM BRONZE

Božidar MATIJEVIĆ, Thota Surya Krishna SUSHMA, B. K. PRATHVI

Abstract: Aluminium bronzes are used for their combination of high strength, excellent corrosion and wear resistance. This paper presents the research of heat treatment parameters of two different chemical compositions of aluminium bronze (Cu-Al-Fe- Ni alloy) on microstructure and mechanical properties. The heat treatment employed in this research were solutionizing and tempering. The solution treatment was carried out at a temperature of 950 °C and the duration in the range of two hours. Similarly, tempering was carried out at 300 °C and 400 °C, wherein the duration was maintained at two hours. The heat treated samples were subjected to the cold water quenching in order to bring them to an ambient temperature. Metallographic studies were performed on samples in order to determine the changes in the microstructure of the hardened bronze, on the metallographic microscope OLYMPUS GX51 with a digital image analysis and the scanning electron microscope TESCAN VEGA 5136MM with EDX along with the digital recording on the computer. Moreover, the Glow Discharge Spectroscopy-GDS was done to determine the chemical composition of the samples. The results of the chemical composition for the aluminium bronze AK2 were: Cu- 78,37%; Al- 10,52%; Fe- 4,44%; Ni- 5,16% and for AK3 alloy: Cu- 78,95%, Al- 10,97%; Fe- 4,16%; Ni- 4,8%. The behavior of the alloy has been assessed in terms of the influence of the temperature and duration of the heat treatment on the microstructural and mechanical properties of the samples. The hardness of samples was measured by using a Vickers hardness tester at an applied load of one kg. The samples were polished metallographically prior to their hardness measurement and an average of three observations has been considered. The hardness of the AK2 alloy increased from 320 HV1 to 425 HV1 after quenching and to 500 HV1 after tempering on 300 °C or 540 on 400 °C. The hardness of the AK3 alloy increased from 300 HV1 to 400 HV1 after quenching and to 475 HV1 after tempering on 300 °C or 470 on 400 °C.

Keywords: aluminium bronze; heat treatment; GDS; mechanical properties; microstructure

1 INTRODUCTION

Aluminium bronze is a type of bronze in which aluminium is the main alloying metal added to copper, in contrast to the standard bronze (copper and tin) or brass (copper and zinc). A variety of aluminium bronzes of differing compositions have found industrial use, with most ranging from 5% to 11% of aluminium by weight, the remaining mass being copper. Other alloying agents such as iron, nickel, manganese, and silicon are also sometimes added to aluminium bronzes [1]. Aluminium bronzes are used for their combination of high strength, excellent corrosion and wear resistance. Aluminium bronze alloys typically contain 9-12% of aluminium and up to 6% of iron and nickel. Alloys in these composition limits are hardened by a combination of a solid solution strengthening, cold work and precipitation of an iron rich phase. The vertical section through the Cu-Al-5%Ni-5%Fe phase diagram is shown in Fig. 1 [2].

High aluminium alloys are quenched and tempered. Aluminium bronzes are used in marine hardware, shafts, pump and valve components for handling sea water, sour mine waters, non-oxidizing acids and industrial process fluids. They are also used in the applications such as heavy duty sleeve bearings and machine tool ways. They are designated by UNS C60800 through C64210 [3]. Aluminium bronzes containing Al above 8.4% respond to heat treatment in a manner similar to steel. The heat-treating processes such as solution treating and tempering are useful for property improvement and have been applied to many Aluminium bronzes in practice. An appraisal of the above suggests that heat treatment plays an important role in controlling the end properties and the resulting microstructural features of Aluminium bronzes [4, 5]. In view of the above, an attempt has been made in this research to optimize the solutionizing and tempering parameters such as the duration and temperature of the treatments, and to characterize their microstructural features and mechanical properties with an objective to establish the microstructure-property correlations and develop the desired combinations of microstructural features and properties.

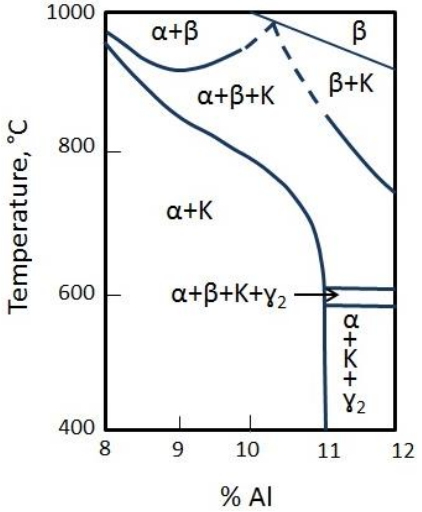

Figure 1 Vertical section through the Cu-Al-5%Ni-5%Fe phase diagram

2 EXPERIMENTAL PROCEDURE

The methodology adopted to carry out the present study essentially involved heat treatment (solutionizing and

tempering) over a range of temperatures and durations, the optimization of heat treatment parameters (temperature and duration), characterization of microstructural features and mechanical properties. The type of heat treatments employed in this research consisted of solutionizing and tempering. The solution treatment was carried out at a temperature of 950 °C and the duration in the range of two hours. Similarly, tempering was carried out at 300 °C and 400 °C maintaining the duration at two hours. The heat treated samples were subjected to cold water quenching in order to bring them to an ambient temperature after solutionizing. The Glow Discharge Spectroscopy-GDS was done to determine the chemical composition of the samples. Metallographic studies were performed on samples in order to determine the changes in the microstructure of the hardened bronze, on the metallographic microscope OLYMPUS GX51 with a digital image analysis, the scanning electron microscope TESCAN VEGA 5136MM with EDX along with the digital recording on the computer. The hardness of the samples was measured by using a Vickers hardness tester at an applied load of one kg. The samples were polished metallographically prior to their hardness measurement. An average of three observations has been considered in this study.

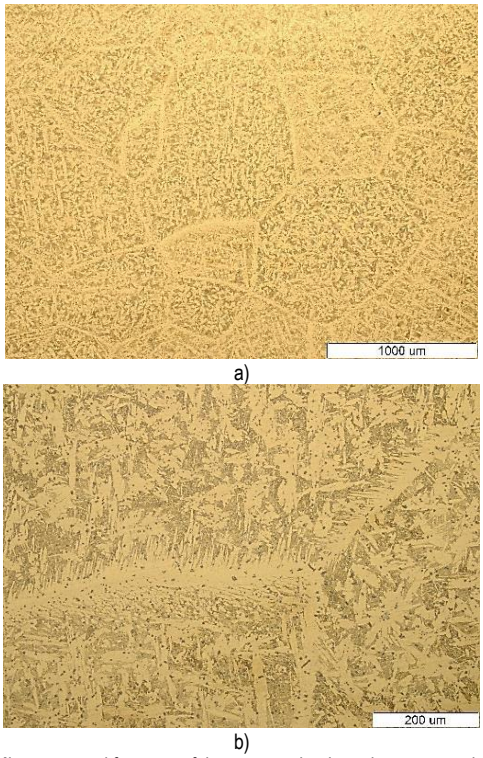

Figure 2 Microstructural features of the as cast aluminum bronze samples showing a dendrite structure and different microconstituents: (a) Primary α; (b) Eutectoid α+γ_2 (100× and 200×)

3 RESULTS

The study deals with the observations made with regard to the characteristics of the samples as influenced by the type of heat treatment (solutionizing and tempering) parameters (duration and temperature). The results of the chemical composition for aluminium bronze AK2 were: Cu- 78,37%; Al- 10,52%; Fe- 4,44%; Ni- 5,16% and for the AK3 alloy: Cu- 78,95%, Al- 10,97%; Fe- 4,16%; Ni- 4,83%. The response of the samples was assessed in terms of their microstructural features and mechanical properties. The figure shows microstructural characteristics of the as cast Aluminium bronze. It shows a granular structure (50× and 200×). Different microconstituents such as the primary α, eutectoid α+γ_2 and Fe-rich phase are shown.

Fig. 2 shows a microstructure of the samples solutionized at 950 °C. Solutionizing at this temperature for two hours led to the breaking of the as cast structure and dissolution of the eutectoid and primary precipitates in the matrix forming coarser β.

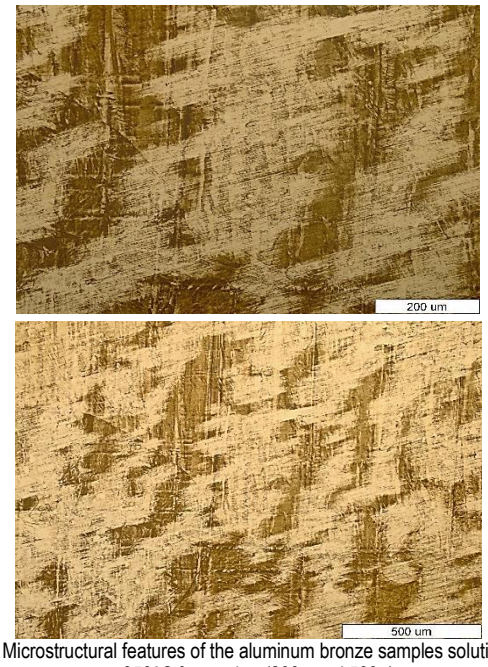

Figure 3 Microstructural features of the aluminum bronze samples solution treated at 950°C for two hrs (200× and 500×)

The microstructures of the samples tempered at 300 °C for two hours are shown in Fig. 3. Tempering at 300 °C for two hrs caused the precipitation of the γ_2 phase in a uniform manner along with some (undissolved) grain boundary precipitates. Increasing the tempering temperature to 400 °C caused a more effective formation of the eutectoid phase, along with a better defined lamellae of the γ_2 phase compared to that at 300 °C.

The heat treated (solutionized and tempered) samples attained a significantly higher hardness than that of their as cast counterpart. The hardness of the solutionized samples tended to increase at the higher temperature (950 °C), while the tempered samples attained the highest hardness amongst all (as cast, solution treated and tempered). Increasing the tempering temperature up to 400 °C led to a decreased hardness. Solutionizing caused the elimination of the as cast structure and microstructural homogeneity along with the formation of a mainly martensite. Increasing the solutionizing temperature of the solution treatment brought about a more effective dissolution of the as cast

microconstituents initially and coarsening of the resulting microconstituents at the latter stages. Similarly, tempering brought about the formation of the eutectoid phase at the cost of the previously formed martensite. A rise in the temperature of tempering led the eutectoid transformation to take place more effectively along with the formation of a better defined lamellae of the (eutectoid) phase and dissolution of the grain boundary precipitates. Solutionizing at 950 °C for two hours led the alloy to attain the highest hardness in the category of solutionized samples, while tempering at 300 °C for two hours offered the maximum hardness amongst the tempered samples. The results of the scanning electron microscope with the EDX analysis are shown in Fig. 5.

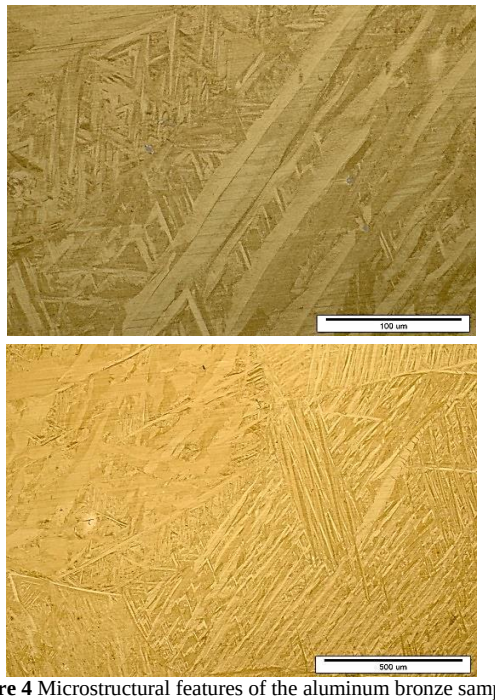

Figure 4 Microstructural features of the aluminum bronze samples tempered at 300 °C for two hours (100× and 500×)

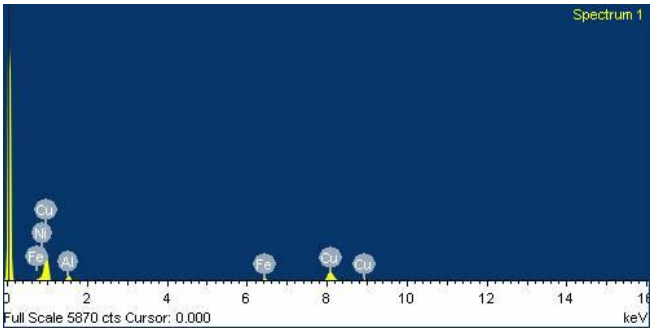

Figure 5 EDX analysis of the examinated alloy

4 DISCUSSION

The microstructural features of the as cast Aluminium bronzes are controlled by the solidification behaviour of the alloy system and the cooling conditions employed during the alloy preparation. Interestingly, equilibrium phases (according to Cu-Al phase diagram) are formed at slow cooling rates such as 500 °C per hour (sand casting of thick sections). Accordingly, the equilibrium of a cast structure comprises of a primary α phase, eutectoid $\alpha+\gamma_2$ and Fe-rich phases (Fig. 2). However, the cooling rates much higher than that of the equilibrium one are generally experienced in practice. This leads to the generation of martensite or bainite depending on the rate of cooling. The presence of Fe leads to microstructural refinement, improved thermal stability, superior mechanical properties through precipitation hardening, restricted growth of grains at high temperatures [6] and a suppressed formation of the unwanted $\alpha+\gamma_2$ phase; the γ_2 phase is hard and brittle and produces embrittlement in the alloy system [7]. Fe-rich particles (Fig. 3) are formed in the temperature range of 350-400 °C [8]. Furthermore, it is not possible to obtain a fully martensitic structure in the alloys even at very high quenching rates [8] since Fe is enriched in the α - phase. This enables Fe to stabilize the α phase and hence suppress the martensitic transformation and favour the formation of bainitic structures [7]. During solutionizing, heating to above 950 °C leads to the generation of 100 % β. Most of the β phase is built up after a few minutes (Fig. 3) at the solution temperature. Prolonged soaking at this temperature leads only to minor changes in the direction of the equilibrium state [8]. The diffusion rate of Al in the β phase is much higher than in the α phase [8]. Accordingly, if there is an α-phase in the structure, there will be no grain growth. Only after a complete dissolution of the α phase does a rapid growth in the grain size occur (Fig. 2) by producing grain sizes in the region of a few millimetres [8]. In complex alloys containing Fe, the solution-treatment temperature has been found to have a significant influence. An increase in the solutionizing temperature leads to the dissolution of more particles; hence higher strength and lower ductility are achieved after subsequent cooling [8]. Holding below ~950 °C results in an increasing amount of β co-existing with α and therefore the quenched alloy has an increasing amount of soft α present. The characteristics of Aluminium bronzes are sensitive to their microstructural features and chemical compositions. The type and parameters employed during the heat treatment also greatly control their microstructural features. Higher hardness of the solutionized alloy samples than that of the as cast specimens could be attributed to the structural homogenization and solid solution hardening and strengthening as also agreed by the formation of martensite or bainite as a result of quenching after solutionizing. Furthermore, higher hardness of the tempered alloy compared to that of the solutionized samples could have resulted from the precipitation of the eutectoid $\alpha+\gamma_2$, which is harder than that of the martensite or bainite formed after solutionizing (Fig. 4). It has been observed that martensite in the case of Cu-Al alloys is slightly softer than that of the corresponding eutectoid ($\alpha+\gamma_2$) phase, the latter in view of the high hardness of the γ_2 phase. Moreover, a reduction in hardness at an increasing tempering temperature was a result of the coarsening of the eutectoid phase. It has been suggested that even though the eutectoid phase is harder than that of the β (martensite), the large amount of primary

α may make the alloy softer even after the formation of the eutectoid phase. The properties of the Cu-Al alloys containing a primary α depend on the grain size and shape of the primary α phase. Moreover, coarser primary α grains reduce the strength and ductility significantly despite the identical hardness values. Rapid cooling from a temperature below the eutectoid one causes the formed structure to offer the minimum strength and a low ductility. The highest strength at a low ductility in a quenched alloy is caused by the formation of the martensite phase. Higher hardness is observed with increasing tempering temperatures from 300 °C to 400 °C in Cu-Al-Fe alloys due to the precipitation hardening. Aluminum bronze attains excellent hardness, tensile and compressive strength at room temperature. From the above detailed discussion, it emerges that the microstructural features of Aluminium bronzes are very much sensitive to their processing steps and associated parameters such as temperature, cooling rate and the duration of processing/treatments. Moreover, the response of the bronzes very much depends on the nature of various microconstituents and their volume fraction and morphology (shape and size). Accordingly, it becomes imperative to exercise due care in optimizing the processing parameters and analyzing the results.

5 CONCLUSIONS

This paper presents conclusions drawn from the results obtained and observations made in this research. The conclusions relate to the microstructural alterations brought about by the heat treatment involving solutionizing and tempering and the corresponding changes in the mechanical properties such as hardness. The conclusions drawn from the research are as follows:

a) The alloy displayed the primary α, eutectoid $\alpha+\gamma_2$ as well as the retained β and martensite β'. Heat treatment led to microstructural alterations significantly depending on the type and parameters employed. For example, solutionizing brought about microstructural homogenization through the disappearance of the as cast structure. The degree of (microstructural) homogeneity increased with the increasing duration and temperature of solutionizing. The coarsening of phases was also observed, especially at higher temperatures and durations of the treatment. Tempering caused the formation of the eutectoid phase, along with the retained/untransformed martensite and microconstituents displayed α. Tempering at 400 °C led to the transformation of martensite into the stable eutectoid structure with a better defined lamellae, while the lamellae were not so well defined at 300 °C.
b) The hardness of the samples improved after heat treatment, compared to the one in as cast condition. Solutionizing temperature showed an increase in hardness. Tempered samples attained the highest hardness amongst all. Moreover, the hardness tended to decrease with the increase of tempering temperature up to 400 °C.

The paper suggests that the microstructural features and mechanical properties of the samples get significantly affected by the heat treatment. The type (solutionizing and tempering) and parameters (temperature and duration) of heat treatment also affected the characteristics of the sample to a considerable extent. Accordingly, it emerges from the study that it is possible to obtain the desired combinations of properties through optimizing the heat treatment type and parameters.

Note: This research was presented at the International Conference MATRIB 2017 (29 June - 2 July 2017, Vela Luka, Croatia).

6 REFERENCES

[1] https://en.wikipedia.org/wiki/Aluminium_bronze
[2] Brezina, P. Gefügeumwandlungen und mechanische Eigenschaften der Mehrstoff-Aluminiumbronzen vom Typ CuAl10 Fe5 Ni5. // Giesserei-Forschung, 25, 3(1973), pp. 1-10.
[3] https://www.copper.org/resources/properties/microstructure/al_bronzes.html
[4] Abdul Hameed, K.; Pravin, K. Singh effect of Heat Treatment parameters on Mechanical Properties of Cu-Al-Fe Alloy. // International Journal of Metallurgical & Materials Science and Engineering (IJMMSE), 5, 6(2015), pp. 19-30.
[5] Pisarek, B. P. Effect of Annealing Time for Quenching CuAl7Fe5Ni5W2Si2 Bronze on the Microstructure and Mechanical Properties. // Archives o f Foundry Engineering, 12, 2 (2012), pp. 187-204.
[6] Gupta, R. K.; Ghosh, B. R.; Sinha, P. P. Choice of heat treatment mode for increasing the hardness of Cu – 9% Al – 6% Ni – 5% Fe alloy. // Metal Science and Heat Treatment, 47, (2005), pp. 526-528.
[7] Alam, S.; Marshallt, R. I.; Sasaki, S. Metallurgical and tribological investigations of aluminum bronze bushes made by a novel centrifugal casting technique. // Tribology International, 29, 6(1996), pp. 487-492.
[8] Brezina, P. Heat treatment of complex aluminum bronzes. // Int. Met. Rev., 27, 2(1982), pp. 77-120.

Authors' contacts:

Božidar MATIJEVIĆ, PhD, Full Professor
Faculty of Mechanical Engineering and Naval Architecture,
University of Zagreb,
Ivana Lučića 5, 10000 Zagreb, Croatia
bozidar.matijevic@fsb.hr

Thota Surya Krishna SUSHMA,
National Institute of Technology Karnataka,
Srinivasnagar PO, Surathkal, Mangalore 575025, India

B. K. PRATHVI
National Institute of Technology Karnataka,
Srinivasnagar PO, Surathkal, Mangalore 575025, India

ISSN 1846-6168 (Print), ISSN 1848-5588 (Online)
ID: TG-20170816143931

Original scientific paper

THERMAL, SURFACE AND MECHANICAL PROPERTIES OF PCL/PLA COMPOSITES WITH COCONUT FIBRES AS AN ALTERNATIVE MATERIAL TO PHOTOPOLYMER PRINTING PLATES

Dino PRISELAC, Tamara TOMAŠEGOVIĆ, Sanja MAHOVIĆ POLJAČEK, Tomislav CIGULA, Mirela LESKOVAC

Abstract: In this paper, methods of thermal, mechanical and surface analyses of biodegradable PCL/PLA composites with the addition of different concentrations of coconut fibres were performed. The aim was to assess the potential of these composite materials for the relief-printing plates as an alternative to classical photopolymer materials. Differential scanning calorimetry, surface free energy calculations and hardness measurements were performed on the samples. Results have shown that most thermal transitions that are characteristic for PLA and PCL do not take place in the area of temperatures applicable in the printing process. Most thermal transitions were not affected by the addition of coconut fibres. Coconut fibres in the composite structure contributed to the increased hardness of the material. Moreover, the hardness range of the prepared PCL/PLA composites was within the range of some classic photopolymer printing plates. By adding coconut fibres in higher concentrations, surface free energy of the materials decreased, which enables a wider application of the material for the production of printing plates. From the obtained results it can be concluded that there is a potential for the use of PCL/PLA biodegradable composite materials in the manufacture of various relief-printing plates for different printing techniques (letterpress, embossing, label printing).

Keywords: biodegradable material; coconut fibres; PCL; PLA; relief printing

1 INTRODUCTION

The application of biodegradable materials in the past years has increased in various industries, from the medical, automotive and agricultural applications to graphic technology, which uses a large proportion of biodegradable materials, primarily in the development of packaging and 3D printing. In the production of printing plates, biodegradable materials were used in the beginning of the development of relief, specifically flexographic printing, when the printing plates were made of rubber. In the middle of 20th century, synthetic polymers have been introduced to graphic technology and quickly replaced natural materials. Until today, most printing plates for various types of relief printing are produced using synthetic photopolymer materials. Printing plates made of photopolymer materials differ in composition, hardness and thickness depending on the printing substrate, the image to be printed and used printed ink. There are three main types of printing inks: solvent-based, water-based and UV-curable, so it is important to choose the printing plate material that will be compatible with the printing ink.

Biodegradable materials are subject to conversion process to water, biomass, carbon dioxide or methane, affected by micro-organisms. They can be of natural or synthetic origin. The process of biodegradation of materials consists of two phases. The first stage is the reduction of the polymer chain by breaking carbon bonds in the conditions of heat, humidity and the presence of microorganisms. The second phase of biodegradation begins when low-molecular carbon chains become energy sources for microorganisms.

Polycaprolactone (PCL) (Fig. 1) is a biodegradable polymer of synthetic origin. It was synthesized in the early 1930s. It is a hydrophobic and a semi-crystalline polymer. Its crystallinity is reduced by the increase in molecular mass. It has a low melting point, at 60 °C, and the glass transition temperature of −60 °C. In order to increase the resistance to cracking it can be mixed with other polymers, such as cellulose propionate, cellulose acetate, butyrate and polylactic acid.

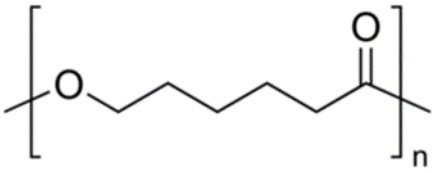

Figure 1 Structural formula of PCL [1]

Because of its properties, it has great potential for use in medical purposes where it is most explored in the field of artificial tissue creation. PCL is biodegradable in nature by bacteria and fungi, but is not degradable within a human or animal organism because of the lack of certain enzymes. Pure PCL requires two to four years to completely disintegrate, depending on the molecular weight of the polymer [2].

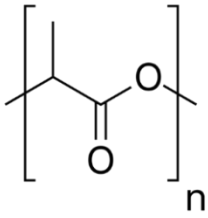

Figure 2 Structural formula of PLA [4]

Polylactic acid (PLA) (Fig. 2) is one of the most widely used biodegradable aliphatic polymers today. It was discovered in the 19th century. It is classified as

thermoplastic polyester. It can be obtained from lactic acid by the fermentation of agricultural crops such as maize. The melting temperature of PLA is 170 °C, while the glass transition temperature is about 60 °C. It is thermally unstable, and above the melting temperature, its thermal degradation begins [3].

PLA is soluble in chlorinated solvents, benzene, tetrahydrofuran and dioxane [5]. The time of biodegradation of polylactic acid in commercial composting plants is from 3 to 6 months [6]. Share of PLA is growing in the production of environmentally friendly packaging materials. It is also used in medicine to make bolts that are embedded in the joints, knees, arms, and rods for ligaments [7]. In 2012, about 180 thousand tons of PLA were produced, and by 2020 this figure would reach up to one million tons in one year [8].

The aim of this paper is to assess the applicability of the environmentally friendly printing plate made of PCL/PLA composites an alternative to conventional photopolymer materials.

Specifically, the new approach to the printing plate production primarily intended for embossing will be achieved through the adjustment of the composition of mixture of biodegradable polylactic acid (PLA) and polycaprolactone (PCL) to meet the necessary qualitative properties. In addition, natural coconut fibres will be added to the produced material in order to improve the mechanical properties of the polymer composite needed for the usage as a printing plate material.

2 EXPERIMENTAL RESEARCH

2.1 Preparation of samples

For this research, 16 PCL/PLA composite samples were prepared (Tab. 1). They were mixed in the Brabender kneader. Weight of all the samples was 40 grams because that is the volume which kneader can take in. The kneader consists of two connected chambers in which the rollers rotate in the opposite direction with narrow interspace along the wall. Walls and rollers are heated by heater.

The samples were placed in the kneader at a temperature of 190 °C because at that temperature the complete melting of PLA will occur. The kneader speed was 60 rpm. The samples were mixed for 5 minutes after which they were taken away and cut into pieces (Fig. 3). Afterward, the tiles were made of cut samples in press at a temperature of 190 °C and a pressure of 16 MPa. The dimensions of tiles were 10 × 10 cm. The pressing procedure lasted for 7 minutes - 2 minutes of preheating and 5 minutes of pressing. Obtained tiles were ready for further tests after cooling. From the tiles, the samples of weight of about 10 milligrams were cut for the differential scanning calorimetry (DSC). For measuring the contact angle and hardness, 1 × 10 cm samples were cut.

Figure 3 Cut samples for press

Table 1 List of the samples

Sample number	Sample name
1	PCL-0
2	PCL + 0.5 % of fibres
3	PCL + 1.5 % of fibres
4	PCL + 3 % of fibres
5	PCL/PLA 90 %/10 %
6	PCL/PLA 90 %/10 % + 0.5 % of fibres
7	PCL/PLA 90 %/10 % + 1.5 % of fibres
8	PCL/PLA 90 %/10 % + 3 % of fibres
9	PCL/PLA 80 %/20 %
10	PCL/PLA 80 %/20 % + 0.5 % of fibres
11	PCL/PLA 80 %/20 % + 1.5 % of fibres
12	PCL/PLA 80 %/20 % + 3 % of fibres
13	PCL/PLA 70 %/30 %
14	PCL/PLA 70 %/30 % + 0.5 % of fibres
15	PCL/PLA 70 %/30 % + 1.5 % of fibres
16	PCL/PLA 70 %/30 % + 3 % of fibres

2.2 Methods of measurement and analysis

Methods of measurement and analysis used in this paper were differential scanning calorimetry (DSC), material hardness measurement, and determination of surface free energy. List and characteristics of the devices used in this paper are shown in Tab. 2.

Differential scanning calorimetry (DSC) is one of the thermal analysis methods. It is used for measuring thermal flow difference between the sample and the reference material during the exposure of the sample to a controlled temperature and atmosphere.

Table 2 List of used devices

Name of the device	Technical characteristics of the device
DSC Mettler Toledo 823e	Temperature data: temperature range with internal refrigerator from −90 to 450 °C, temperature accuracy from ±0.2K, heating speed from 0.01 to 300 K/min; cooling speed from 0.01 to 50 K/min; calorimetric data: sensor type – ceramic, number of thermocouples – 56, resolution – 0.04 μW, measuring speed – max. 50 values per second.
Goniometer Dataphysics OCA 30	Contact angle: 0 ÷ 180°; ± 0.1° Surface tension: $10^{-2} \div 2\times10^{3}$ mN/m resolution: ± 0.01 mN/m USB-CCIR camera: 768 × 576 pixels FOV: 1.32 × 0,99 ÷ 8.50 × 6.38 mm Integrated thermometer: −60 ÷ 700 °C
Durometer Zwick Roell	Shore A and Shore D scale

The material used as the reference sample is aluminium oxide (Al_2O_3). DSC analysis has ability to monitor the transformations in the solid state, phase changes and to determine the thermodynamic parameters during the controlled heating and cooling of the sample. The parameters that can be determined by DSC analysis are glass transition temperature, crystallization temperature, melting temperature, polymer crystallinity percentage, specific heat capacity, transformation enthalpy and many others [9].

The device used in this paper was Mettler Toledo 823e. The samples of the weight of about 10 mg were put in an aluminium bowl, hermetically sealed by a press and then placed in a device where glass transition temperature, melting temperature, crystallization temperature and possible changes caused by coconut fibre were determined. The tests were conducted in a stream of nitrogen at the flow rate of 50 cm^3/min with refrigerator cooling with heating/cooling rate of 10 °C/min. Measurements were performed in two heating cycles and one cooling cycle in a temperature range of −90 to 200 °C. First heating cycle was performed to erase the thermal history of the sample preparation [10, 11].

Hardness of the material is defined as the ease with which the material can be cut, punctured or subject to abrasion. The process is carried out by placing few layers of polymer (minimal height is 4 mm) at top of one another and placing them beneath the needle. The hardness value is being read on the digital screen on the Shore A scale [12]. The device used in this measurement was durometer Zwick Roell. Eight measurements were performed for each of 16 samples and average value of the Shore A hardness has been calculated.

To determine the surface free energy of biodegradable printing plates, it was first necessary to determine the contact angles for the three reference liquids: water, diiodomethane and glycerol. Contact angle measurements were performed by means of goniometer Dataphysics OCA 30.

The contact angle was measured using Sessile drop method. Eight drops of every liquid were applied at the different places on the sample. The drop volume was 1 μm. Average value of the contact angle was calculated for each of the three liquids and then surface free energy of biodegradable printing plates was calculated by OWRK method which is suitable for this type of the material [13, 14].

3 RESULTS AND DISCUSSION

3.1 Differential scanning calorimetry

The results of DSC measurements for all samples are presented in Tab. 3. They were obtained from the DSC diagrams. As an example, Fig. 4 presents the DSC diagram of the 16th sample (PCL/PLA 70 %/30 % + 3 % of fibres). DSC diagram of 16th sample shows three thermograms. Red thermogram represents the first heating cycle, green thermogram represents the second heating cycle and blue thermogram represents the cooling cycle. The first and the second heating cycles have 4 transitions.

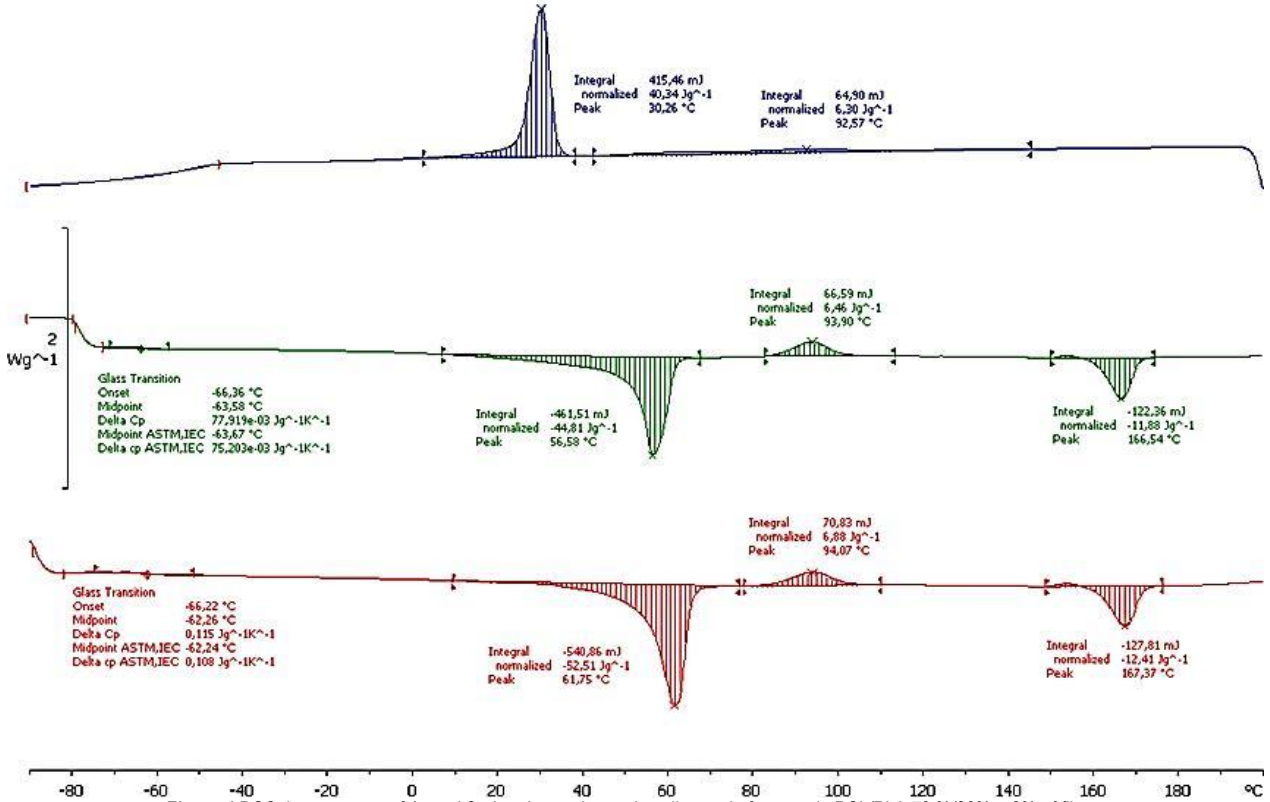

Figure 4 DSC thermograms of 1st and 2nd heating cycles and cooling cycle for sample PCL/PLA 70 %/30% + 3% of fibres

Table 3 DSC data for PCL/PLA mixtures, 2nd heating cycle

Share of PCL/PLA / Share of fibres		PCL			PLA				
		T_g / °C	T_m / °C	ΔH_m / J g^{-1}	T_g / °C	T_{cc} / °C	ΔH_{cc} / J g^{-1}	T_m / °C	ΔH_m / J g^{-1}
PCL	0 %	−63.21	57.06	−74.43	/	/	/	/	/
	0.5 %	−62.66	56.92	−71.42	/	/	/	/	/
	1.5 %	−63.70	57.90	−69.87	/	/	/	/	/
	3 %	−63.41	56.94	−70.46	/	/	/	/	/
PCL/PLA 90/10	0 %	−62.72	58.03	−67.66	*	96.84	2.10	167.79	−3.72
	0.5 %	−62.96	57.07	−63.88	*	91.71	1.86	166.68	−3.61
	1.5 %	−63.70	56.77	−57.64	*	90.43	1.26	166.41	−4.08
	3 %	−62.20	56.80	−55.29	*	90.13	2.29	166.28	−3.75
PCL/PLA 80/20	0 %	−57.33	57.62	−52.82	*	98.28	4.80	168.26	−7.38
	0.5 %	−63.20	57.10	−53.13	*	94.42	3.81	167.22	−7.87
	1.5 %	−61.10	57.38	−52.49	*	94.36	4.21	167.65	−8.49
	3 %	−62.62	56.93	−53.10	*	91.91	4.57	166.72	−7.84
PCL/PLA 70/30	0 %	−63.95	56.61	−43.83	*	99.43	8.29	167.75	−11.97
	0.5 %	−62.84	56.76	−47.88	*	99.75	6.04	167.39	−11.56
	1.5 %	−63.50	56.81	−43.55	*	95.47	7.41	167.12	−11.48
	3 %	−63.67	56.58	−44.81	*	93.30	6.46	166.54	−11.88

It can be seen in Fig. 4 that first transition is at −63.37 °C and it represents the glass transition temperature. Next transition is in the interval from 0 to 70 °C and it represents PCL melting. Endothermic peak of melting is at 56.58 °C. Third transition is cold crystallization of PLA in the interval from 80 to 110 °C. Exothermic peak of cold crystallization is at 93.90 °C. The last transition is PLA melting. It begins at 150 °C and ends at 180 °C. Endothermic peak of PLA melting is at 166.54 °C. Thermogram of cooling cycle shows two transitions. The first is PCL crystallization in the interval from 0 to 40 °C with exothermic peak at 30.26 °C and the second one is PLA crystallization which begins at 50 °C and ends at 130 °C with exothermic peak at 92.57 °C.

Tab. 3 shows results of the second heating cycle from DSC analysis for all the samples. In the table one can find values of PCL glass transition temperature (T_g), PCL melting temperature (T_m), PCL melting enthalpy (ΔH_m), PLA cold crystallization temperature (T_{cc}), PLA cold crystallization enthalpy (ΔH_{cc}), PLA melting temperature (T_m), and PLA melting enthalpy (ΔH_m). PLA glass transition temperature (T_g) is marked with asterisks, which means it could not be determined because it overlaps with PCL melting interval.

Table 4 DSC data for PCL/PLA mixtures, cooling cycle

Share of PCL/PLA / Share of fibres		PCL		PLA	
		T_c / °C	ΔH_c / J g^{-1}	T_c / °C	ΔH_c / J g^{-1}
PCL	0 %	27.25	66.49	/	/
	0.5 %	27.76	62.93	/	/
	1.5 %	30.25	60.52	/	/
	3 %	28.78	60.47	/	/
PCL/PLA 90/10	0 %	32.05	59.63	59.20	0.07653
	0.5 %	31.41	54.69	/	/
	1.5 %	31.78	52.97	/	/
	3 %	31.97	48.70	60.46	0.36
PCL/PLA 80/20	0 %	31.79	50.68	61.45	1.34
	0.5 %	30.94	45.34	95.42	3.07
	1.5 %	30.90	48.19	94.36	6.92
	3 %	30.77	44.14	92.74	3.18
PCL/PLA 70/30	0 %	30.62	42.10	60.78	4.06
	0.5 %	30.77	41.44	91.42	5.79
	1.5 %	30.48	37.43	59.14	3.86
	3 %	30.26	40.34	92.57	6.30

Tab. 4 shows results of cooling cycle from DSC analysis for all samples. In the table one can find values of PCL crystallization temperature (T_c), PCL crystallization enthalpy (ΔH_c), PLA crystallization temperature (T_c), and PLA crystallization enthalpy (ΔH_c). It is possible to conclude that the addition of coconut fibres causes changes in some of the thermal properties of the prepared composites. Specifically, the fibre addition does not significantly affect the glass temperature, nor does the melting temperature, as expected.

This result suggests that the addition of coconut fibres to the polymeric mixture does not significantly affect the mobility of the polymer in the polymer network. Visible changes are present in the cold crystallization temperature and enthalpy of crystallization for all measured samples and in the melting enthalpy for the PCL/PLA 90 %/10 % sample. The values are shifted to lower points after addition of higher fibre concentration, which is common for composite materials.

3.2 Measurement of hardness

Shore A method of hardness measurement showed the highest hardness of sample PCL/PLA 70 %/30 % + 0.5 % of fibres, 92.7 (Fig. 5). Lowest hardness was measured on sample PCL/PLA 90 %/10 % + 3 % of fibres - 86.98. However, a decrease in hardness of the sample PCL/PLA 90 %/10 % + 3 % of fibres can be attributed to measuring method due to high concentration of fibres in tough polymer material. Due to the surface structure which is created by fibres in higher concentration in material, measurement of hardness can be difficult and give imprecise result.

Except for the sample that deviates from the trend, it is possible to conclude that coconut fibres in polymer structure contribute to the increased hardness of the material. The highest general hardness of the material, regardless of the amount of added fibres, is present for the sample with the highest share of PLA. Also, the hardness range of tested polymer materials is within the range of some classical photopolymer printing plates. Therefore, it is possible to conclude that by a combination of ratios of PCL and PLA

and the amount of added fibres it is possible to adjust the hardness of material to the needs of the printing plate.

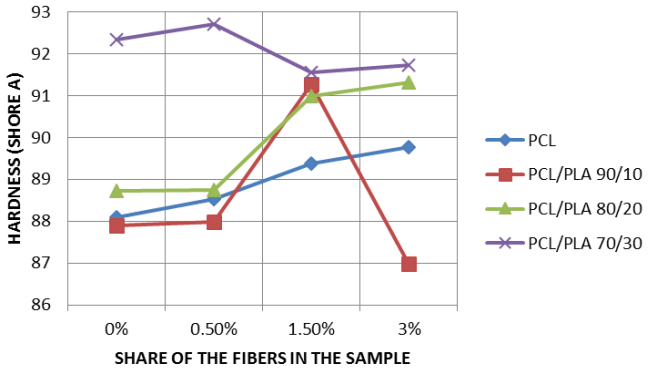

Figure 5 Material hardness (Shore A)

3.3 Calculation of surface free energy

The highest surface free energy was calculated for the sample PCL/PLA 80 %/20 % + 1.5 % of fibres and its value is 41.92 mN/m. The lowest surface free energy was calculated for the sample PCL + 3 % of fibres and its value is 33.1 mN/m (Fig. 6).

It is possible to conclude that the addition of coconut fibres in higher concentrations causes the decrease in free surface energy. The possible cause of that is shortening of the chains in the polymer network, and the properties of the fibres. This change of the surface properties of tested material is actually positive in the terms of applicability for the production of the relief printing plate.

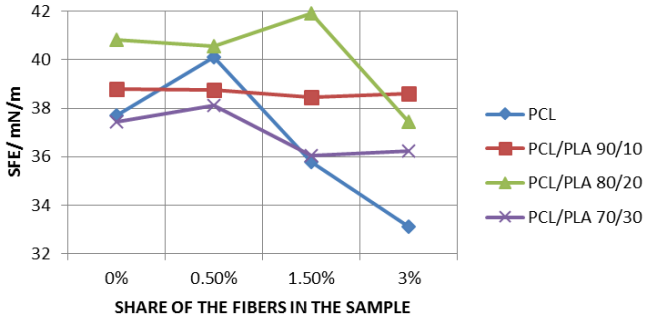

Figure 6 Surface free energy of samples

Namely, the surface free energy range of photopolymer printing plates for some relief printing techniques is in the range of measured surface free energy of PCL/PLA mixtures with fibres. Needed surface free energy of the photopolymer printing plate depends on the type of printing ink which will be used (solvent-based, water-based or UV-curable ink). Consequently, the results show that by choosing the right ratio of used biodegradable polymers in mixture and amount of coconut fibres it is possible to obtain the desired surface free energy of material and ensure its application in form of relief printing plate.

4 CONCLUSION

In this paper, thermal, mechanical and surface analyses of biodegradable PCL/PLA composites with the addition of different coconut fibres weight shares were carried out. The aim was to use different methods of measurement and analysis to determine potential applicability of used materials for production of the relief printing plate as an alternative to conventional photopolymer materials. From the research results of this paper, the following can be concluded:

- Most thermal changes characteristic for PLA and PCL do not take place in the applicable temperature range for relief printing. Exceptions are: PCL melting temperature at 60 °C which is not affected by the addition of fibres – this prevents the application of the obtained material for the foil stamping; second is PCL crystallization temperature during the cooling cycle at 30 °C. The influence of crystal transition on surface properties of the polymer mixtures should be examined in the following research;
- Coconut fibres in the composite structure contribute to the increased material hardness. The hardness range of the tested polymers is within the range of some classical photopolymer printing plates, so it can be concluded that the combination of PCL and PLA ratios and specific amount of added fibres enable adjustment of the material hardness;
- Addition of coconut fibres in higher concentrations causes the decrease in free surface energy which is positive change in terms of application for the production of relief printing plate. Surface free energy range of photopolymer printing plates is within the range of the measured surface free energy of PCL/PLA mixtures with fibres. Furthermore, calculated surface free energy is in the range applicable for the relief printing application;
- Materials produced and tested in this research have the potential for the application for various types of relief printing plates (letterset, embossing, printing plates for label printing).

Note: This investigation was presented at the International Conference MATRIB 2017 (29. 6. - 2. 7. 2017, Vela Luka, Croatia).

5 REFERENCES

[1] http://www.sigmaaldrich.com/catalog/product/aldrich/440744?lang=en&region=US (Accessed on 2 June 2017)

[2] Woodruff, M. A.; Hutmacher, D. W. The return of a forgotten polymer - Polycaprolactone in the 21st century. // Progress in Polymer Science, 35-10, pp. 1217-1256 (2011).

[3] Ebnesajjad, S. Handbook of Biopolymers and Biodegradable Plastics, 1st edition, Elsevier, 2012.

[4] https://en.wikipedia.org/wiki/Polylactic_acid (Accessed on 29 May 2017)

[5] Garlotta, D. A Literature Review of Poly(Lactic Acid). // Journal of Polymers and the Environment, 9, 2(2001), pp. 63-84.
[6] https://www.biogreenchoice.com/category_s/1866.htm (Accessed on 29 May 2017)
[7] Hamad, K.; Kaseem, M.; Yang, H. W.; Deri, F.; Ko, Y. G. Properties and medical applications of polylactic acid. // eXPRESS Polymer Letters, 9, 5(2015), pp. 435-455.
[8] http://www.bakeryandsnacks.com/Processing-Packaging/PLA-bioplastics-production-could-hit-1m-tonnes-by-2020-nova-Institut (Accessed on 30 May 2017)
[9] Kodre, K. V.; Attarde, S. R.; Yendhe, P. R.; Patil, R. Y.; Barge V. U. Differential Scanning Calorimetry: A Review. // Journal of Pharmaceutical Analysis, 3, 3(2014), pp. 11-22.
[10] http://hr.mt.com/dam/LabDiv/Campaigns/gp/gtap/thermal_analysis_of_polymers _en.pdf (Accessed on 2 Jun 2017)
[11] Day, M.; Nawaby, A. V.; Liao, X. J. A DSC study of the crystallization behaviour of polylactic acid and its nanocomposites. // Journal of Thermal Analysis and Calorimetry, 86, 3(2006), pp. 623-629.
[12] https://www.fkit.unizg.hr/_download/repository/Struktura_i_svojstva_materijala-nastavni_materijal.pdf (Accessed on 2 Jun 2017)
[13] Żenkiewicz, M. Methods for the calculation of surface free energy of solids. // Journal of Achievements in Materials and Manufacturing Engineering, 24, 1(2007), pp. 137-145.
[14] Tomašegović, T. Functional model of photopolymer printing plate production process. Doctoral thesis, 2016.

Authors' contacts:

Dino PRISELAC
Tamara TOMAŠEGOVIĆ
Sanja MAHOVIĆ POLJAČEK
Tomislav CIGULA
University of Zagreb, Faculty of Graphic Arts,
Department for Graphic Materials and Printing Plates,
Getaldićeva 2, 10000 Zagreb, Croatia
dino.priselac@grf.hr

Mirela LESKOVAC
University of Zagreb, Faculty of Chemical Engineering and Technology,
Marulićev trg 19, 10 000 Zagreb, Croatia

ISSN 1846-6168 (Print), ISSN 1848-5588 (Online)
ID: TG-20170815201209

Original scientific paper

RECIPE-TECHNOLOGICAL FEATURES OF CARBONIZATION HARDENING OF LIGHTWEIGHT CONCRETE

Aleksandr GARA, Aleksej ANISKIN, Matija OREŠKOVIĆ

Abstract: The work is devoted to researching the parameters of expanded clay lightweight concrete technology by using carbonation hardening that allows to maximally intensify the process of carbonization using methods such as decreasing the total water content in the system, applying optimal structure and formula concrete compositions, processing the products in carbon dioxide environment. The mechanism of structure formation of concrete compositions in conditions of artificial carbonation was studied. It was formulated using the basic techniques of rational intensification of the hardening process. Rational formulation and technological parameters of carbonization technology of lightweight aggregate concrete wall products were proposed: effective replacement of almost 30 per cent of concrete by powdered lime rock in process of carbonization without changing the physical and technical properties of material; the optimal size of porous aggregates; the optimal modes of composite carbonization that include preliminary placement in vacuum and step processing in carbon dioxide environment. The maximum demoulding strength of expanded clay lightweight concrete was received by using maximum concentration of carbon dioxide during carbonization in reaction area that is characterized by the maximum pressure value. In addition, the properties of concrete in an early stage after the carbonization were explored.

Keywords: carbonating hardening; cement stone; compounding-technological parameters; expanded clay lightweight concrete; kinetics of growth of durability.

1 INTRODUCTION

The task of the concrete hardening acceleration becomes very important in developing the saving technologies that save the concrete products. The maximum speed of the concrete hardening can be obtained by treatment compositions in carbon dioxide. The continuous process of carbonization gives an opportunity to make the material with specified properties. To achieve this effect, it is necessary to optimize the recipe and the processing modes.

2 THE PURPOSE AND OBJECTIVES

The purpose of the work is to develop rational technological methods and parameters of the expanded clay lightweight concrete products processed in carbon dioxide that allows getting the material with specified physical and technical properties with minimal duration of hardening.

3 MECHANISM OF STRUCTURING OF THE CEMENT COMPOSITIONS

The increased initial strength of the concrete is connected with acceleration of the hardening process of the cement in the very early period. Slowing the rate of hydration of binders can be explained by formation of a colloidal dispersion of the hydration shells around the grains. The reasons for the formation of such shells are small diffusion coefficients of hydrate neoplasms and supersaturation in the boundary layer that prevents the dissolution of the new cement portions and slows down its hydration and hardening. The supersaturation of the liquid phase of the cement paste is caused by calcium hydroxide. Thus the acceleration of the formation of a new phase and the reduction in the degree of supersaturation can be obtained by using the reaction of compound of calcium oxide with carbon dioxide. Carbon dioxide transforms a stand-lime to practically insoluble calcium carbonate. At the beginning the crystals of such calcium carbonate turn to crystallization basis and then give an additional bond to strengthen the cement stone.

In theory, all calcium-containing components of the cement stone are capable of carbonation. The only exception is the compounds that include $CaSO_4$. The reaction of CO_2 with $Ca(OH)_2$ proceeds with the evolution of one mole of water. As a result, the humid state of the material can be changed. In that case, an exothermic effect that causes intense drying of the system will be favourable. On the other hand, by carbonation hardening water will mostly be the environment in which the dissolution of the initial binder phase and the transportation to a reaction zone take place. The water becomes the main structural part of the emerging neoplasms only when the water carbonates form. Neoplasms were mostly formed in a reaction zone that located at a distance from the surface of the dissolving starting material. Neoplasms can also be formed in a close proximity to the surface of the dissolving starting material if the humidity of the carbonized samples is decreased noticeably. As a result, that will further block the passing reaction and the process will slow down significantly.

Along with hydrates carbonization "carbonate" dissolution of initial minerals can take place [1]. This is due to the fact that the irreversible transfer of $Ca(OH)_2$ to $CaCO_3$ disturbs the dynamic balance between the initial phase and the solute in Ca_2+ ions that leads to intensive dissolution. The selective dissolution and carbonization of the separate component parts of cement occur in the downstream row that matches to the downlink solubility and hydrated oxides of compounds. At first the calcium hydroxide enters into the reaction and is followed by hydrated calcium oxide compounds. In addition to reactions

described above the calcium hydrosilicates polymerization can also take place when CO_2 affects cement paste. That leads to the insoluble polysilicate formation [1].

During carbonation hardening the changes in a moisture state of the material can slow down the carbonization process. Therefore, it is necessary to work out the technological methods that will reduce the water content of concrete compound on the stage of its preparation and that will provide the excess water extraction from the cement matrix during the hardening. Moreover, for the efficient continuous flow of carbonation reaction it is necessary to make an optimally developed structure of the compacted concrete compound. Such structure will enable bulk diffusion of carbon dioxide into the product and, in relation to this, volumetric change of neoplasms on one side and the mudding of the pore structure with neoplasms as a result of the local bulk increase of the solid phase during the carbonization process on the other.

All these actions and the optimization of the binder composition and the processing modes have to provide efficiency of the carbonization process of the product that allows obtaining the material with specified mechanical and physical properties while dramatically reducing the production cycle.

4 THE OPTIMISATIONAL COMPOSITION METHODS

The optimization of the recipe and technological parameters of the carbonized expanded clay lightweight concrete includes the following: working out economical concrete compositions; working out the optimal carbonization modes; researching the possibility to intensify the carbonization process by inserting a binder into the composition (milled limestone) and by decreasing the total water content of the concrete mixture.

The carbonization process can be activated by intensive introduction of gas reagent into the reaction zone. That can be achieved by using carbonization regimes with preliminary vacuuming and subsequent filing of carbon dioxide under pressure. The vacuuming of freshly made concrete provides the creation of rarefaction in capillary-porous system. After that the carbon dioxide pressure drop in the initial period provides the vacuum removal, effective self-consumption of the reagent and the intensification of the carbonization process.

The process of "carbonate" dissolution of initial cement minerals accelerates proportionally to concentration of carbon dioxide in reaction zone. That is why the use of regimes with CO_2 overpressure allows ruling the structuring process of cement compositions. At the same time carbonization of the product under the pressure leads to creation of high satiations in the system and to local increase of the solid phase bulk. That entails the emergence of a significant internal tension and the development of destructive processes in the concrete structure. In these circumstances the use of stepwise pressure rise of CO_2 to the desired value allows to eliminate destructive processes that take place during the single-stage carbonization. It was established experimentally that the use of stepwise pressure rise of CO_2 allows increasing the demoulding strength of the expanded clay lightweight concrete in 10-30 % [2].

The efficient replacement of 20-30 % of the cement on the milled limestone without changing the physical and mechanical properties of the material was found [3]. During the carbonization hardening the basic component of the crystal structure is calcite; the results of the X-ray examination and the differential thermal studies of the cement stone confirmed it. Massive morphological changes arise under the CO_2 effect in the cement matrix. The increase of the pressure, processing time and temperature leads to the matrix compaction and to the reduction of micropores and microcapillaries as compared with untreated samples. The flat, plate-like structures (inherent in portland lime stone) and thin needle-like crystals of ettringite are absent. Instead of them, there are rounded, densely arranged round crystals without any pores and the crystals in the structure of treated samples.

In relation to the aforesaid, it is obvious that crystallization of neoplasm occurs at the surface of carbonate grains. As a result, such carbonate grains accrete with the fused between well-developed crystals of a new phase. The electron microscopic analysis confirmed the lasting nature of accretion between a carbonate rock and a secondary calcite generation. That leads to the structure hardening. The carbonate rock serves as a substrate. That occurs thanks to the proximity of crystallographic cells.

In conditions of carbonization hardening adding of the super plasticizer into the concrete mix provides technological concrete mixtures with low water content. After the cement mixture compaction the dehydration of cement mixture occurs as a result of self-evacuation. In this case the capillaries are exempted from moisture and become gas-proof. The volume of solid increases during the process of binding up CO_2 with hydrolysis products of cement minerals. That process is accompanied by pore structure mudding and leads to the increase of concrete strength.

The increased CO_2 concentration noticeably affects the initial concrete strength in the reaction zone [4]. The increase of the amount of CO_2 pressure from 0.6 to 1.2 MPa leads to increase of the CO_2 concentration and as a result to increase of the concrete strength in one hour after the carbonization of 25-60 %. The increase of the duration of treatment from 30 to 60 minutes leads to increasing concrete strength of 5-20 %. The influence of carbonization regimes on the concrete strength is equalized with increasing concrete age. As a result, the strength of the same dense concrete can vary widely after the carbonization (Fig. 1).

5 EXPERIMENTS AND RESULT DISCUSSION

The four tested lightweight aggregate compositions were selected for researching the growth of the kinetic strength during time. All compositions have different consumption and composition of the binder.

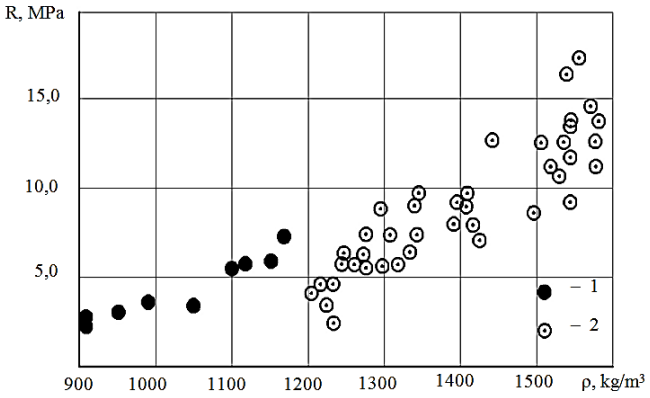

Figure 1 The relationship between the demoulding strength and the density of the carbonized keramsit;
1 – concrete based on expanded clay aggregate gravel ($\rho_{bulk.}$ = 450 kg/m³); 2 – concrete based on expanded clay aggregate gravel ($\rho_{bulk.}$ = 720 kg/m³).

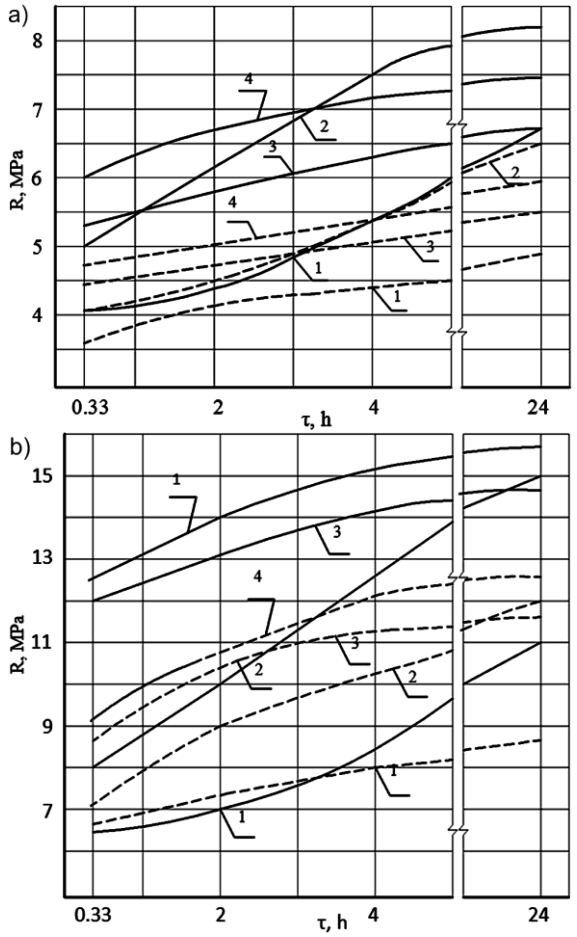

Figure 2 The growth of expanded clay lightweight concrete strength in early age after the carbonization (a – compositions 1 and 2; b – compositions 3 and 4). 1 – carbonization by regime: R_c= 0.6 MPa, τ_c = 20 min; 2 – carbonization by regime: R_c = 0.6 MPa, τ_c = 40 min; 3 – carbonization by regime: R_c = 1,2 MPa, τ_c = 20 min; 4 – carbonization by regime: R_c = 1.2 MPa, τ_c = 40 min.

The analysis of strength changes of expanded clay lightweight concrete in early age (20 min, 2 hours, 4 hours, 24 hours after carbonization) showed the maximal demoulding strength after applying the carbonization regimes with the maximal CO_2 concentration and pressure value in the reaction zone. After applying the carbonization regimes with pressure value 1.2 MPa and carbonization time 20-40 min, the demoulding strength was 70-75 % of the one after 28 days (Fig. 2 a, b).

The decrease of the CO_2 concentration by applying carbonization regimes with pressure value 0.6 MPa provides reaching 50-60 % of the concrete strength of the ones after 28 days for concrete classes B5-B7.5 (compositions 1 and 2) and 34-45 % of the concrete strength for concrete classes B10-B15 (compositions 3 and 4).

The use of porous sands in structurally-insulated concretes leads to producing the products with residual moisture above permissible. During the carbonization process the free water is released with exothermic effect as a result of the chemical interaction of carbon dioxide and hydration and hydrolysis products of binder minerals. In consequence, after the demoulding the residual moisture of the expanded clay, lightweight concrete was 9.4-13.5 % for concretes with 920-1000 kg/m^3 density and 10.6-13.1 % for concretes with 1200-1550 kg/m^3 density. The injection of the superplasticizer allows to reduce the residual moisture by 0.5-3.5 % depending on concrete composition.

6 CONCLUSION

The mechanism of structuring of the cement compositions in conditions of artificial carbonization has been studied. The main rational methods of intensification of hardening process were found.

The rational technological parameters and formulas of carbonization technology of the lightweight aggregate concrete wall products have been offered:

- effective replacement of 30 % of cement by milled limestone without changing the level of indexes of physical and mechanical properties of the material;
- optimal granulometry of porous fillers;
- optimal carbonization regimes that use the preliminary mixture vacuuming and the step processing mode in carbon dioxide.

The maximal demoulding strength has been provided under carbonization regimes with a maximal CO_2 concentration in reaction zone that is characterized by maximal pressure value.

Note: This investigation was presented at the International Conference MATRIB 2017 (29. 6. - 2. 7. 2017, Vela Luka, Croatia).

7 REFERENCES

[1] Ramachadran, V.; Feldman, R.; Boduen, J.: The science of concrete, Stroyizdat, Moskva, 1986.
[2] Michailenko, G. V.; Solomatov, V. I.; Gara, A. A.: The method of manufacturing concrete products, C.A. 1320202 the USSR, MKI C 04 B 40/2., Pub. In B.I., 1987, №24- 6p.
[3] Michailenko, G. V.; Gara, A. A.: The physical and mechanical properties of keramsit that had been hardened under carbonization, Proc. The new effective materials in building, Ashhabad, 1986, 93-94
[4] Lubomirsky, N. V.; Srebnyk, V. M.; Bahtin, A. S.: The building composites on the lime basis of the carbonated hardening type Motrol, Proc. Motoryzacja i energetyka rolnictwa, Simferopol-Lublin, 2009, Vol. 11A., 229 – 238

Authors' contacts:

Aleksandr GARA, PhD
Odessa State Academy of Civil Engineering and Architecture,
4th Didrikhsona str., Odessa, Ukraine
garaogasa@ukr.net

Aleksej ANISKIN, PhD
University North,
Department of Civil Engineering,
104. brigade 3, Varaždin, Croatia
aaniskin@unin.hr

Matija OREŠKOVIĆ, PhD
University North,
Department of Civil Engineering,
104. brigade 3, Varaždin, Croatia
moreskovic@unin.hr

ISSN 1846-6168 (Print), ISSN 1848-5588 (Online)
ID: TG-20170816140212

Original scientific paper

MODIFIED EXPANDED CLAY LIGHTWEIGHT CONCRETES FOR THIN-WALLED REINFORCED CONCRETE FLOATING STRUCTURES

Andrey MISHUTN, Sergii KROVIAKOV, Oleg PISHEV, Božo SOLDO

Abstract: Reinforced concrete floating structures have much more durable metal structures and do not require frequent repairs. Heavy and lightweight shipbuilding concrete is used for these structures. Floating structures are operated in difficult climatic conditions. Properties of modified expanded clay concrete for thin-walled reinforced floating structures were investigated. The experiment was carried out according to the 3-factor optimal plan. Concretes with the strength of up to 43 Mpa, with water resistance up to W12 and the average density of up to 1750 kg/m^3 were obtained. Due to the use of expanded clay lightweight concrete, the carrying capacity of a ship, in particular, the floating dock, is increasing, and the comfort of people and technological equipment is increasing. Regulations for the technology of manufacturing modified shipbuilding expanded clay lightweight concrete for the construction of thin-walled floating structures and floating docks were developed and approved. The results of the research were used in the development of the national standard of Ukraine "Shipbuilding Concrete".

Keywords: expanded clay; floating structures; lightweight concrete; plasticizer; silica fume; water resistance

1 INTRODUCTION

Reinforced concrete has been used to build ships for more than a hundred years. Nowadays, parking floating structures are mainly built from reinforced concrete: docks, wharves, pontoons, houses, hotels and oil platforms. Floating structures are operated in difficult climatic conditions. They are exposed to water, freezing and thawing, sulfate corrosion, and dynamic impacts. Concrete floating structures are much more durable then metal structures and do not require frequent repairs [1].

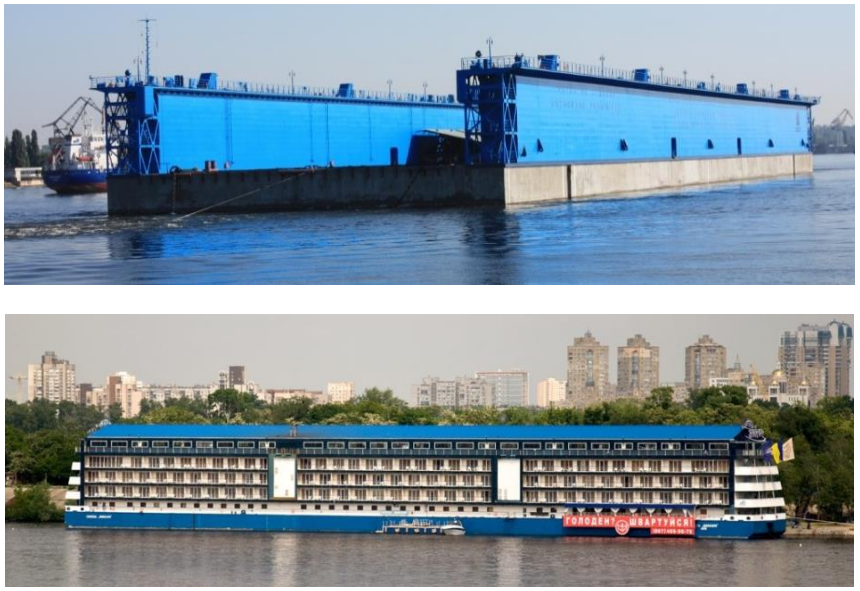

Figure 1 Floating dock and hotel with reinforced concrete pontoons. These structures were built at Kherson state plant "Palada".

Heavy and lightweight shipbuilding concrete is used for reinforced concrete floating structures. The main type of lightweight ship-building concrete is high-strength expanded clay concrete. Through the use of expanded clay weight construction is reduced. Reducing the weight of structures increases the carrying capacity of the floating structure. Morover, the use of lightweight concrete improves the working conditions of equipment and people on a reinforced concrete vessel. In particular, light concrete class LC-60 constructed "Heidun" floating oil platform. This platform operates in the Norwegian sector of the North Sea [2]. Concrete with porous aggregates has shown excellent durability in the harsh operating conditions in waters with sulfates and chlorides. Also, concrete with porous aggregates has a high frost resistance [3]. The first arctic floating structure made of concrete with porous aggregates is the caisson Tarsiut Island in the Beaufort Sea (Canada). It was built for extraction of sand in 1982 and is still in operation [4]. Positive experience was gained in the construction of lightweight aggregate concrete floating

docks in Ukraine at the reinforced concrete shipbuilding Kherson state plant "Palada" (Kherson) [5]. Fig. 1 shows a floating dock and hotel with reinforced concrete pontoons. These structures were built at Kherson state plant "Palada".

Different types of modifiers are used to improve the durability of shipbuilding concretes. Most often, plasticizers, colmatizing additives and active fillers are used. Silica fume is one of the most commonly used modifiers of shipbuilding concretes. It is also important than the silica fume is produced in Ukraine. Accordingly, the study of the properties and durability of modified expanded clay lightweight concrete for thin-walled reinforced concrete floating structures is relevant.

2 MATERIALS AND METHODS

Studies of the shipbuilding expanded clay concrete properties were conducted using the methods of planning the experiment [6]. The experiment was carried out according to the 3-factor 15-point optimal plan.

The following materials were used: sulfate-resistant Portland cement M400, expanded clay gravel fractions 5-10 mm, quartz sand with fineness modulus 2.7, additive superplasticizer S-3 and silica fume. The following factors had varied compositions: x_1 – sulphate-resistant Portland cement, from 500 to 600 kg/m^3; x_2 – silica fume, from 0 to 50 kg/m^3; x_3 – additive S-3, from 0.5 to 1 % of cement weight. All expanded clay lightweight concrete mixes have mobility equal 3 ± 1 cm.

3 RESULTS AND DISCUSSION

As noted above, all the mixtures had an equal mobility of 4 to 6 cm. Therefore, *W/C* ratio of mixtures depended on the composition of expanded clay concrete. According to data obtained at 15 experimental points, an experimental statistical model of the influence of composition factors on the *W/C* was constructed:

$$W/C = 0.318 - 0.025x_1 + 0.012x_2 - 0.032x_3 + 0.022x_1^2 + 0.021x_2^2 + 0.009x_3^2 + 0.007x_1x_3 \quad (1)$$

According to the model (1), a diagram in the form of a cube was constructed, which is shown in Fig. 2. The analysis of the diagram shows that an increase in the amount of Portland cement and the addition of S-3 reduces the *W/C* mixture. With the introduction of silica fume in an amount of up to 30 kg/m^3, the concrete mixture *W/C* varies insignificantly. Increasing the amount of silica fume to 50 kg/m^3 necessitates an increase in the *W/C* or an increase in the amount of the additive S-3 to stabilize the mobility of the mixture.

Fig. 3 shows a diagram that shows the effect of the composition on the compression strength of concrete. This diagram is constructed from a similar (1) experimental-statistical model. The analysis of the diagram shows that the compressive strength of concrete is in the range of 32 to 43 MPa. By increasing the amount of Portland cement expanded clay lightweight concrete strength increases. Addition of 30-35 kg/m^3 of silica fume increase the compressive strength of concrete at average of 2 MPa. This effect is not significant, but the main goal was the addition of silica fume increase water resistance and durability of concrete. With the increasing amount of additive S-3 to 0.8-1 % by reducing the mixture W/C concrete compressive strength is increased by 2-2.5 MPa.

Importantly, expanded clay lightweight concrete has high tensile strength compared with the heavy concrete compressive strength equal. The tested concretes had tensile strength at flexure in the range from 5.6 to 7.0 MPa. This expanded clay lightweight concrete is effective for thin-walled structures.

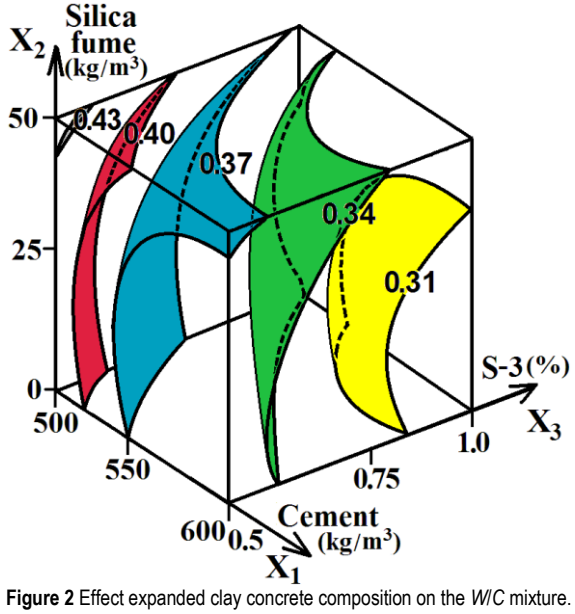

Figure 2 Effect expanded clay concrete composition on the *W/C* mixture.

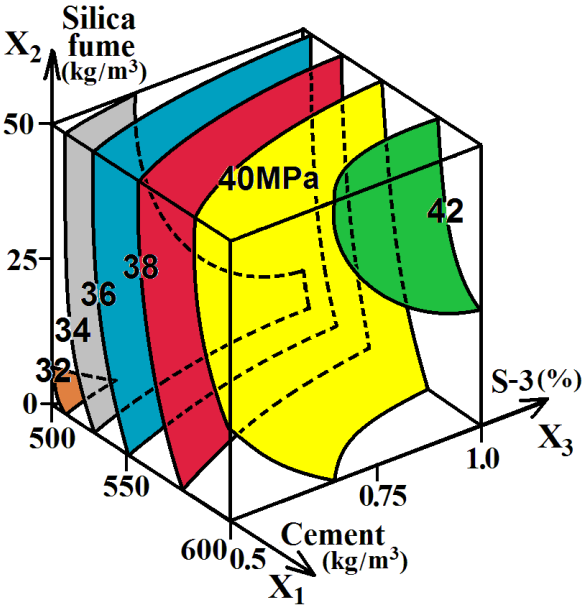

Figure 3 Effect of composition on the compression strength of expanded clay concrete.

Moreover, the water resistance of concrete was investigated. This quality score is very important for concrete floating structures. Water resistance determines the durability of reinforced concrete structures in water. The diagram in Fig. 4 shows the effect of composition factors on the water resistance of concrete.

As it can be seen from the diagram, the amount of Portland cement most significantly affects the level of water resistance concrete. In addition, 30-35 kg/m^3 silica fume concrete increases the water resistance of more than 2 atmospheres. By increasing the amount of superplasticizer S-3 from 0.5 to 0.9 %, the resistance of concrete increases by almost 2 atmospheres. Maximum water resistance was W12. This level of water resistance ensures the durability of concrete.

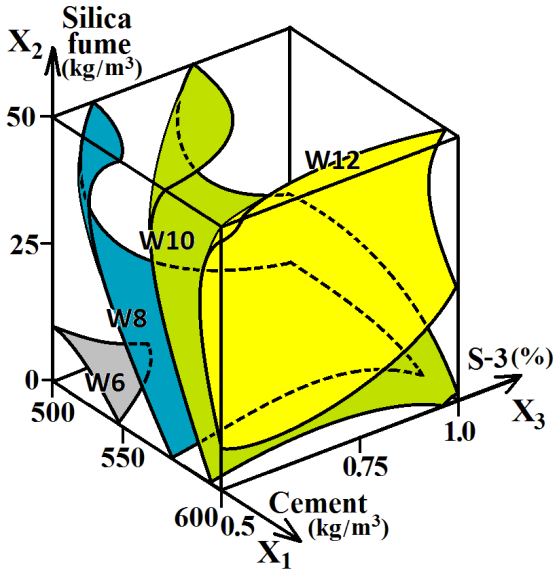

Figure 4 Effect of composition on the water resistance of expanded clay concrete.

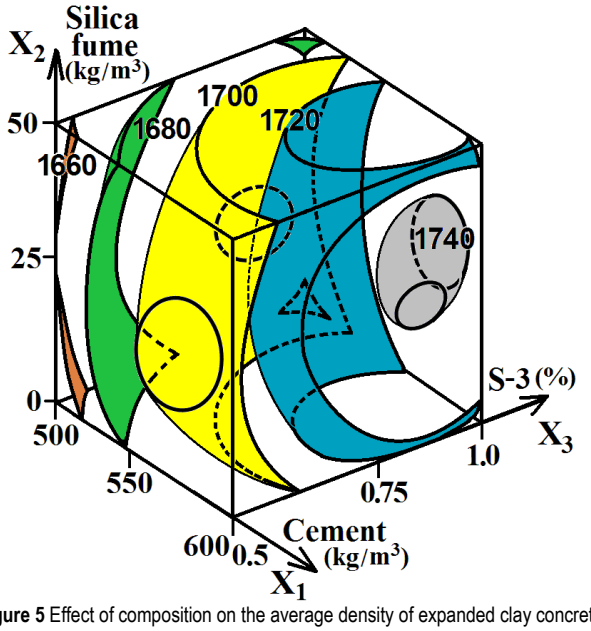

Figure 5 Effect of composition on the average density of expanded clay concrete.

Due to the use of lightweight concrete, the weight of the structures is reduced. This increases the carrying capacity of reinforced concrete floating structures, including floating docks. Fig. 5 is a diagram which shows the effect of the composition on the average density of the concrete in a dry state. As can be seen in the diagram, the density of expanded clay concrete in a dry state was from 1640 to 1750 kg/m^3. The amount of cement and superplasticizer S-3 most significantly affects the density of concrete. Also, the density increases with the addition of silica fume in an amount of 30-35 kg/m^3. It can be concluded that denser concrete had higher strength. After saturation with water, the average density was from 1750 to 1900 kg/m^3. This density corresponds to industrial shipbuilding standards. It was also found that modified shipbuilding concretes had frost resistance of F500 or more.

Therefore, modified expanded clay lightweight concrete complies with Maritime Register and can be used for the thin-walled floating structures. Optimal compositions of shipbuilding expanded clay lightweight concrete have been selected [7]. Technological methods of the production and the use of expanded clay lightweight concrete were developed for thin-walled floating hydraulic engineering structures. The regulations for the technology of manufacturing modified shipbuilding expanded clay lightweight concrete for the construction of thin-walled floating structures and floating docks were developed and approved at State shipbuilding plant "Pallada". Moreover, the results of the research were used in the development of the national standard of Ukraine "Shipbuilding Concrete".

4 CONCLUSION

The compressive strength of shipbuilding expanded clay lightweight concrete is in the range of 32 to 43 MPa. The tensile strength of concrete was in the range of 5.6 to 7.0 MPa. The water resistance of the modified concrete was in the range of W6 to W12, and the average density was from 1640 to 1750 kg/m3. Therefore, modified expanded clay lightweight concrete complies with Maritime Register and can be used for the construction of floating docks, hotels, houses, marinas, oil platforms and other floating structures. The replacement of heavy shipbuilding concrete with expanded clay lightweight concrete increases load-carrying capacity of a ship, in particular a floating dock, and increases people's comfort and technological equipment. In addition, lightweight shipbuilding concrete has high durability.

Note: This investigation was presented at the International Conference MATRIB 2017 (29. 6. - 2. 7. 2017, Vela Luka, Croatia).

5 REFERENCES

[1] Mishutin, A. V.; Mishutin, N. V. Increased durability of concrete of marine reinforced concrete floating and stationary structures. - Odessa: Ewen, 2011. - 292 p. [in Russian]

[2] Helland, S.; Aarstein, R.; Maage, M. In-field performance of North Sea offshore platforms with regard to chloride resistance – Structural Concrete (J. of fib). 2010, Vol. 11, no. 1 – pp. 15-24.

[3] Aïtcin, P.-C. High performance concrete (Modern concrete technology) – E & FN Spon: 2011 – 624 p.

[4] Fitzpatrick, J.; Stenning, D. G. Design and construction of Tarsiut island in the Canadian Beaufort Sea. - 15th Annual offshore technology conference, Houston, United States; Journal Volume: 2; 2-5 May, 1983, Paper No. OTC 4517 – pp. 51-60.

[5] http://www.pallada-doc.com - Official site of Kherson State Plant "Palada" (Accessed on 5 May 2017).

[6] Voznesensky, V. A.; Lyashenko, T. V.; Ogarkov, B. L. Numerical methods for solving construction and technological problems on a computer - Kyiv: High School, 1989. - 327 p. [in Russian]

[7] Increasing the durability of expanded clay lightweight concretes for thin-walled hydraulic engineering structures / V. Mishutin, S. Kroviakov, M. Zavoloka, V. Bogutsky, I. Stanchyk / Meridian Ingineresc, Journal of technical university of Moldova and Moldavian engineering association, 2016, №4 – pp. 42-45.

Authors' contacts:

Andrey MISHUTN
Sergii KROVIAKOV
Oleg PISHEV
Odessa State Academy of Civil Engineering and Architecture,
Department of Design, Construction and Operation of Road,
4 Didrihsona st., 65029 Odessa, Ukraine
skrovyakov@ukr.net

Božo SOLDO
University North,
Department of Civil Engineering,
104. brigade 3, 42000 Varaždin, Croatia

ISSN 1846-6168 (Print), ISSN 1848-5588 (Online)
ID: TG-20170816141410

Original scientific paper

ANALYSIS OF POROUS AND CHEMICAL ADDITIVES EFFECTS ON THE CEMENT-LIME MORTAR PROPERTIES

Khrystyna MOSKALOVA, Marin MILKOVIĆ, Goran KOZINA

Abstract: Cement-lime (CL) mortar has a number of properties and most important property of this mortar type is dependent on the admixtures and aggregates. By varying the ratio of ingredients, the characteristics of CL mortar can be adapted to specific mortar applications. This paper discusses those mortar properties that EU standards and engineers consider important. For each of these properties, the influence of admixtures and aggregates in the mortar is explored. Properties detailed in the paper include bond strength, compressive strength and workability.

Keywords: admixtures; cement; hydrated lime; mortar; workability

1 INTRODUCTION

The main components that form a strong structure of solid plasters based on the dry building mixes (DBM) are binders and fillers. Cement of various brands and lime in hydroxyl form are predominantly used as binders for coating materials. Fillers with rationally selected grading, dispersion and the optimum ratio in the texture composition contribute to the improvement of the quality of the plaster. They also contribute to minimization of added chemical additives, which are the most expensive component. In case the material is a complex system consisting not only of binders and fillers, but also of high molecular substances, its structure will be unique due to the structure and properties of polymer modifiers. This system will not obey the generally accepted idealized laws of recoverability, plasticity, which proceed from the theory of an ideal model of a body possessing the properties of continuity, homogeneity and isotropy.

2 RESEARCH AND RESULTS

The ability to quantitatively describe and analyse the multidimensional relationships between the parameters of mixtures, operating conditions, ratio and technological factors and the properties of materials - the properties of the mixture, characteristics of the structure, operational properties with the purpose of controlling the structure and properties of the material - it is expedient to use computer material science tools based on the concept of property plains [1, 2].

The cement-lime light plaster on the basis of perlite was adopted as a baseline mixture, which is developed by the company "Henkel-Bautechnik (Ukraine)". The composition consists of a polymer-cement mixture containing perlite sand, redispersible powders Vinnapas, as well as water-retaining and air-entraining additives.

The experiment was carried out according to the optimal 18-points plan [3]. Four factors of the composition were varied (relative to 1000 weight parts (w.p.) of a premised plaster):

X_1 - powdered to S_{ss} = 400 m^2 / kg limestone rock, 80 ± 20 w.p.;

X_2 - expanded perlite sand of mark 100, 40 ± 10 w.p.;

X_3 - methylhydroxyethyl cellulose Tylose 60010 (water-soluble, non-ionic cellulose ethers), 1.15 ± 0.15 w.p.;

X_4 - polymer redispersible powder Vinnapas RE 5034N (copolymer of vinyl chloride, ethylene and vinyl laurate), 1.5 ± 0.5 w.p.

Table 1 Generalized parameters of plaster mortar

Parameter Y		W/C		W_{OUT}, %		R_A, MPa	
		min	max	min	max	min	max
Y_{exp}		0.92	1.2	99.7	99.9	0.08	0.49
Coordinates Y_{exp}	x_1	−1	0.99	0.37	1	−1	−1
	x_2	1	0.99	1	1	1	1
	x_3	1	1	−1	1	−1	−1
	x_4	0.41	−1	−1	−1	−1	−1
ΔY		0.28		0.2		0.41	
δY		1.3		1		6.1	
S		0.03		0.03		0.03	

Based on the results obtained in the experiment, four-factor experimental-statistical (ES) models were constructed describing the explored quality criteria (1-3). For the construction of ES models, the COMPEX system [4] created in the Odessa State Academy of Civil Engineering and Architecture is quite effective, which is used to process experimental-statistical models data, optimize and make engineering decisions. The COMPEX program provides interaction with Windows, and allows the construction of models with a generated experimental error [5], calculation of generalized indices of the material properties fields [6], etc. The fields which were described by these models can be characterized by generalizing indicators that facilitate their comparative analysis, Tab. 1. The basic generalizing exponents of the property Y in the boundaries of the field under study are the minimum Y_{min} and the maximum Y_{max} levels, as well as their coordinates x_{min} and x_{max}.

3 PROPERTIES OF CEMENT-LIME MORTARS

3.1 Workability

One of the most important properties of plastic mortar is its workability. Lime is the primary contributor to workability of cement-lime mortars. The lack of workability of mortar mix makes it difficult to align the surface of the plaster coatings, reduces the adhesion properties, reduces the degree of hydration of the binder in the mortar, and leads to the shedding of the surfaces of the plaster coating.

Water requirement of dry mortars was attributed to the cement as a water-cement ratio and was determined at different water-cement relations chosen so that all proportions had the same workability.

The workability of the mortar mixture was determined by the European standard DIN 18555 on a jolt-table. According to the standard, all plasters mortar mixes are divided by diameter of flow into: rigid <14 cm; plastic - 14÷20 cm and soft > 20 cm. To ensure equal workability all the examined plasters should have the same workable consistency. As a result, the flow diameter of all mixtures corresponded to 16÷17 cm and this classifies all mixtures as plastic. This condition is chosen based on the results of the analysis of the behaviour of produced dry mixtures and equipment parameters. Equal workability of all mixtures was ensured by the selection of mixing water.

The diagram (Fig. 1) in the form of squares on a square is shown; it represents the influence of composition factors on the water demand of the mixture. Factors - methylhydroxyethyl cellulose (x_3) and polymeric redispersible powder (x_4) were chosen as square-bearing. The fields that show the effect of limestone (x_1) and perlite (x_2) are constructed at nine points. In the squares on the square, the isolines of the maximum values of water demand W/C_{max}, water-cement ratio are shown, which can be achieved with a fixed ratio of methylhydroxyethyl cellulose and polymer redispersible Vinnapas powder, with varying amounts of limestone and perlite. Analysis of the diagram allows saying that the water requirement of a plaster mixture of equal mobility slightly increases as the amount of porous components - limestone (x_1) and expanded perlite (x_2) in the formulation increase.

Varying the dosage of methylhydroxyethyl cellulose within the factor space of the experiment does not produce significant effect on water requirement. The minimum of water-cement ratio shows compositions with an average (about 1.5 w.p.) amount of redispersible powder Vinnapas. In general, it is possible to establish a slight (up to 16 %) change in water requirement and, respectively, water-cement ratio (W/C) mixes of equal mobility with varying composition factors, which is explained by a rather "narrow" range of factors, approximating to the baseline composition.

3.2 Water retention

The water retention ability plays an important role in the formation of a strong adhesion of the mortar to the base. With insufficient water retention capacity in the contact area with a base, the liquid phase is formed, which leads to a complete disruption of the adhesion. The water-retaining capacity of the compositions was estimated by water loss in %,. As a result, an ES model was obtained (1).

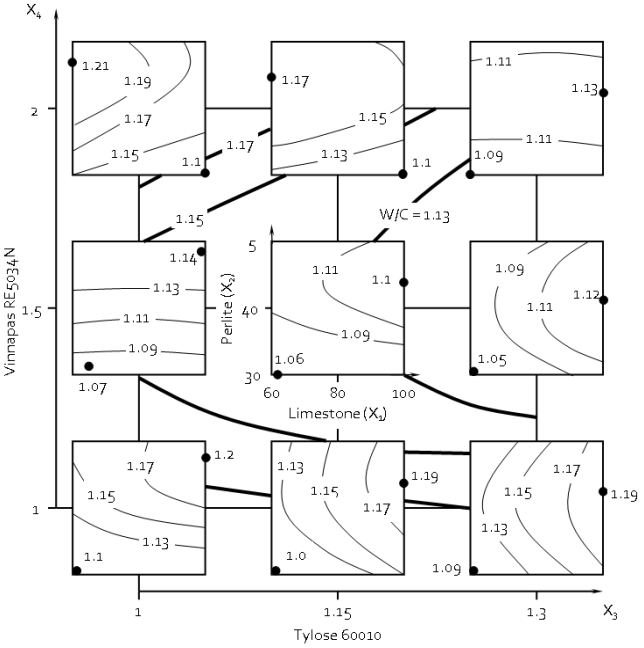

Figure 1 The diagram of change in the water requirement of the W/C plaster compositions of the same workability under the influence of composition factors

$$W_{out} = 99.8 \pm 0x_1 + 0.06x_1^2 + 0.03x_1x_2 + 0.04x_1x_3 + 0.03x_1x_4 \pm 0x_2 \pm 0x_2^2 + 0.02x_2x_3 + 0.01x_2x_4 \pm 0x_3 - 0.04x_3^2 - 0.08x_3x_4 \pm 0x_4 + 0.3x_4^2 \quad (1)$$

The water-retaining capacity of all 18 compositions proved to be higher than the regulatory requirements and it is within W_{out} = 99.65÷99.9 %, which is achieved by adding high-molecular compounds into the mixture. However, as expected, the greatest positive effect on the mixture is provided by the water-retaining additive Tylose, with growth of which the water-retention is increased.

3.3 Hardened mortar property

3.3.1 Adhesion

One of the most important quality indicators for all types of plaster mixture, including lightweight ones, is adhesion to the base [7]. The adhesion was measured on DYNA Z16 instrument, and based on the results of its determination, the following experimental statistical model (ES) was constructed for 18 experimental compositions (S_e = 0.0307):

$$R_A \text{ (MPa)} = 0.304 \pm 0x_1 - 0.06x_1^2 - 0.04x_1x_2 - 0.02x_1x_3 - 0.02x_1x_4 + 0.04x_2 \pm 0x_2^2 + 0.04x_2x_3 + 0.07x_2x_4 \pm 0x_3 - 0.04x_3^2 \pm 0x_3x_4 + 0.05x_4 \pm 0x_4^2 \quad (2)$$

According to the model (2), the diagram shown in Fig. 2 was constructed in the form "Squares on a square", reflecting the influence of variable factors on the adhesion of light-weight plaster composition. In this case, in the field

of each small square, as in Fig. 1, the effect of the amount of ground limestone and perlite is shown, and depending on the coordinate of the small square on the carrier square, the amount of methylhydroxyethyl cellulose and Vinnapas changes.

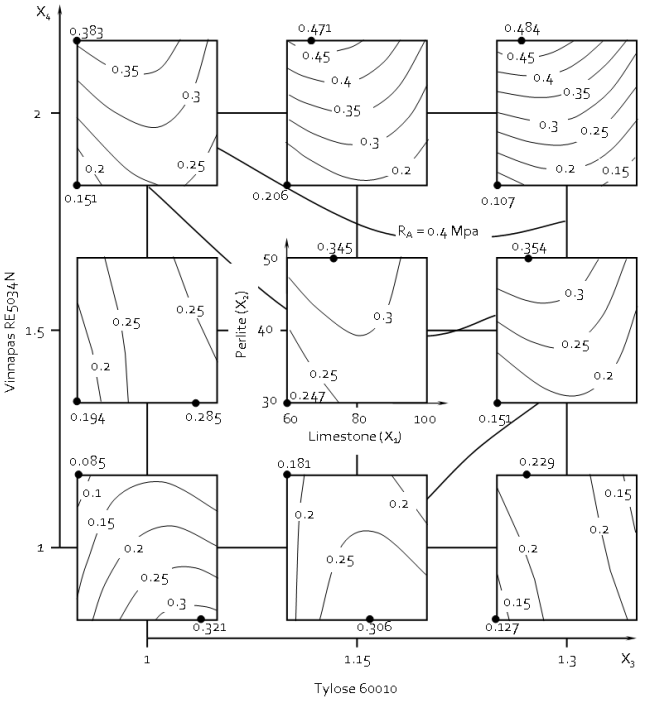

Figure 2 Influence of the composition factors of the on the adhesion of the light-weight plaster mixture

Analysis of the diagram allows saying that the adhesion of the plaster mixture to the base significantly increases with the increase of the amount of redispersible powder Vinnapas, which is a quite expected effect. At the maximum dosage of Vinnapas, an adhesion level above 0.4 MPa is achieved, which can be considered desirable for the durable work of the solution in real conditions. The change in the amount of methylhydroxyethyl cellulose affects the adhesion less significantly. This increase of the amount of this component increases the level of adhesion for the compositions with the maximum dosage of Vinnapas and slightly reduces for formulations with a small amount of redispersible powder.

It is important to note that almost for all of the examined compositions, with the exception of the zone with $x_3 = x_4 = -1$, the adhesion was increased with increasing of perlite amount and reached a maximum at a dosage of limestone close to 70 w.p.

4 CONCLUSION

From the presented materials it can be noted that water requirement of mortar was maximally reduced and slightly increases with increasing of porous components; water requirement can also be reduced by rational dosage of redispersible additive Vinnapas.

Water retention ability of compositions is increased to almost 100 % (due methylhydroxyethyl cellulose and redispersible powder with optimal amount content of fillers), which reduces the risk of shrinkage and peeling of plaster layer during the migration of water in the porous base from the lower layers and evaporation from the upper layers at higher temperatures.

Adhesion of plaster to the base is significantly increased by increasing the ratio of redispersible powder Vinnapas, which purposefully affects this property. At the maximum dosage of Vinnapas the level of adhesion is achieved above 0.4 MPa, which can be considered a satisfactory mark for such building materials.

Note: This investigation was presented at the International Conference MATRIB 2017 (29. 6. - 2. 7. 2017, Vela Luka, Croatia).

5 REFERENCES

[1] Lyashenko, T.: Fields of properties of building materials (concept, analysis, optimization), Abstract of the thesis for degree Doctor of technical sciences, 2003.
[2] Lyashekno, T.: The concept of the fields of properties is the methodological basis for extracting information from ES models in computer material science, Bulletin OSACEA, 12 Edition (2003) 171–179.
[3] Kazarnovskyy, Z.; Omelchenko, L.; Saville, G.; Warming of enclosing structures, sanitation and waterproofing with the use of dry mixes, Building materials, No. 3 (1999) 24–25.
[4] Voznesenskiy, V.: Modern methods of optimization of composite materials, Budivelnik, Kiev, 1989.
[5] Voznesenskiy, V.: Models with a generated experimental error for special quality criteria of composites, A collection of scientific articles, Odesa: Building materials, structures and engineering systems (1996) 144–155.
[6] Lyashekno, T.: The Generalizing properties of fields for the development of effective composites, A collection of scientific articles, Odesa: Building materials, structures and engineering systems (1996) 172–186.
[7] Popov, O.; Moskalova, K.: Technology influence of the mineral and polymer additives on adhesion of plaster solutions, Tehnički glasnik, Vol. 1, No. 9, (2015) 33−34.

Authors' contacts:

Khrystyna MOSKALOVA, PhD, Assistant Professor
Odessa State Academy of Civil Engineering and Architecture
4 Didrihsona St., Odessa, Ukraine
krisogasa@gmail.com

Marin MILKOVIĆ, Ph.D, Professor
Goran KOZINA, Ph.D, Associate Professor
University North
104. brigade 3, Varaždin, Croatia
rektor@unin.hr
goran.kozina@unin.hr

ISSN 1846-6168 (Print), ISSN 1848-5588 (Online)
ID: TG-20170316142642

Subject review

AN OVERVIEW: THE IMPACT OF DATA MINING APPLICATIONS ON VARIOUS SECTORS

Mümine KAYA KELEŞ

Abstract: In recent years, it has become difficult to reach to the reliable information with increasing complicated, non-significant, unclear, large and raw data. The need for accurate analysis of reliable information from large data has also increased in direct proportion to the rate of data growth. The Data Mining Method, which is a statistical application, is used in any desired area to be accessed to the reliable and meaningful information. In this study, the areas where data mining methods are used were explained, a literature review about banking and finance, education, telecommunication, health, public, construction, engineering and science sectors was made, and the impact of the data mining was discussed. This study is aimed to provide a contribution to the literature eliminating the gap in the mentioned area and to bring an innovation to the applications and work in these areas.

Keywords: data mining; engineering; knowledge discovery process; science; statistic

1 INTRODUCTION

Data are raw facts or measurements that can be recorded about events and assets, and indirectly meaningful [1]. The data needs to be collected, organized, summarized, analyzed and synthesized for decision-making purposes. According to Akpınar [2], data analysis is defined as the collection, organization, modeling, and testing of information access. Data analysis requires a systematic approach involving several important steps. Data analysis is involved in many disciplines such as data mining and statistics.

Statistics are defined as the art of learning from data. In its most general form, statistics deals with the collection of data, the description of data following it, and the analysis of data that often leads to the conclusion [3]. In almost all areas of work, statistical data analysis has great importance for the results to be valid and reliable. There is no statistical method applied from the field and subject, independent of the measurement and research problem. So, it is not possible to propose a single statistical method that can provide results depending on multiple purposes in the data analysis process. For this reason, in various fields, for different purposes, there are quite a number of statistical methods defined according to different data structures.

Data mining is a scientific discipline that takes the origin of statistics. Although data mining is basically a statistical application, the methods of data mining are somewhat different from the statistical methods [4]. The most obvious difference is that, unlike data mining methods, it is not easy to analyze the large-scale data with traditional statistical methods [5]. Data mining is widely used in diverse and interdisciplinary fields. In recent years, data mining has gained a great deal of importance due to the large amount of data in different applications belonging to various fields.

The aim of this study is to discuss the applications and the trend of data mining. For this reason, in this study, it has been decided to focus on the data mining method and its applications and determine the impact of these applications on various sectors.

For this purpose, this study focuses on presenting the data mining applications with examples in the various sectors including banking and finance, education, telecommunication, health, public, construction, engineering, and science sectors. This study contains a general overview of data mining and discusses the main fields for which data mining can be applied. This study also presents the main areas of the data mining applications used: banking and finance, education, telecommunication, health, public, construction, engineering, and science sectors.

In the first part of this study, the concept of data mining is in focus. In the second part, data mining applications which have been put forward in various international disciplines are examined in general perspective. Then, in the last part of the study, comments on the effects of systematic analysis of data are presented.

2 MATERIAL AND METHODS

In this section, firstly the definitions of data mining are explained, and then the method is defined briefly.

2.1 Data mining

There are many definitions of the data mining method, which is often used by data analysts. According to Kleinberg and his colleagues [6], data mining is "an interesting pattern extraction process from the raw data". According to the Gartner Group [7], data mining is the process of "discovering new correlations, patterns and trends that are meaningful by passing a large number of data stored in a vault". According to Fayyad [8], data mining is "a systematic process that is a step in the process of information discovery and is based on algorithms to produce patterns and data analysis applications". According to another definition, data mining is the process of accessing valuable information among the mass data collected by the enterprises [9].

Data mining is a major discipline that has foundation in statistics. Data mining has emerged in order to uncover the workable data in the databases, to remove redundant data, and to achieve accurate data in the fastest possible way. Data mining makes it easier to search for a set of rules within a large amount of data in order to find some predictions about the future. It also helps extract and use valuable data from a large amount of data.

Data mining, which is a meaningful, interesting and useful process of extracting very large amount information, consists of seven steps as a part of the Knowledge Discovery Process as shown in Fig. 1. These steps are as follows: data cleaning step, in which the noisy, erroneous and inconsistent data in the data is removed and the missing data is completed; data integration step, in which a plurality of data sources from different sources are consistently combined in one source; data selection step, in which the data relating to the analysis to be performed is determined and taken from the database; data transformation step, in which the data is prepared for the data analysis methods to be used at the modeling stage and the conversion is performed; data mining step, in which intelligent methods are applied to extract data patterns; pattern evaluation step that defines the correct and interesting patterns representing the information obtained according to the measurements made; and finally, knowledge presentation step that the obtained information is presented to the user through information exploration methods.

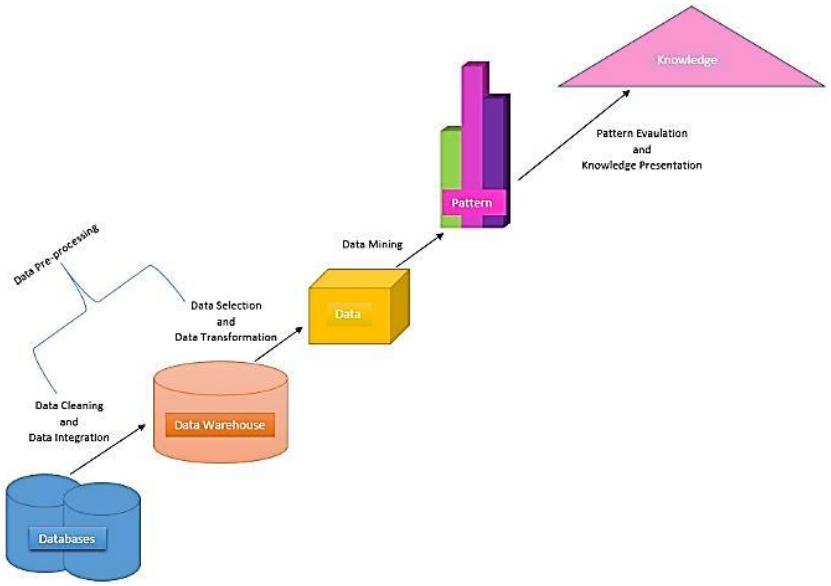

Figure 1 Knowledge Discovery (KDD) Process

2.2 Method

In this study the concepts of data and data analysis are briefly described and mentioned and the application areas of data mining are explained. The studies done in these subjects are explained and the data mining's contributions to these areas are brought into focus.

2.2.1 Data Mining Application Fields and Studies Done In These Fields

Data mining has application fields in many branches such as banking, stock exchange, marketing management, retail sales, signal processing, insurance, telecommunication, electronic commerce, health, medicine, biology, genetics, industry, construction, education, intelligence, science, and engineering [5, 10, 11]. Various businesses apply data mining to critical business processes to gain competitive advantage and help businesses grow. In this study, data mining applications in the main sectors covering the mentioned sectors were researched and explained with examples of how and for what purpose data mining was used.

2.2.1.1 Banking and Finance Sector

Data mining is mostly used in the banking and finance sectors to determine what, when, and why the customer profile prefers. At the same time, it is also used in these fields to find appropriate solutions for the right demand creation and presentation the right time demands. Furthermore, it is also used in

- financial forecasting,
- estimation of stock prices,
- management of new investments,
- determination of investment portfolio,
- formation of marketing strategies,
- making risk analyses,
- making the right choice in terms of human resources for business, credit and credit card fraud estimates,
- credit limit determination and fee management.

Data mining applications are used extensively to improve the performance of some core business processes in the banking sector [12, 13]. Some banks, for example Garanti Bank in Turkey, use data mining methods to have information about the behavior models of customers and offer appropriate and successful promotions by examining

the relationship between customer 'credit cards' selectivity and their character.

2.2.1.2 Education Sector

It has been observed that data mining has been used in many studies in the education sector including:

- determining the status of students' pass and fail,
- factors affecting the success of the students enrolling at the university,
- creating the preference of university department, determining the factors that influence the preference order of new enrolled students,
- choosing a profession according to the demographic and personal characteristics [14],
- preventing students from failing and determining the factors that affect success,
- determine the relationships between the type of school in which students graduate and their university departments [15, 16] evaluating the study activities of distance education students [16, 17],
- determining the profiles and preferences of students entering the university entrance exam [18],
- determining the relationship between academic success and participation in extracurricular activities of university students,
- determining the relationships between the socio-economic level of students and the level of academic learning [14],
- determining whether there is a relationship between student entry scores and school achievement.

These usage areas in educational sector help teachers to manage their classes, to understand their students' learning, and to provide proactive feedback to learners.

2.2.1.3 Telecommunication Sector

Data Mining can be used in the telecommunication sector:

- to predict mobile user movements in the communications sector,
- to determine the future movements of mobile users,
- to detect frauds,
- to reduce much of human-based analysis,
- to determine the factors that influence customers to call more at certain times,
- to determine user templates for social network usage [19],
- to identify new prospects using demographic data [20],
- to identify the characteristics of customers who need special action as suspension or deactivation [20],
- to prevent customer loss.

In order to prevent customer loss, telecommunication organizations can eliminate this problem by resorting to strategies for developing strategies, low cost and effective campaigns.

A good example of the use of data mining in this sector, regarding customer loss, is Verizon, America's largest wireless communications provider. In the study, Verizon has resorted to data mining methods to identify customers whom they are likely to lose and the factors that cause customer loss.

2.2.1.4 Health Sector

Data mining techniques and application tools are more valuable for health sector. Data mining applications are used extensively to reduce the complexity of the healthcare data transactions' study in the health sector [21-24]. Data Mining is used in the health sector:

- to diagnose the disease,
- to determine the treatment method to be applied to the disease,
- to estimate the resource use and patient numbers in hospitals,
- to set the success of treatment methods applied in the hospital,
- to classify the patient data according to factors such as age, gender, race and treatment,
- to determine the high risk factors in surgeries,
- to prevent corruption in hospital expenditures.

One of the best examples of data mining studies in the health field is the one conducted at the San Francisco Heart Institute. In this study, some data such as the patient's history, laboratory data, and other medical data which are obtained from the patients to improve patient outcomes and reduce patient's hospital stay, were converted to information through data mining methods.

2.2.1.5 Public Sector

Data Mining is often used to predict public safety and security problems in the public sector. Data mining techniques offer open opportunities for the public sector to optimize decisions. These decisions are based on general trends extracted from past experience and historical data [25]. Apart from that, it is necessary:

- to determine the tax related corruption,
- to predict the impact of changes in the tax system on the budget,
- to determine waste and prevent damage caused by waste, estimate population,
- to forecast the weather, determine new job opportunities,
- to measure performance of employees, manage the business processes,
- to classify public expenditures, plan the correct use of resources,
- to forecast the future of public investment, analyze the data in defense industry,
- to determine which offenders are likely to commit crimes in terms of safety.

One of the most important examples in this area is E-Government application in Turkey. Faster feedback is being received as data mining methods are used in conjunction with the web page re-arrangement according to the behavior of the user in the past by determining the simultaneous

access of the information and the order in which the web pages on E-Government are visited.

2.2.1.6 Construction Sector

Data Mining is used in the construction sector in construction, project management, hydraulics, occupational health and safety applications, analysis of earthquake data, groundwork studies and many other areas. In view of the studies carried out in this context, it has been found that studies have been done:

- to create the information classification scheme in project documents [26],
- to determine the tax related corruption,
- to predict the impact of changes in the tax system on the budget,
- to determine waste and prevent damage caused by waste,
- to estimate the cost of highway construction [27],
- to estimate population, forecast the weather, determine new job opportunities,
- to estimate the compressive strength of the cement product [28],
- to measure performance of employees, manage the business processes,
- to define the characteristics of occupational accidents in the construction industry [29],
- to classify public expenditures, plan the correct use of resources,
- to measure worker productivity [30, 31],
- to determine the concrete compressive strength [32],
- to forecast the future of public investment, analyze the data in defense industry,
- to determine the relationship of leadership-motivation between the chief and the worker [33],
- to determine which offenders are likely to commit crimes in terms of safety,
- to determine the location of data mining method in construction management [34, 35].

One of the most important examples in this area is E-Government application in Turkey. Faster feedback is being received as data mining methods are used in conjunction with the web page re-arrangement according to the behavior of the user in the past by determining the simultaneous access of the information and the order in which the web pages on E-Government are visited.

2.2.1.7 Engineering and Science Sector

Large quantities of data have been collected from scientific fields such as astronomy, bioinformatics, computing, criminal science, engineering, geosciences, mathematics, software etc. Data Mining provides many benefits in engineering and science sector including:

- managing the process of the software used in firms,
- reducing the amount of tasks,
- increasing the speed of the Software Development Life Cycle,
- saving time and effort,
- providing competitive advantage to the organizations with the predicted analysis,
- improving the manufacturing process [20],
- biological literature analysis,
- remote sensing,
- soil quality analysis [20],
- detecting crime pattern,
- real-time feature extraction for turbulent flow analysis,
- obtaining good quality seed [20],
- evolving new crop breeds [20],
- classifying the astronomical objects,
- ecosystem modeling,
- discovering the relationships for best utilization of the cold storages and use of canal water [20],
- classifying the sequences in bioinformatics.

These usage areas in engineering and science sector help users to improve system performance of software used, to provide insight into many parts of used engineering software development processes, and to plan the future decision making process.

3 RESULTS AND CONCLUSIONS

In this study, the application areas and the contributions of data mining are examined. In the light of the literature studies examined within the scope of this study, it is observed that data mining is applied to many areas in our country. Many researchers in many different disciplines have found that meaningful results can be achieved by providing data mining methods and analysis of data. The transformation of raw data into meaningful information by processing through these studies is thought to provide economic contributions to businesses and public enterprises.

Based on these studies it can be observed that useful results can be obtained if data mining methods are used when there is an estimation or determination process in terms of cost in any sector.

It is obvious that data which are considered unnecessary and which are not recognized due to the volumetric magnitude of the preconceptions will benefit many subjects from loss of potential workforce to cost reduction, from prediction of potential customers to marketing strategies by being analyzed by data mining methods as well as statistical methods and by connecting to a system.

The important result of this study is that data mining methods, which have been used frequently in almost every field in recent years, can be applied to any kind of data obtained in the sectors mentioned in this study, and economically beneficial results can be achieved by providing competitive advantage to businesses.

4 REFERENCES

[1] Ercil Çağıltay, N., Tokdemir, G., 2010. Veritabanı Sistemleri Dersi Teoriden Pratiğe, Ada Matbaacılık, Ankara.

[2] Akpınar, H., 2014. DATA Veri Madenciliği Veri Analizi, Papatya Yayıncılık Eğitim, 1. Basım, İstanbul.

[3] Ross, S. M., 2012. Introduction to Probability for Engineers and Scientists, Academic Press.
[4] Kaya Keleş, M., 2016. İstatiksel Yöntemler ile Veri Madenciliği Yöntemlerinin Karşılaştırması (A Comparison of Statistical Methods and Data Mining Methods), Sosyal Bilimler Metinleri, 2016 Aralık ICOMEP Special Issue, pp. 20-24.
[5] Özkan, Y., 2008. Veri Madenciliği Yöntemleri, Papatya Yayıncılık Eğitim, İstanbul.
[6] Kleinberg, J., Papadimitriou, C., Raghavan, P., 1998. A microeconomic view of data mining, Data mining and knowledge discovery, 2.4, pp. 311-324.
[7] Larose, D. T., 2005. Discovering Knowledge in Data, A John Wiley & Sons, Inc., Publication, New Jersey.
[8] Fayyad, U., Piatetsky-Shapiro, G., Smyth, P., 1996. From Data Mining to Knowledge Discovery in Databases, American Association for Artificial Intelligence, 17(3), pp. 37-54.
[9] Sümersan Köktürk, M., Dirsehan, T., 2012. Veri Madenciliği ile Pazarlama Etkileşimi, Nobel Yayın, 1st Edition.
[10] Kaya, M., Özel, S. A., 2014. Açık Kaynak Kodlu Veri Madenciliği Yazılımlarının Karşılaştırılması (Comparison of Open Source Data Mining Software), Akademik Bilişim'14 - XVI. Akademik Bilişim Konferansı (AB2014), AB2014 Proceedings, 47-53.
[11] Silahtaroğlu, G., 2008. Kavram ve Algoritmalarıyla Temel Veri Madenciliği, Papatya Yayıncılık Eğitim, İstanbul.
[12] Pulakkazhy, S., Balan R.V.S., 2013. Data Mining In Banking And Its Applications-A Review, Journal of Computer Science, 9(10), pp. 1252-1259.
[13] Bhambri, V., 2011. Application of Data Mining in Banking Sector, International Journal of Computer Science and Technology (IJCST), 2(2), pp. 199-202.
[14] Kurt, Ç., Erdem, A., 2012. Öğrenci Başarısını etkileyen Faktörlerin Veri Madenciliği Yöntemleriyle İncelenmesi, Politeknik Dergisi, 15(2), pp. 111-116.
[15] Ayık, Y. Z., Özdemir, A., Yavuz, U., 2007. Lise Türü ve Lise Mezuniyet Başarısının Kazanılan Fakülte ile İlişkisinin Veri Madenciliği Tekniği ile Analizi, Sosyal Bilimler Enstitüsü Dergisi, 10(2), pp. 441-454.
[16] Savaş, S., Topaloğlu, N., Yılmaz, M., 2012. Veri Madenciliği ve Türkiye'deki Uygulama Örnekleri, İstanbul Ticaret Üniversitesi Fen Bilimleri Dergisi, 21, pp. 1-23.
[17] Çiftçi, S., 2006. Uzaktan Eğitimde Öğrencilerin Ders Çalışma Etkinliklerinin Log Verilerinin Analiz Edilerek İncelenmesi, Yüksek Lisans Tezi, Gazi Üniversitesi, Eğitim Bilimleri Enstitüsü.
[18] Dolgun, M. O., Özdemir, T. G., Deliloğlu, S., 2007. Öğrenci Seçme Sınavında (ÖSS) Öğrencilerin Tercih Profillerinin Veri Madenciliği Yöntemleriyle Tespiti, Bilişim 07 Kongresi, Ankara.
[19] Bozkır, A. S., Mazman, S. G., Sezer, E. A., 2010. Identification of User Patterns in Social Networks by Data Mining Techniques: Facebook Case, 2nd International Symposium on Information Management in a Changing World", Hacettepe University, Ankara, pp. 145-152.
[20] Shahbaz, M., Rahman, M., 2008. Data mining for engineering sector in pakistan: Issues and implications, Proceedings of the World Congress on Engineering and Computer Science 2008 (WCECS 2008), San Francisco, USA, ISBN: 978-988-98671-0-2.
[21] Avşar Aydın, E., Kaya Keleş, M., 2017. Breast cancer detection using K-nearest neighbors data mining method obtained from the bow-tie antenna dataset, International Journal of RF and Microwave Computer-Aided Engineering.
[22] Durairaj, M., Ranjani, V., 2013. Data Mining Applications In Healthcare Sector: A Study, International Journal Of Scientific & Technology Research, 2(10), pp. 29-35.
[23] Avşar Aydın, E., 2014. Meme Kanseri Tespitinde Mikrodalgaların Önemi ve Kanserli/Sağlıklı Meme Dokularının Yapay Zeka Algoritmaları ile Tanımlanabilmesi, Çukurova Üniversitesi Mühendislik-Mimarlık Fakültesi Dergisi, 29(2), pp. 27-38.
[24] Aydın, A., AVŞAR AYDIN, E., 2017. Evaluation of Limestone Layer's Effect for UWB Microwave Imaging of Breast Models Using Neural Network, Technical Journal, 11(1-2).
[25] Wang, J, Hu, X., Zhu, D., 2008. Data Mining in Public Administration, Handbook of Research on Public Information Technology, IGI Global, Chapter LI, pp.556-567.
[26] Caldas, C., Soibelman, L., Han, J., 2002. Automated Classification of Construction Project Documents, J. Comput. Civ. Eng., 16(4), pp. 234-243.
[27] Wilmot, C. G., Cheng, G., 2003. Estimating Future Highway Construction Costs, J. Constr. Eng. Manage, 129 (3), pp. 272-279.
[28] Baykasoğlu, A., 2005. Veri Madenciliği ve Çimento Sektöründe Bir Uygulama, Akademik Bilişim Konferansları, pp.82-83.
[29] Liaoa, C. W., Perng, Y. H., 2008. Data Mining for Occupational Injuries in The Taiwan Construction Industry, Safety Science, 46(7), pp. 1091-1012.
[30] Kaya, M., Keleş, A. E., Laptalı Oral, E., 2013. Construction Crew Productivity Prediction by Using Data Mining Methods, Proceedings of the 4th World Conference on Learning, Teaching and Educational Leadership, Procedia - Social and Behavioral Sciences, 141, pp. 1249–1253.
[31] Keleş, A. E., Kaya, M., 2014. Duvar İnşa Edilmesinde Verimliliği Etkileyen Faktörlerin Apriori Veri Madenciliği Yöntemi Kullanılarak Analizi (The Analysis of the Factors Affecting the Productivity in the Wall Construction of the Using Apriori Data Mining Method), Akademik Bilişim Konferansları, AB 2014 Proceedings, pp.831-836.
[32] Özel, C., Topsakal, A., 2014. Veri Madenciliği Kullanarak Beton Basınç Dayanımının Belirlenmesi, Cumhuriyet Üniversitesi Fen Fakültesi Fen Bilimleri Dergisi, 35(1), pp. 43-57.
[33] Keleş, A. E., 2016. İnşaat Projelerinde Şantiye Şeflerinin Liderliği ve Çalışan Motivasyonu İlişkisinin Veri Madenciliği ile Belirlenmesi. Çukurova Üniversitesi Fen Bilimleri Enstitüsü PhD Thesis, Adana.
[34] Keleş, A. E., 2016. İnşaat Sektöründe Veri Madenciliği Uygulamalarına Genel Bakış Ve Ekonomik Etkilerinin Yorumlanması, Balkan Journal of Social Sciences, International Congress of Management Economy And Policy Special Issue, pp. 55-61.
[35] Kaya Keleş, M., Keleş, A. E., 2017. Veri Madenciliği Uygulamalarının ve Sezgisel Optimizasyon Algoritmalarının Yapım Yönetimindeki Yeri (The Place of Data Mining Applications and Heuristic Optimization Algorithms in Construction Management), Çukurova Üniversitesi Mühendislik-Mimarlık Fakültesi Dergisi, 32(1), pp. 235-242.

Author's contact:

Mümine KAYA KELEŞ, Assistant Prof. Dr.
Adana Science and Technology University,
Department of Computer Engineering
Seyhan/Adana-TURKEY, +90-0538 548 35 00
mkaya@adanabtu.edu.tr, muminekayakeles@gmail.com

ISSN 1846-6168 (Print), ISSN 1848-5588 (Online)
ID: TG-20170815203704

Subject review

MATHEMATICAL PROPERTIES OF FORMULATIONS OF THE GAS TRANSMISSION PROBLEM

Daniel DE WOLF

Abstract: The paper presents the mathematical properties of several formulations for the gas transmission problem that account for the nonlinear flow pressure relations. The form of the nonlinear flow pressure relations is such that the model is in general nonconvex. However, we show here that under a restrictive condition (gas inlet or gas pressure fixed at every entry/outgoing node) the problem becomes convex. This result is obtained by use of the variational inequality theory. We also give a computational method to find a feasible solution to the problem and give a physical interpretation to this feasible solution.

Keywords: OR in natural resources: natural gas; variational inequalities theory: applied to prove convexity; convexity: sufficient conditions for

1 INTRODUCTION

The problem considered is a real world problem in the field of engineering applications. It is to determine the optimal transportation plan for a gas transmission company which must satisfy demands at different nodes at a minimal guaranteed pressure. The model consists of a linear objective function subject to a set of linear and nonlinear constraints. The linear constraints express flow conservation at each node of the network. The nonlinear equations give the relation between the flow along each arc and the pressure at its two ends.

This problem was first introduced by O'Neill et al. [12]. It was also considered by Wilson, Wallace and Furey [15], who also use integer variables to describe the state of the compressors. More recently, it was considered by André et al. [1] for the case of hydrogen. For a complete discussion of advantages and disadvantages of several mathematical models that address gas transport within the context of its technical and regulatory framework, see Koch et al [9]. For a review on the most relevant research works conducted to solve natural gas transportation problems via pipeline systems, see Rios-Mercado [14]. In the paper Rios-Mercado et al. [13] address the problem of minimizing the fuel consumption incurred by compressor stations in steady-state natural gas transmission networks. In the practical world, these types of instances are very large, in terms of the number of decision variables and the number of constraints, and very complex due to the presence of non-linearity and non-convexity in both the set of feasible solutions and the objective function. In this paper, the authors present a study of the properties of gas pipeline networks, and exploit them to develop a technique that can be used to reduce problem dimension significantly, making it more amenable to the solution.

In the present paper, we consider the same problem, show the convexity of the problem and present an auxiliary problem to find a feasible solution to the problem. Moreover, we give a physical interpretation to the auxiliary problem never published before.

Finally, Geißler et al. [7] present a solution algorithm for problems from steady-state gas transport optimization taking into account the nonlinear and nonconvex physics as well as discrete variables to control the active network devices. The proposed method is based on mixed-integer linear techniques using piecewise linear relaxations of the nonlinearities. For two recent theses on the subject, see A. Morsi [11] and J. Humpola [8] who also consider convex relaxation of the problems with only passive elements (pipes and valves). In [3], Borraz-Sanchez et al. consider a convex mixed-integer second-order cone relaxation for the gas expansion planning problem.

We present the problem formulation in section 2. Then, in section 3, attention is given to identifying circumstances that guarantee the problem to be convex. If gas inlet is fixed at every entry/outgoing node, the problem becomes convex. Then, in section 4, we show how to compute a feasible solution to the problem by solving a convex optimization problem where nonlinearities are only in the objective function. We also give a physical interpretation of this feasible solution. This gives a practical solution method to find an initial solution for the more complete problem. Section 5 explains the gain to proceed first through this auxiliary problem. Finally, Section 6 presents some conclusions.

2 PROBLEM FORMULATION

Consider the problem of a gas transmission company operating a network. If the company is an integrated one, it must decide the quantities of gas to buy from different producers in order to satisfy the demand spread over different nodes of the network at the minimal guaranteed pressure requested by the consumers. The problem can be considered at different levels of aggregation. The higher level is to look at the management of the gas purchases. Contracts often differ in their flexibility and each company only has limited storage capacities. The problem of planning the purchase and the storage activities is a multitemporal one. It is formulated as a single node problem, or using a simplified representation of the

network. It is assumed here that this problem has been solved and that the gas transmission company considers the more disaggregated problem of optimizing the quantity taken from the different production contracts and from storage in order to meet the demand at some moment of time. The question is no longer focused on storage but on network operations.

More and more, the two functions (buying gas and transportation) are separated. For example, in many European countries, the former national gas company is separated in two or more companies: one or more for the distribution of gas and one for the operation of the network. If we consider the transportation company, the quantities of gas taken from contracts are fixed. The transportation company must decide on the transportation plan in order to satisfy several demands of the clients at a minimal transportation cost (which are essentially the compression costs).

The network of a gas transmission company consists of several supply points where the gas is injected into the system, several demand points where gas flows out the system, and other intermediate nodes where the gas is simply rerouted. Pipelines are represented by arcs linking the nodes. Some of them can include compressors. We do not include the compressors in the present formulation.

The following mathematical notation is used. The network is defined as the pair (N, A) where $N = \{1, 2, ..., n\}$ is the set of nodes and $A \subseteq N \times N$ is the set of arcs connecting these nodes. A network example is represented in Fig. 1.

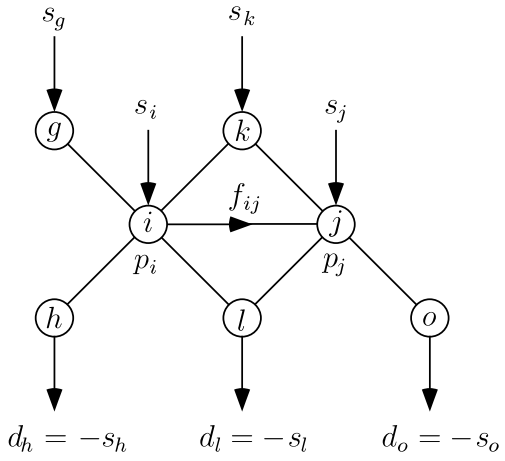

Figure 1 Network example

To each node i of the network a number p_i is associated, which represents the gas pressure at this node. We distinguish three types of nodes: the set of demand nodes, denoted N_d, the set of supply nodes, denoted N_s, and the set of connection nodes, denoted N_c. The gas supply at node i is denoted s_i. The gas demand at node i is denoted d_i. A gas flow f_{ij} is associated to each arc (i,j) from i to j. The arcs here correspond to pipelines.

The **constraints of the model** are as follows. The *flow conservation equation* at node i simply establishes the gas balance at this node. Mathematically, the gas balance at a node i is written as follows:

$$\forall i \in N, \quad \sum_{j|(i,j)\in A} f_{ij} + d_i = \sum_{j|(j,i)\in A} f_{ji} + s_i \tag{1}$$

At a supply node i, the gas inflow s_i must remain within the lower and upper bounds specified in the contract. A gas contract specifies a nominal daily quantity to be taken by the transmission company from the producer. Still, depending on the flexibility of the contract, the transmission company has the possibility of taking a quantity ranging from a certain fraction lower than one (e.g. 80 % ⋯ 90 %) to a certain fraction higher than one (e.g. 110 % ⋯ 115 %) of the nominal contracted quantity. Mathematically:

$$\forall i \in N_s, \ \underline{s}_i \le s_i \le \bar{s}_i \tag{2}$$

It is clear that if we consider the problem of the pure transmission company, these quantities are fixed, in other words:

$$\forall i \in N_s, \ s_i = \bar{s}_i$$

The gas must be provided at the demand nodes at a minimal pressure $\underline{p}_i$ which is requested by the consumers. At the supply nodes, the pressure is bounded above by the maximum pressure $\bar{p}_i$ that the producer can provide. In general, these two pressure bounds can be summarized in the following form:

$$\forall i \in N, \ \underline{p}_i \le p_i \le \bar{p}_i \tag{3}$$

Now, consider the constraints on the arcs. The relation between the flow f_{ij} in the arc (i, j) and the pressure p_i and p_j is of the following form (see O'Neill et al. [12]):

$$\forall (i,j) \in A, \ \text{sign}\,(f_{ij}) f_{ij}^2 = C_{ij}^2 (p_i^2 - p_j^2) \tag{4}$$

where C_{ij} is a constant which mainly depends on the length and on the diameter of the pipe. Thus, for each pipeline where the gas can move in both directions, we consider that the f_{ij} are unrestricted in sign. If $f_{ij} < 0$, the flow $-f_{ij}$ goes from node j to node i. This form also answers to the question: what about the case of $p_i = p_j$? In this case, the flow f_{ij} is equal to zero.

The **objective function** of the integrated transmission company is to minimize the total cost of the supplies. We can write:

$$\min z = \sum_{j \in N_S} c_j s_j$$

where c_j is the purchase price of the gas delivered at node j. In the case of a pure transmission company, the objective is to minimize the compressor costs (if the pressure goes

under the minimal pressure requested by the client, one can increase the pressure using compressors).

Substituting new variables π_i defined as the square of the pressure variables p_i^2 and defining $\pi_i = p_i^2$, the problem of the integrated company can be summarized as follows:

$$\min z = \sum_{j \in N_S} c_j s_j$$
$$\text{s.t.} \begin{cases} \sum_{j|(i,j)\in A} f_{ij} - \sum_{j|(j,i)\in A} f_{ji} - s_i = 0 & \forall i \in N \\ \underline{s}_i \le s_i \le \overline{s}_i & \forall i \in N \\ \underline{\pi}_i \le \pi_i \le \overline{\pi}_i & \forall i \in N \\ \text{sign}(f_{ij}) f_{ij}^2 - C_{ij}^2(\pi_i - \pi_j) = 0 & \forall (i,j) \in A \end{cases} \quad (5)$$

3 CONVEXITY OF THE SOLUTION SET

It is well known that it is easier to compute a global solution for convex problems than for nonconvex ones. It is thus relevant to identify under which circumstances problem (5) is convex. The objective function being linear, we need only identify when the constraints define a convex set.

Proposition 1. If π_i or s_i is fixed $\forall i \in N_d \cup N_s$, then the feasible set for the gas transmission problem is convex.

Proof: See Koch [9, page 128].

Remark also that the assumption of Proposition 1 is satisfied in the case of a pure transmission company for which, as previously said:

$$\forall i \in N_s,\ s_i = \overline{s}_i .$$

4 COMPUTATION OF A FEASIBLE SOLUTION

Let us now consider the problem of the computation of a feasible solution. Following the same lines as Maugis [10], we shall show that a feasible solution can be found by solving the following mathematical programming problem:

$$\min h = \sum_{(i,j)\in A} \frac{|f_{ij}| f_{ij}^2}{3C_{ij}^2}$$
$$\text{s.t.} \quad \sum_{j|(j,i)\in A} f_{ji} - \sum_{j|(i,j)\in A} f_{ij} + s_i = 0 \quad \forall i \in N \quad (6)$$

We shall also give a physical interpretation to the objective function of this mathematical problem.

Proposition 2. The optimal solution of problem (6) is a feasible solution to the gas transmission problem (5).

Proof: Noting by π_i, the Lagrange multiplier associated to constraint of node i for (6), Maugis [10] has proved that the nonlinear flow-pressure equations of problem (5) are the Kuhn Tucker optimality conditions for the convex problem (6).

Since the objective function is strictly convex, there is only a single optimal solution in f. Note that uniqueness is guaranteed only for the flow variables and not for the pressure variables.

This mathematical programming problem can be given an interesting physical interpretation in the case of a pure transmission company (i.e. when $s_i = \overline{s}_i,\ \forall i$). Extending the work of Maugis for distribution network, we have the following proposition.

Proposition 3. The objective function of problem (6) corresponds up to a multiplicative constant to the mechanical energy dissipated per unit of time in the pipes (the mechanical energy being defined as the energy necessary for compressing f_{ij} from pressure p_j to pressure p_i).

Proof. At node i, the power W_i given by a volumetric outflow of Q_i units of gas per second at pressure p_i can be calculated in the following manner, where the total energy released by the gas when changing pressure from the reference pressure p^0 to pressure p_i is:

$$W_i = \int_{p^0}^{p_i} Q(p)\mathrm{d}p .$$

By using the perfect gas state relation ($p^0 Q^0 = pQ$), we can write:

$$W_i = \int_{p^0}^{p_i} p^0 Q^0 \frac{\mathrm{d}p}{p} = p^0 Q^0 \log\left(\frac{p_i}{p^0}\right).$$

Denote the volumetric flow going though arc (i, j) under standard conditions by Q_{ij}^0 and the pressures at the two ends of the arc by p_i and p_j. The power lost in arc (i, j) can be calculated by:

$$W_{ij} = W_i - W_j = Q_{ij}^0 p^0 \log\left(\frac{p_i}{p_j}\right) = Q_{ij}^0 \frac{p^0}{2} \log\left(\frac{p_i^2}{p_j^2}\right).$$

Introducing the mean of square of pressure p_M defined by

$$p_M^2 = \frac{p_i^2 + p_j^2}{2}$$

the power discharge W_{ij} can be expressed through the head discharge variable $H_{ij} = p_i^2 - p_j^2$ as:

$$W_{ij} = Q_{ij}^0 \frac{p^0}{2} \log\left(\frac{p_M^2 + \frac{H_{ij}}{2}}{p_M^2 - \frac{H_{ij}}{2}}\right) =$$
$$= Q_{ij}^0 \frac{p^0}{2}\left[\log\left(1+\frac{H_{ij}}{2p_M^2}\right) - \log\left(1-\frac{H_{ij}}{2p_M^2}\right)\right]$$

Note that since H_{ij} is small with respect to p_M^2, we obtain the following as a first order approximation

$$W_{ij} \approx Q_{ij}^0 p^0 \frac{H_{ij}}{p_M^2}.$$

The power discharge through the whole network is thus (we suppose that p_M is similar for each arc (i, j) and can be factored out in the following sum):

$$W = \sum_{(i,j)\in A} W_{ij} \approx \frac{p^0}{p_M^2} \sum_{(i,j)\in A} Q_{ij}^0 (p_i^2 - p_j^2) =$$
$$= \frac{p^0}{p_M^2} \sum_{(i,j)\in A} \frac{\left(Q_{ij}^0\right)^3}{C_{ij}^2} \operatorname{sign}(Q_{ij})$$

which corresponds, up to a multiplicative constant, to the first term of the objective of problem (6). We can thus conclude that the function h corresponds to the mechanical energy dissipated per unit time in the network due to the flow of gas in the pipes up to a multiplicative constant.

This proposition was suggested to the author by Mr. Zarea of Gaz de France.

5 UTILITY OF PROPOSITION

As said in the introduction, the motivation for our work is algorithmic. We are looking for the solution of the nonlinear nonconvex problem (5). Looking for a sufficient condition for the problem (5) to be convex, we found the following condition: fix the gas net inlet at each node. We have also emphasized that this condition is satisfied for a pure transmission company.

We have also showed that a feasible point to the non-convex problem (5) can be found as the solution of a strictly convex problem (6). The use of the solution of this auxiliary problem as a starting point for the general non-convex problem has two main advantages:

- For a non-convex optimization problem, it is well known that starting far from the optimal solution can give a local optimal solution far from the global optimum. We hope to reduce this risk with our starting point. In fact, we have proved in proposition 3 that the initial solution computed by the auxiliary problem as a meaningful interpretation: the minimization of the energy used to push the gas through the pipes.
- Using this point as a starting point can reduce computational times for the general problem.

The gain in processing time achieved by resorting to the first problem was studied and earlier proved by De Wolf and Smeers [5] for several representations of the Belgian gas transmission network, the gain of efficiency increase with the size of the problem. For small examples, the reduction of the computational time achieved in the problem (5) is completely lost due to the time spent in solving the problem (6). In contrast, for larger problems the cost of processing first the problem (6) is largely compensated by the savings achieved in the complete problem. Specifically, the global time necessary to successively solve the two problems is about half the time needed for solving the problem (5) directly from scratch. For the greater sizes of problems considered now (see for example Geißler [7]), the utilization of this auxiliary problem is totally justified.

More recently, De Wolf and Bakhouya [6] use the same auxiliary problem to find an initial solution for a larger network, namely the French high pressure natural gas network. They also show the important gain in computer time to solve first this auxiliary problem. Note that the physical interpretation given by proposition 3 explains why this starting point is a very good initial solution for the complete problem. In fact, in proposition 3, we have proved that the objective function corresponds to the minimization of the mechanical energy dissipated per unit of time in the pipes (the mechanical energy being defined as the energy necessary for compressing f_{ij} from pressure p_j to pressure pi). And the objective of a pure transmission company (the new case considered by De Wolf and Bakhouya [6]) is precisely the minimization of the used of compressors to push the gas through the pipes.

6 CONCLUSIONS

Several aspects of the gas transmission problem have been considered in this paper. The gas transmission problem is convex if the gas net inlet is fixed at all supplies and demand nodes. We have shown how to compute a feasible solution to the problem by solving a strictly convex problem with nonlinearity only in the objective function.

Based on these results, an auxiliary problem can be defined for producing an initial solution to the general problem. This auxiliary problem has a natural physical interpretation namely the minimization of the mechanical power dissipated in the pipes. This also corresponds to the objective for a pure transmission company. The use of this starting point can reduce the computing time as pointed by De Wolf and Smeers [5].

Even for more recent and realistic situation where the gas selling company and the network operators are separated (See De Wolf and Bakhouya [6]), this formulation gives a good starting point for the general nonconvex problem.

The tool there appears also to be useful in investment problem. This was used with success by De Wolf and Smeers [4] for the two stages problem of optimal

dimensioning and operating of a gas transmission problem. More recently, for the case where the gas selling company and the network operators are separated, it also allows to solve this difficult non convex integer problem (see Andre et al [1, 2] for the case of hydrogen).

Acknowledgments

Many thanks are due to the Norwegian State Oil Company Statoil A. S. which provided most of the funding for this work. Our gratitude also extends to Mr. Zarea of Gaz de France for helping us to find the physical interpretation. This research was also supported by the ANR research program EcoTransHy.

7 References

[1] Andre, J.; Auray, S.; Brac, J.; De Wolf, D.; Maisonnier, G.; Ould-Sidi, M.; Simonnet, A. Design and dimensioning of hydrogen transmission pipeline networks. European Journal of Operational Research, 229, 1(2013), pp. 239-251.

[2] Andre, J.; Auray, S.; De Wolf, D.; Memmah, M. M.; Simonnet, A. Time development of new hydrogen transmission pipeline networks for France. International Journal of Hydrogen Energy 39, 20(2014), pp. 10323-10337.

[3] Borraz-Sanchez, C.; Bent, R.; Backhaus, S.; Hijazi, H.; Van Hentenryck, P. Convex relaxations for gas expansion planning. arXiv preprint arXiv:1506.07214.

[4] De Wolf, D.; Smeers, Y. Optimal dimensioning of pipe networks with application to gas transmission networks. Operations Research 44, 4(1996), pp. 596-608.

[5] De Wolf, D.; Smeers, Y. The Gas Transmission Problem Solved by an Extension of the Simplex Algorithm. Management Sciences. 46, 11(2000), pp. 1454-1465.

[6] De Wolf, D.; Bakhouya, B. Optimal dimensioning of gas transmission networks when the distribution and the transportation functions are separated. in D. Klatte et al (eds.), Operations Research Proceedings 2012, Springer Verlag, Berlin, (2012), pp. 369-374.

[7] Geißler, B.; Morsi, A.; Schewe, L.; Schmidt, M. Solving power-constrained gas transportation problems using an MIP-based alternating direction method. Computers & Chemical Engineering. 82, 2(2015), pp. 303-317.

[8] Humpola, J. Gas Network Optimization by MINLP, Ph.D. Thesis. TU Berlin, Logos Verlag, Berlin, 2017.

[9] Koch, T.; Hiller, B.; Pfetsch, M. E.; Schewe, L. Evaluating Gas Network Capacities. MOS SIAM Series in Optimization, 2015.

[10] Maugis, M. J. J. Etude de Réseaux de Transport et de Distribution de Fluide. RAIRO 11, 2(1977), pp. 243-248.

[11] Morsi, A. Solving MINLPs on Loosely-Coupled Networks with Applications in Water and Gas Network Optimization. Dissertation Universitat Erlangen-Nurnberg, 2013.

[12] O'neill, R. P.; Williard, M.; Wilkins, B.; Pike, R. A Mathematical Programming Model for Allocation of Natural Gas. Operations Research 27, 5(1979), pp. 857-873.

[13] Rios-Mercado, R. Z.; Wu, S.; Scott, L. R.; Boyd, E. A. A Reduction Technique for Natural Gas Transmission Network Optimization Problems. Annals of Operations Research. 117, 1-4(2002), pp. 217-234.

[14] Rios-Mercado, R. Z.; Borraz-Sanchez, C. Optimization problems in natural gas transportation systems: A state-of-the-art review. Applied Energy 147, (2015), pp. 536-555.

[15] Wilson, J. G.; Wallace, J.; Furey, B. P. Steady-state Optimization of Large gas transmission systems. in Simulation and optimization of large systems, A. J. Osiadacz Ed, Clarendon Press, Oxford, 1988.

Author contact:

Daniel DE WOLF, Professor
TVES, Université du Littoral Côte d'Opale
189B avenue Maurice Schumann, BP 5526
59379 Dunkerque, France
E-mail: daniel.dewolf@univ-littoral.fr

ISSN 1846-6168 (Print), ISSN 1848-5588 (Online)
ID: TG-20170816163807

Subject review

CURRENT STATE OF THE PLASTIC WASTE RECYCLING SYSTEM IN THE EUROPEAN UNION AND IN GERMANY

Irena ŽMAK, **Carina HARTMANN**

Abstract: The paper presents the results of the analysis of the current state in waste management of plastic bottles in Germany. A data overview of the differences in recycling policies between different countries in the European Union is presented. The application of twelve different polymeric materials by five different application sectors in Europe shows the predominated usage areas of selected polymeric materials. A detailed insight into the German Dual System (DSD) for plastic recycling is presented, with the reference to the famous label the "Green Dot". The evolution of the recovery rates of packaging in Germany from 1991 to 2014 is presented for glass, aluminium, tinplate, polymers, paper and cardboard and liquid packaging board. It was observed that the plastic recycling rate has risen from ~ 15 % to almost 100 %, i.e. nowadays almost the whole plastic waste is either incinerated or recycled. Current data for PET-bottles return is determined as well, and detailed current information regarding the deposit system is presented. The actual applications and specific data showing the industry sectors that use the PET from recovered bottles are presented.

Keywords: Germany; PET; plastics; recycling; waste

1 INTRODUCTION

The Earth's population is ever-increasing and with this development comes the increase in waste. In Europe, a single person is currently producing half a ton of waste per year. If industrial waste is taken into account as well, it becomes clear that the overall amount of waste is enormous. In 2010, for example, the total waste production in the EU amounted to around 2.5 bn tons. [1] However, the increasing population is not the only reason for this development. Rather, each person is producing more waste. Consumers now have more choices and products are designed to have shorter lifespans. Apart from that, more single-use and disposable products are produced. Generally, it can be stated that people, relatively, earn more money, consume more products and, thus, generate more waste. If all of it were put onto the landfills, the Earth could soon be entirely covered with waste. If all waste were incinerated, the resulting air pollution could destroy the planet's climate. The only reasonable answer to this issue is recycling.

Since plastic has become one of the most common materials, plastic waste has, in this respect, become one of the most pressing issues. Unfortunately, the properties which make plastic so useful, such as durability, light-weight and low-cost, often cause problems when it comes to the end-of-life options. Processes of degradation, incineration and recycling are not as easy for plastics as they are for other materials. This paper discusses the issue of recycling of plastics and depicts a practical example of the plastic recycling in Germany.

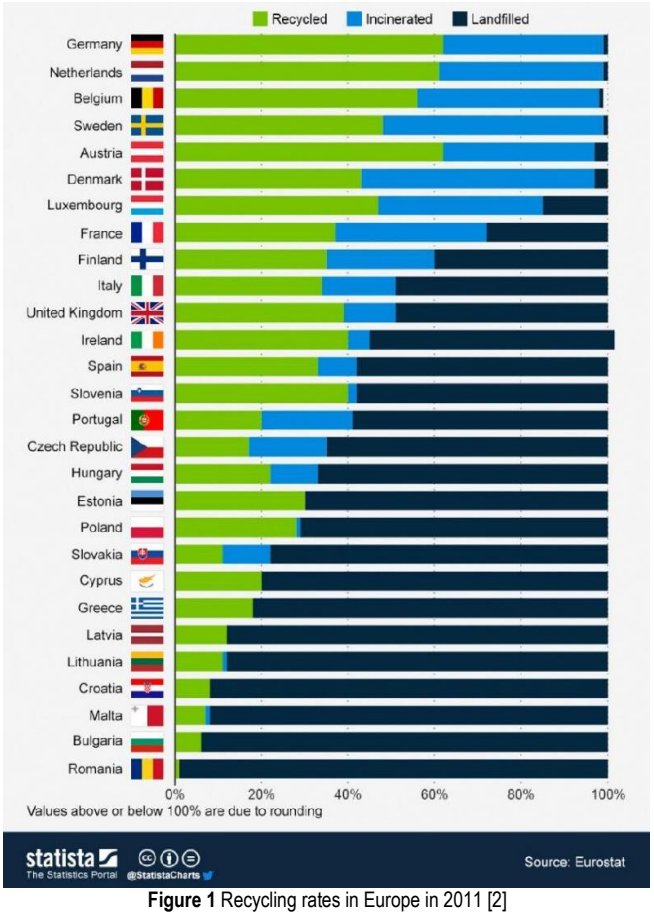

Figure 1 Recycling rates in Europe in 2011 [2]

2 CURRENT EUROPEAN RECYCLING RATES

This infographic in Fig. 1 shows a significant difference in recycling between different countries in the European Union. [2] Germany, the Netherlands and Belgium recycle 62 %, 61 % and 56 % of their waste, respectively, while

Croatia, Malta, Romania and Bulgaria are listed at the end of the list. Croatia is the fourth country from the bottom, with only 8 % of the waste recycled, while the remaining of 92 % ends up on landfills. Bulgaria recycles only 6 % and Romania 1 % of its waste. In 2013, according to the European Environment Agency, an analysis of the recycling vs. landfill vs. incineration rate has shown that Northern and Western Europe differ strongly compared to Eastern European countries. The case of Estonia is an exception, since the recycling-rate there is relatively high, while there is no incineration at all, which leads to a high the landfill-rate.

The EU has introduced policies forcing its member states to reach certain recycling quotas until 2020. This recycling rate for example for the building sector will be 70% of its waste. In order to fulfil the criteria, a lot of states have to change their deposal systems completely. [4]

The "Zero plastics to landfills by 2020" concept is a challenging, although not an unrealistic goal, as suggested by the European Association of Plastics Recycling and Recovery Organisation. [1] Other European Commission policies which will be due until 2030 are as folows: common EU target for recycling 65 % of municipal waste, common EU target for recycling 75 % of packaging waste, a binding landfill target to reduce landfill to a maximum of 10 % of municipal waste, and a ban on landfilling of separately collected waste. [1]

If these goals set by the EU Commission will be met, it would be a major step forward in the fight against waste.

3 POLYMERIC MATERIALS APPLICATIONS

The first association which comes to one's minds when talking about plastics are probably plastic bags or food packaging since it constitutes a major fraction in the applications. Nevertheless, there are more fields of applications - for example the building and construction sector. With 20 % of the total European plastic consumption it is the second largest group after packaging. Plastic is used for equipment like insulation, pipes or window frames. Another branch is transportation, including the car and aircraft industries. By lowering the weight of vehicles, which can be achieved through the use of plastic components, emissions can be decreased. Other sectors are agriculture, electronic devices or leisure. The medical sector uses plastic for different devices, prostheses and pill capsules made of special polymers. [5] Different demands of several plastic types, sorted by the different application sectors are shown in Fig. 2.

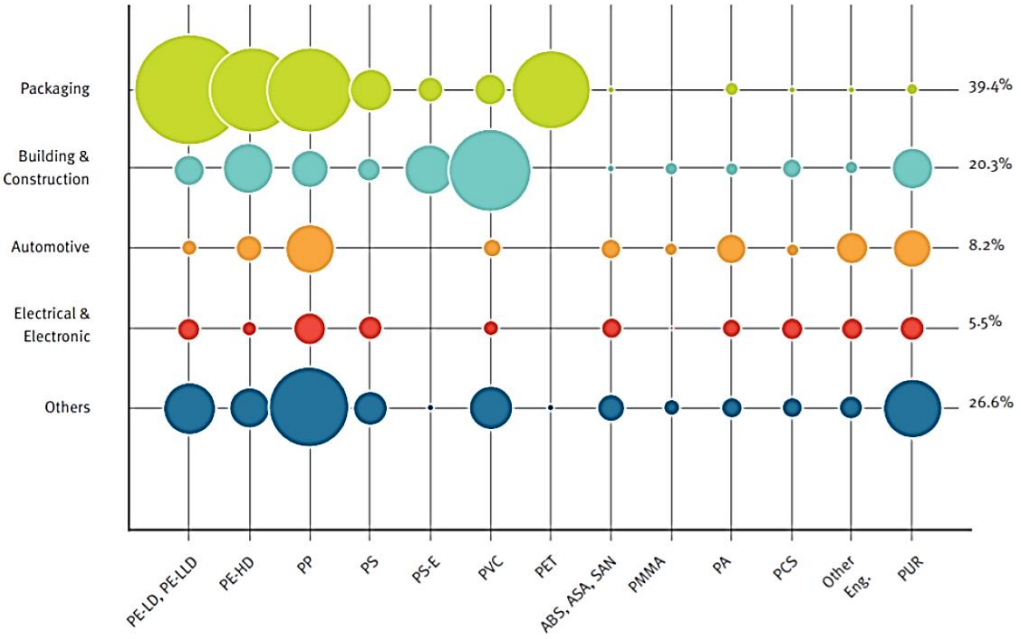

Figure 2 European plastics demand by segment and resin type in 2012 [3]

4 ANALYSIS OF PLASTIC RECYCLING IN GERMANY

As mentioned before, the rate of Germany landfill waste is the lowest in the EU. Also, Germany is producing the largest part of the European plastic waste. In 2015, the European plastic demand was 49 megatons and 24.6 % of that came from Germany. [3] Since the early 1990s, a considerable effort has been made to recycle plastics in Germany. As a result, Germany is the largest market for recycled plastics in Europe today, followed by Spain. [7]

4.1 German Dual System (DSD)

In 1991 a rapid entry into plastic recycling occurred in Germany with the implementation of the German Ordinance on Packaging Waste ("Verpackungsverordnung"). As a result of that law, the privately operated German Dual System (DSD), also known as "Green Dot" (in German: "Der grüne Punkt"), was established. [8] In order to liberate industrial firms and retailers from their individual take-back

and recovery obligations under the German Packaging Ordinance, on the basis of this ordinance DSD established a second (dual) disposal system besides the public-sector waste disposal service. As the first system of this kind worldwide, it has been providing a nationwide collection of used sales packages since 1991. [9]

In Germany, private households receive a yellow barrel or a yellow bag ("Gelber Sack"), what is part of the Dual System. In that they can put every packaging, which is labelled with the "Green Dot". The companies have to pay for the deposal of the packaging beforehand, if they want to participate in the German Dual System. DSD only collects packaging material from manufacturers who pay a license fee to DSD. These license fee payers can then add the Green Dot logo to their package labelling to indicate that this package should be placed into the separate yellow bags bins that will then be collected and emptied by DSD-operated waste collection vehicles and sorted in DSD facilities. German license fees are calculated using the weight of packs, each material type used and the volumes of product produced per annum. [9]

Since the population is relieved from the charge of the plastic waste in the yellow bags, but has to pay fees for the municipal waste, the motivation for separating the waste is huge. The system for the waste fees differs in different federal states, but in general, people only pay for the municipal waste. The separated waste in the paper bins, organic and plastic waste is not charged. If a household is not separating the trash correctly, the garbage collection will not take it away. Furthermore the household may be forced to pay a penalty.

The dual system is one of the largest purchasers for waste management services too. Not only in Germany but in many countries in Europe, the DSD delegate the collection and processing of used sales packaging to waste deposal companies. [7]

4.2 Recycling and incinerating rates for plastic waste

Fig. 3 shows the evolution of the recovery rates of packaging in Germany from 1991 until 2014. The blue line constitutes the plastics and is very close to the 100 %-mark since 2013. This means that nowadays nearly the whole plastic waste is either incinerated (energetic recovery) or recycled (material recycling).

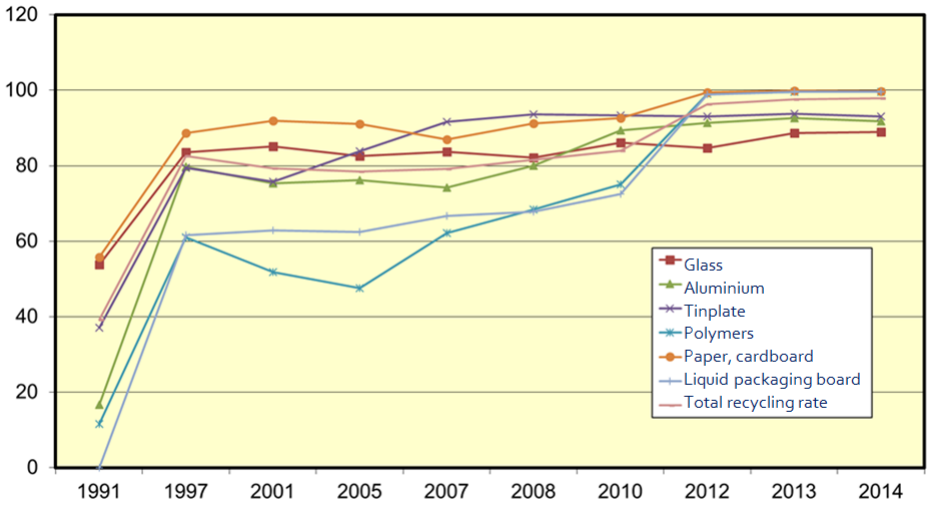

Figure 3 Evolution of recovery rates in Germany from 1991 to 2014 [6]

In 2001 only 51.8 % of the amount of plastic packaging waste was recovered or recycled. In 2013 it was already 99.6 %. [10]

Currently there are 68 waste incinerating plants in operation in Germany, which have a capacity of 20 million tons. The plants have to follow strict restrictions of emission control [11] to avoid water and air pollution. [12]

The waste management in Germany has been privatized since the 80s, so there are no specifics about the number of recycling plants in Germany. Furthermore, many companies are recycling their waste themselves. Because of their usual economic inefficiency, the plastic recycling plants are typically subsidized by the German state.

One large plastic recycling company in Germany is Multipet in Bernburg, which produces recyclates of PP, PET and HDPE in form of flakes or granulates. Moreover they sell drainage channels and cable ducts, which are 100 % recycled products made by the injection moulding. [13]

4.3 Plastic bottle deposit system

The huge demand of PET, mostly caused by the PET-bottles produces greenhouse gas emissions of 1.5 tonnes of CO_2-e per ton of recycled PET as well as a reduction in landfill and in energy consumption. An average net reduction of 1.45 tonnes of CO_2-e per ton of recycled plastic has been estimated. Most of the net energy and emission benefits arise from the substitution of the virgin polymer production. [14]

In order to avoid PET-bottles contaminations for easier recycling, the system of deposit is introduced. A lot of

countries have a deposit system for plastic bottles, but the deposit in Germany is the largest: 25 cents for each plastic bottle. A side effect of that are people collecting these bottles from trashcans, streets or parks. The system in Germany is very strict - except for a few juice bottles, most plastic bottles are included in the deposit system. Since the system was introduced in 2006, nowadays, i.e. 10 years later, it is possible to take a review of the deposit system.

4.4 Recollection of PET-bottles

In 2005, the DPG (Deutsche Pfandsystem GmbH), the German Deposit-system company, was founded. Since then every shop with more than 200 m^2 shop area is obliged to take back every drink packages of the same kind of material which they are selling. Nowadays the recycling-rate of PET-bottles with the deposit in Germany is 97.2 %. For the PET-bottles without a deposit the recycling-rate is 93.6 %. The deposit of 25 cent has to be on every plastic bottle which has a volume between 0.1 and 3 litres and has a one-way-use. They are labelled with the logo of the DPG, which is shown in Fig. 4.

Figure 4 DPG – logo [15]

This high PET-return is due to the consumers, which are bringing back 96 % of the plastic bottles. Also, bottles thrown-away in the waste are filtered out, and brought back to the recycling route.

4.5 Recycled PET-bottles usage

New PET-bottles were made from more than 26 % recycled PET-material in Germany in 2013. In this example of the recycled PET-bottles usage, the lifecycle of PET-bottles is closed. Other sectors too are increasingly using the recovered material of plastic bottles. Recycled PET is used in the textile industry, in the foil industry or for other applications, such as ribbons or detergent packaging, with the exact values shown in Tab. 1.

Table 1 Sectors using the PET from recovered bottles [16]

Recovered PET used for:	PET-bottles	Textile industry	Foil industry	Other
	32.1 %	29.4 %	27.3 %	11.2 %

According to the increased usage of the recycled PET, the deposit system on PET-bottles in Germany has proved to be a huge gain in conserving resources.

5 CONCLUSION

Recycling is a promising strategy for the end-of-life management of plastic products. It is slow, but it does make increasing economic sense, as well as an undoubtful positive environmental impact. Recent trends demonstrate a substantial increase in the rate of recovery and recycling of plastic wastes. These trends are likely to continue, but some significant challenges still exist from both technological factors and from economic or social behaviour.

The recycling of plastics is a very important issue in the modern society, with aims to the reduction of waste on the landfills and saving the environment. Material recycling is the most efficient way of recycling, with less energy or feedstock lost as compared to incineration.

Finally, the common people thinking should evolve, from a throwing-away to an exchange-community.

Note: This investigation was presented at the International Conference MATRIB 2017 (29. 6. - 2. 7. 2017, Vela Luka, Croatia).

6 REFERENCES

[1] European Commission (2017). http://ec.europa.eu/environment/waste/index.htm (accesed on 20 Jan 2017)
[2] Recycling Remains a Rarity in Eastern Europe. OneEurope. http://one-europe.net/eurographics/recycling-remains-a-rarity-in-eastern-europe (accesed on 20 Jan 2017)
[3] PlasticsEurope (2017). http://www.plasticseurope.org/plastics-sustainability-14017/zero-plastics-to-landfill.aspx (accesed on 20 Jan 2017)
[4] European Environment Agency (2013). http://www.eea.europa.eu/about-us/competitions/waste-smart-competition/recycling-rates-in-europe/view (accesed on 20 Jan 2017)
[5] Sevenster. Use of plastics. http://www.plasticseurope.org/use-of-plastics/building-construction.aspx (accesed on 20 Jan 2017)
[6] Bundesministerium für Umwelt, Naturschutz, Bau und Reaktorsicherheit. http://www.bmub.bund.de/fileadmin/Daten_BMU/Bilder_Infografiken/verpackungen_verwertungsquote_linien.png (accesed on 20 Jan 2017)
[7] Martin Patel (1999). Recycling of plastics in Germany. http://aceee.org/files/proceedings/1999/data/papers/SS99_Panel1_Paper37.pdf (accesed on 20 Jan 2017)
[8] Wollny V., Dehoust G., Fritsche U. R., Weinem P., Comparison of Plastic Packaging Waste Management Options: Feedstock Recycling versus Energy Recovery in Germany, Journal of Industrial Ecology, 5, pp. 49-63, (2001).
[9] Duales System Deutschland. Der Grüne Punkt. https://www.gruener-punkt.de (accesed on 20 Jan 2017)

[10] Abfallwirtschaft in Deutschland – Fakten, Daten, Grafiken. http:/www.bmub.bund.de/fileadmin/Daten_BMU/Pools/Broschueren/abfallwirtschaft_2016.pdf (accesed on 20 Jan 2017)
[11] 17. BImSchV-Siebzehnte Verordnung zur Durchführung des Bundes-Immissionsschutzgesetzes, https://www.gesetze-im-internet.de/bimschv_17_2013/BJNR104400013.html, consulted on 20 Jan 2017.
[12] Bundesministerium für Umwelt, Naturschutz, Bau und Reaktorsicherheit. http://www.bmub.bund.de/fileadmin/Daten_BMU/Bilder_Infografiken/verpackungen_verwertungsquote_linien.png (accesed on 20 Jan 2017)
[13] Multiport GmbH und MultiPet GmbH. https://www.mp-bbg.eu/de/ (accesed on 20 Jan 2017)
[14] Plastics recycling: challenges and opportunities: http://rstb.royalsocietypublishing.org/content/364/1526/2115#sec-20 (accesed on 20 Jan 2017)
[15] DPG Deutsche Pfandsystem GmbH. http://www.dpg-pfandsystem.de/index.php/de/die-pfandpflicht-fuer-einweggetraenkeverpackungen.html (accesed on 20 Jan 2017)
[16] IK Industrievereinigung Kunststoffverpackungen. http://www.kunststoffverpackungen.de/getraenkeflaschen_aus_pet___meister_des_recyclings_5657.html (accesed on 20 Jan 2017)

Authors' contacts:

Irena ŽMAK
University of Zagreb,
Faculty of Mechanical Engineering and Naval Architecture,
Ivana Lučića 5, HR-10000 Zagreb, Croatia
irena.zmak@fsb.hr

Carina HARTMANN
Friedrich-Alexander University Erlangen-Nürnberg,
Technical Faculty,
Paul-Gordan-Strasse 3/5, D-91052 Erlangen, Germany

ISSN 1846-6168 (Print), ISSN 1848-5588 (Online)
ID: TG-20……..

14pt
14pt

ARTICLE TITLE ONLY IN ENGLISH (Style: Arial Narrow, Bold, 14pt)

14pt

Ivan HORVAT, Thomas JOHNSON (Style: Arial Narrow, Bold, 11pt)

11pt
11pt

Abstract: Article abstract contains maximum of 150 words and is written in the language of the article. The abstract should reflect the content of the article as precisely as possible. TECHNICAL JOURNAL is a trade journal that publishes scientific and professional papers from the domain(s) of mechanical engineering, electrical engineering, civil engineering, multimedia, logistics, etc., and their boundary areas. This document must be used as the template for writing articles so that all the articles have the same layout. (Style: Arial Narraw, 8pt)

10pt

Keywords: keywords in alphabetical order (5-6 key words). Keywords are generally taken from the article title and/or from the abstract. (Style: Arial Narraw, 8pt)

10pt
10pt

1 ARTICLE DESIGN
(Style: Arial Narrow, Bold, 10pt)

10pt

(Tab 6 mm) The article is written in Latin script and Greek symbols can be used for labelling. The length of the article is limited to eight pages of international paper size of Letter (in accordance with the template with all the tables and figures included). When formatting the text the syllabification option is not to be used.

10pt

1.1 General guidelines
(Style: Arial Narrow, 10pt, Bold, Align Left)

10pt

The document format is Letter with margins in accordance with the template. A two column layout is used with the column spacing of 10 mm. The running text is written in Times New Roman with single line spacing, font size 10 pt, alignment justified.

Article title must clearly reflect the issues covered by the article (it should not contain more than 15 words).

Body of the text is divided into chapters and the chapters are divided into subchapters, if needed. Chapters are numbered with Arabic numerals (followed by a period). Subchapters, as a part of a chapter, are marked with two Arabic numerals i.e. 1.1, 1.2, 1.3, etc. Subchapters can be divided into even smaller units that are marked with three Arabic numerals i.e. 1.1.1, 1.1.2, etc. Further divisions are not to be made.

Titles of chapters are written in capital letters (uppercase) and are aligned in the centre. The titles of subchapters (and smaller units) are written in small letters (lowercase) and are aligned left. If the text in the title of the subchapter is longer than one line, no hanging indents.

10pt

Typographical symbols (bullets), which are being used for marking an item in a list or for enumeration, are placed at a beginning of a line. There is a spacing of 10pt following the last item:

- Item 1
- Item 2
- Item 3

10pt

The same rule is valid when items are numbered in a list:

1. Item 1
2. Item 2
3. Item 3

10pt

1.2 Formatting of pictures, tables and equations
(Style: Arial Narrow, 10pt, Bold, Align Left)

10pt

Figures (drawings, diagrams, photographs) that are part of the content are embedded into the article and aligned in the centre. In order for the figure to always be in the same position in relation to the text, the following settings should be defined when importing it: text wrapping / in line with text.

Pictures must be formatted for graphic reproduction with minimal resolution of 300 dpi. Pictures downloaded from the internet in ratio 1:1 are not suitable for print reproduction because of unsatisfying quality.

10pt

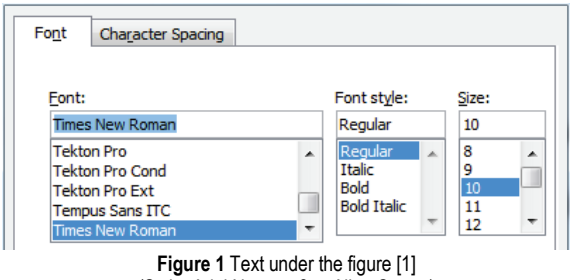

Figure 1 Text under the figure [1]
(Style: Arial Narraw, 8pt, Align Centre)

10pt

The journal is printed in black ink and the figures have to be prepared accordingly so that bright tones are printed in a satisfactory manner and are readable. Figures are to be in colour for the purpose of digital format publishing. Figures in the article are numbered with Arabic numerals (followed by a period).

Text and other data in tables are formatted - Times New Roman, 8pt, Normal, Align Center.

When describing figures and tables, physical units and their factors are written in italics with Latin or Greek letters,

while the measuring values and numbers are written upright.

10pt

Table 1 Table title aligned centre
(Style: Arial Narraw, 8pt, Align Centre)

	1	2	3	4	5	6
ABC	ab	ab	ab	ab	ab	ab
DEF	cd	cd	cd	cd	cd	cd
GHI	ef	ef	ef	ef	ef	ef

10 pt

Equations in the text are numbered with Arabic numerals inside the round brackets on the right side of the text. Inside the text they are referred to with equation number inside the round brackets i.e. ".... from Eq. (5) follows ...." (Create equations with MS Word Equation Editor - some examples are given below).

10pt

$$F_{\text{avg}}(t,t_0)=\frac{1}{t}\int_{t_0}^{t_0+t}F\big(q(\tau),p(\tau)\big)\,\mathrm{d}\tau, \tag{1}$$

10pt

$$\cos\alpha+\cos\beta=2\cos\frac{\alpha+\beta}{2}\cdot\cos\frac{\alpha-\beta}{2}. \tag{2}$$

10pt

Variables that are used in equations and also in the text or tables of the article are formatted as *italics* in the same font size as the text.

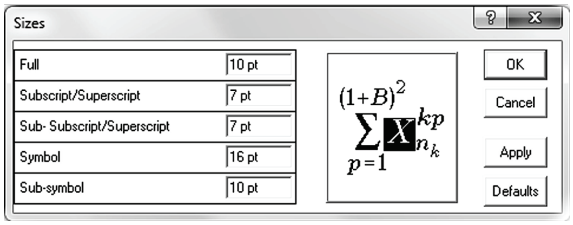

Figure 2 The texts under figures
(Style: Arial Narraw, 8pt, Align Centre)

Figures and tables that are a part of the article have to be mentioned inside the text and thus connected to the content i.e. „ … as shown in Fig. 1…" or „data from Tab. 1…" and similar.

10pt

2 PRELIMINARY ANNOTATION

10pt

Article that is offered for publication cannot be published beforehand, be it in the same or similar form, and it cannot be offered at the same time to a different journal. Author or authors are solely responsible for the content of the article and the authenticity of information and statements written in the article.

Articles that are accepted for publishing are classified into four categories: original scientific papers, preliminary communications, subject reviews and professional papers.

Original scientific papers are articles that according to the reviewer and the editorial board contain original theoretical or practical results of research. These articles need to be written in such a way that based on the information given, the experiment can be repeated and the results described can be achieved together with the author's observations, theoretical statements or measurements.

Preliminary communication contains one or more pieces of new scientific information, but without details that allow recollection as in original scientific papers. Preliminary communication can give results of an experimental research, results of a shorter research or research in progress that is deemed useful for publishing.

Subject review contains a complete depiction of conditions and tendencies of a specific domain of theory, technology or application. Articles in this category have an overview character with a critical review and evaluation. Cited literature must be complete enough to allow a good insight and comprehension of the depicted domain.

Professional paper can contain a description of an original solution to a device, assembly or instrument, depiction of important practical solutions, and similar. The article need not be related to the original research, but it should contains a contribution to an application of known scientific results and their adaptation to practical needs, so it presents a contribution to spreading knowledge, etc.

Outside the mentioned categorization, the Editorial board of the journal will publish articles of interesting content in a special column. These articles provide descriptions of practical implementation and solutions from the area of production, experiences from device application, and similar.

10pt

3 WRITING AN ARTICLE

10pt

Article is written in the English language and the terminology and the measurement system should be adjusted to legal regulations, standards (ISO 80 000 series) and the SI international system of units. The article should be written in third person.

Introduction contains the depiction of the problem and an account of important results that come from the articles that are listed in the cited literature.

Main section of the article can be divided into several parts or chapters. Mathematical statements that obstruct the reading of the article should be avoided. Mathematical statements that cannot be avoided can be written as one or more addendums, when needed. It is recommended to use an example when an experiment procedure, the use of the work in a concrete situation or an algorithm of the suggested method must be illustrated. In general, an analysis should be experimentally confirmed.

Conclusion is a part of the article where the results are being given and efficiency of the procedure used is emphasized. Possible procedure and domain constraints where the obtained results can be applied should be emphasized.

10pt

4 RECAPITULATION ANNOTATION

10pt

In order for the articles to be formatted in the same manner as in this template, this document is recommended for use when writing the article. Finished articles written in MS Word for Windows and formatted according to this

template must be submitted using our The Paper Submission Tool (PST) (https://tehnickiglasnik.unin.hr/authors.php) or eventually sent to the Editorial board of the Technical Journal to the following e-mail address: tehnickiglasnik@unin.hr

The editorial board reserves the right to minor redaction corrections of the article within the framework of prepress procedures. Articles that in any way do not follow these authors' instructions will be returned to the author by the editorial board. Should any questions arise, the editorial board contacts only the first author and accepts only the reflections given by the first author.

10pt

5 REFERENCES

10pt

The literature is cited in the order it is used in the article. Individual references from the listed literature inside the text are addressed with the corresponding number inside square brackets i.e. "… in [7] is shown …". If the literature references are web links, the hyperlink is to be removed as shown with the reference number 8. Also, the hyperlinks from the e-mail addresses of the authors are to be removed. In the literature list, each unit is marked with a number and listed according to the following examples (omit the subtitles over the references – they are here only to show possible types of references):

10pt

books:

[1] Franklin, G. F.; Powel, J. D.; Workman, M. L.: Digital Control of Dynamic System, Addison-Wesley Publishing Company, Massachusetts, 1990

[2] Kostrenčić, Z.: Teorija elastičnosti, Školska knjiga, Zagreb, 1982.

articles in journals:

[3] Michel, A. N.; Farrell, J. A.: Associative Memories via Artificial Neural Networks, IEEE Control System Magazine, Vol. 10, No. 3 (1990) 6-17

[4] Dong, P.; Pan, J.: Elastic-Plastic Analysis of Cracks in Pressure-Sensitive Materials, International Journal of Solids and Structures, Vol. 28, No. 5 (1991) 1113-1127

[5] Kljajin, M.: Prijedlog poboljšanja proračuna parametara dodira na primjeru evolventnih bokova zubi, Tehnički vjesnik/Technical Gazette, Vol. 1, No. 1,2 (1994) 49-58

articles published in conference proceedings:

[6] Albertsen, N. C.; Balling, P.; Laursen, F.: New Low Gain S-Band Satellite Antenna with Suppressed Back Radiation, Proc. 6th European Microwave Conference, Rome, September 1976, 14-17

[7] Kljajin, M.; Ergić, T.; Ivandić, Ž.: Izbor robota za zavarivanje uvjetovan konstrukcijom proizvoda, Zbornik radova - 3. međunarodno savjetovanje proizvodnoga strojarstva/3rd International Conference on Production Engineering CIM '95, Zagreb, November 1995, C-35 - C-41

links:

[8] http://www.sciencedaily.com/articles/w/wind_power.htm (Accessed: 19.06.2012.)

10pt

10pt

Authors' contacts:

10pt

Full Name, title
Institution, company
Address
Tel./Fax,e-mail

Full Name, title
Institution, company
Address
Tel./Fax,e-mail